(12)

AFGL-TR-82-0299

SINGLE AND MULTIPLE SCATTERED SOLAR RADIATION

W.L. RIDGWAY
R.A. MOOSE
A.C. COGLEY

SONICRAFT, INC.
8859 S. GREENWOOD AVENUE
CHICAGO, ILLINOIS 60619

30 AUGUST 1982

Final Report

(Sept. 1980 - June 1982)

Approved for public release; distribution unlimited

Prepared for:

AIR FORCE GEOPHYSICS LABORATORY
AIR FORCE SYSTEMS COMMAND
UNITED STATES AIR FORCE
HANSCOM AFB, MASSACHUSETTS 01731

DISCLAIMER NOTICE

THIS DOCUMENT IS BEST QUALITY PRACTICABLE. THE COPY FURNISHED TO DTIC CONTAINED A SIGNIFICANT NUMBER OF PAGES WHICH DO NOT REPRODUCE LEGIBLY.

UNCLASSIFIED

SECURITY CLASSIFICATION OF THIS PAGE (When Data Entered)

REPORT DOCUMENTATION PAGE		READ INSTRUCTIONS BEFORE COMPLETING FORM
1. REPORT NUMBER AFGL-TR-82-0299	2. GOVT ACCESSION NO. AD-A126 323	3. RECIPIENT'S CATALOG NUMBER
4. TITLE (and Subtitle) Single And Multiple Scattered Solar Radiation		5. TYPE OF REPORT & PERIOD COVERED Final Report Sept. 1980 - June 1982
		6. PERFORMING ORG. REPORT NUMBER
7. AUTHOR(s) W.L. Ridgway R.A. Moose A.C. Cogley		8. CONTRACT OR GRANT NUMBER(s) F19628-80-C-0180
9. PERFORMING ORGANIZATION NAME AND ADDRESS Sonicraft, Inc. 8859 South Greenwood Avenue Chicago, Illinois 60619		10. PROGRAM ELEMENT, PROJECT, TASK AREA & WORK UNIT NUMBERS 62101F 767009AN
11. CONTROLLING OFFICE NAME AND ADDRESS Air Force Geophysics Laboratory Hanscom AFB, Massachusetts 01731 Monitor/William O. Gallery/OPI		12. REPORT DATE August 30, 1982 13. NUMBER OF PAGES 196
14. MONITORING AGENCY NAME & ADDRESS (if different from Controlling Office)		15. SECURITY CLASS. (of this report) UNCLASSIFIED 15a. DECLASSIFICATION/DOWNGRADING SCHEDULE

16. DISTRIBUTION STATEMENT (of this Report)

Approved for public release; distribution unlimited

17. DISTRIBUTION STATEMENT (of the abstract entered in Block 20, if different from Report)

18. SUPPLEMENTARY NOTES

19. KEY WORDS (Continue on reverse side if necessary and identify by block number)

Radiative Transfer
Scattering Properties
Solar Scattering
Multiple Scattering
Thermal Radiation
Scattering Radiance
Atmospheric Radiance

20. ABSTRACT (Continue on reverse side if necessary and identify by block number)

Mie calculations are performed to produce complete scattering properties for various aerosol models contained in LOWTRAN'S model atmospheres. Those properties are used in a solar single scattering approximation for inhomogeneous spherical atmospheres based on LOWTRAN'S transmission functions. A multiple scattering adding/doubling code for plane-paralle atmospheres is developed and can be used to represent muldiple scattered radiative fields in spherical atmospheres over a wide range of angle and path parameters. All data and codes are documented so they can be used in future research.

DD FORM 1 JAN 73 1473 EDITION OF 1 NOV 65 IS OBSOLETE

UNCLASSIFIED

SECURITY CLASSIFICATION OF THIS PAGE (When Data Entered)

TABLE OF CONTENTS

TABLE OF CONTENTS (cont'd)

LIST OF FIGURES

LIST OF TABLES

1. INTRODUCTION

For the past ten to fifteen years the Air Force Geophysics Laboratory (AFGL), Optical Physics Division has been developing the expertise to calculate radiative transfer (direct point-to-point transmittance and radiance) in the earth's atmosphere. At the focus of this research are two computer codes called LOWTRAN [Ref. 1] and FASCODE [Ref. 2,3,4]. LOWTRAN is a low spectral resolution code (typical resolution is 20 wavenumbers) that uses spectrally averaged and empirically derived direct transmittance functions for spherically symmetric and refractive model atmospheres that include aerosols. FASCODE uses the same spherical geometry and atmospheric models found in LOWTRAN, but retains the spectral resolution inherent in molecular and atomic line models. The developments described in this report concern solar/lunar scattering phenomena in the atmosphere and how such processes can be included in these two codes (mainly LOWTRAN in this study) which are under continual development at AFGL.

Mie calculations have been performed at AFGL for some time to obtain scattering and absorption coefficients for the various atmospheric aerosol models that have been developed. When scattering phenomena beyond zeroth order (attenuation only) are to be considered, the phase function must also be obtained from Mie calculations. Section 2 describes the complete Mie calculations which were done for all of the atmospheric aerosol models comprising the model atmospheres of LOWTRAN. The Mie code and aerosol models are described only briefly since they were developed by others and are well documented in the literature. The computed scattering data are parametrically defined and all unconventional approximations and assumptions are discussed. The format of the available data is described so that the

reader can more readily obtain access to it through AFCL.

Since LOWTRAN uses spherical geometry and spectrally averaged direct radiative transmission functions which do not obey Beer's law, there is no established method to compatibly calculate mutiply scattered radiative fields due to solar/lunar illumination. As a first step toward including scattering in LOWTRAN, Section 3 develops a single-scattering calculation procedure compatible with LOWTRAN and describes its integration with a recent version of the LOWTRAN code, the result being designated LOWTRANSX. Example calculations made with the newly developed code are presented and the parametric range of all calculations performed to date is discussed. An independent verification of the code is also presented along with a discussion of the effects of spherical geometry and refraction on the single-scattering results.

Section 4 begins an analysis of multiple scattering in an atmosphere of unidirectional illumination from an external source like the sun. As an initial step along the difficult path to calculate multiple scattering in spherical atmospheres, an Adding/Doubling (A/D) computer code [Ref. 5,6,7] for plane-parallel media is modified to model radiation from external sources (the code was originally developed for infrared isotropic internal sources). A Fast Fourier Transform of the azimuth dependence of the phase function is taken and each Fourier component is used in a separate A/D run. The results are then inverse transformed to obtain intensity fields throughout the plane-parallel medium. The codes that perform these operations are described and the results are checked against other independent results for certain special values of the parameters (optical depth, albedo, and angular variables). A parallel but independent single-scattering code is developed, partly to check the A/D code in the limit of sufficiently small single

scattering albedoes. Appropriate intercomparisons are made between the A/D, LOWTRANSX, and plane-parallel single-scattering predictions to show their commonality and differences. The effects of spherical geometry, refraction, and multiple scattering are quantified within the context of the present codes. The A/D code is also used to study how spectral redundancy in realistic, inhomogeneous atmospheres may be used to reduce computational times for high resolution multiple scattering calculations.

Several appendices are used to present details of the codes and special mathematical developments that will be of interest only to the reader who must use the codes or their derivatives developed subsequently by AFGL.

2. AEROSOL PHASE FUNCTIONS

The model atmospheres contained in LOWTRAN 5 [Ref. 1] include a number of aerosol models for which Mie computations have been made to produce normalized aerosol scattering and absorption coefficients. When scattering (beyond zeroth order) is considered in the radiative transfer, the phase function must also be known. This chapter describes the complete Mie calculations carried out for all the aerosol models contained in LOWTRAN 5. Section 2.1 briefly delineates the aerosol models while Section 2.2 discusses the Mie code used, along with any pertinent assumptions. Appendix A describes a short code that will access the resulting data, and Section 2.3 discusses AFGL's plan to prepare a single, comprehensive aerosol-model report to guide the reader who may want to use the data. Details of how these Mie data were used in LOWTRAN can be found in Appendix C.

2.1 Aerosol Models

Molecular or Rayleigh scattering is well understood and accurately modeled by a simple empirical expression [Ref. 8]. Aerosol scattering properties, on the other hand, must be obtained numerically and models must be constructed that attempt to duplicate those found in the atmosphere. The aerosol models used here are identical to those described in LOWTRAN 5 [Ref. 1], which are revisions of those found in earlier versions of LOWTRAN [Refs. 9, 10]. Further details of their development can be found in References 11 and 12. Only a brief summary of these aerosol models will be given here to orient the reader.

The atmosphere is divided into four regions that contain distinct aerosol models as follows:

1) 0-2Km, Boundary or Mixing Layer; within this layer there are four

basic models, namely rural, urban, maritime, and tropospheric, each having properties specified at four different relative humidities. Two additional models represent light and heavy fog conditions which brings the total number of boundary layer aerosol models to eighteen.

2) 2-10 Km, Upper Tropospheric Layer; The model used in this region is identical to the boundary layer tropospheric model with 70% relative humidity.

3) 10-30 Km, Lower Stratospheric Layer; This region contains three models called background statospheric, aged volcanic, and fresh volcanic.

4) 30-100 Km, Upper Atmospheric Layer; One meteoric dust model is used throughout this region.

There are, therefore, a total of 22 aerosol models. Each model is defined by a unique size distribution and composition. All models assume that the aerosols are spherical and homogeneous. The humidity dependent models, however, are actually two-component aerosols (a particulate surrounded by water) but are treated as a single substance using a method discussed below. Within each of the four altitude regions discussed above the model parameters are constant except for an altitude dependent loading or effective density, which does not effect the Mie calculations. The complex refractive index for each model has been tabulated [Ref. 11 and 12] for forty spectral points over the range from 0.2 to 40 μm.

2.2 Mie Calculations.

The Mie [Ref. 13] code used here and called Mie 2 [Ref. 14] was developed specifically for use on the AFGL CDC-6600 computer system. It has

been modified to allow direct input of the desired scattering angle grid and to provide output in a form suitable for use in the LOWTRANSX code [see Section 3]. This Mie code handles only homogeneous aerosols but offers advantages of multiple run capability and improved computational time.

For aerosols containing water, an effective refraction index is formed by taking a volume weighted average of the refraction index of the substance and that for water [Ref. 11]. In addition, the rural and urban models each contain two distinct size distributions that lead to slightly different indices of refraction. These are sufficiently similar such that a simple numerical average is taken of the indices. The maritime model, on the other hand, has two distinct size distributions which are run through the Mie code separately. A combined phase function is then formed for the maritime model by forming a scattering-coefficient weighted average on these two phase functions. All the other aerosol models are homogeneous with a given size distribution.

The Mie code could be run at each of the forty spectral points with a fine scattering-angle grid for each of the twenty-two models. The data base would then be very large and the computational time excessive. Considerable discussion with the staff at AFGL led to the following spectral points (27) and scattering-angle grid (34) that is a compromise between accuracy and practicality.

a) Spectral points (μm): 0.2, 0.3, 0.55, 0.6943, 1.06, 1.536, 2.0, 2.5, 2.7, 3.0, 3.2, 3.3923, 5.0, 6.0, 7.2, 7.9, 8.7, 9.2, 10.6, 10.591, 12.5, 15.0, 17.2, 18.5, 21.3, 30.0, 40.0.

b) Scattering-angle Grid (degrees): 0° → 12° (increments of 2°), 12° → 40° (increments of 4°), 40° → 120° (increments of 10°), 120° → 180° (increments of 5°).

The data resulting from the 594 (22 models times 27 spectral points) Mie runs are quite extensive and was, therefore, divided into two parts. A truncated version of the output containing only the normalized phase function ($\int P(0)\, d\Omega = 1$) at the 34 scattering angles was generated for direct use with LOWTRANSX (see Section 3). The full output file containing the wavelength, complex index of refraction, extinction and scattering coefficients, normalized phase matrix, and cosines for equal probability intervals was written in binary form to a disk file. A small separate program found in Appendix A is required to retrieve this data. A word of caution is necessary. Some of the early runs of the Mie code produced incorrect results for some of the data as a result of underdimensioned arrays. Fortunately the phase matrix was calculated correctly and this is what these calculations were for. The other quantities such as attenuation coefficients, albedos, and asymmetry parameters have been found previously. Because of computational costs, these calculations were not repeated. A full discussion of this problem is given in Appendix A.

2.3 Concluding Remarks

In an effort to reduce the size of the phase function data base, researchers at AFGL have recently performed a statistical analysis of the phase function data. While the details of this study have not yet been made public, early reports indicate that the number of aerosol-spectral models has been reduced from 594 to about 70. AFGL has also recognized the need for a single comprehensive reference describing all aspects of the aerosol models. Such a future report should contain refractive indices, attenuation coefficients, albedos, and asymmetry parameters as a function of wavelength, along with size distributions and normalized phase functions for each of the aerosol models.

3. LOWTRAN SINGLE SCATTERING MODEL

This section of the report develops a solar/lunar single scattering model based on LOWTRAN radiative transfer and outlines the new (LOWTRANSX) code structure. Subsection 3.2 presents the geometric perspective required to connect observer and illumination source locations to reference space and time coordinates on the earth. The code structure and users guide for LOWTRANSX are given in Appendices B and C, respectively, while Subsection 3.3 discusses an example calculation and independent verifications that the code functions properly. Finally, Subsection 3.4 contains concluding remarks and Appendix D contains a note on finding the subsolar point.

3.1 Radiative Transfer

The LOWTRAN code has been constructed to calculate point-to-point transmittance and observed thermal radiance along a line-of-sight in model spherical atmospheres made up of homogeneous layers. Refractive bending is computed and aerosol attenuation (zeroth order scattering and absorption) is included. Radiative transfer is calculated by way of spectrally averaged transmittance functions (resolution of about 20 wavenumbers) that are derived from experimental data and theoretical relationships. This code is extended here to include the source function due to single scattering within the atmosphere of the extraterrestrial sources, sun or moon. At the present time, reflection (scattering) off the earth's surface or other objects within the atmosphere is not considered. The observed scattering radiance is obtained by summing the properly attenuated scattering source function along any specified line-of-sight.

Before proceeding further, it will be helpful to introduce the following nomenclature:

SUPERSCRIPTS:	A	aerosol
	M	molecular
SUBSCRIPTS:	e	extinction
	a	absorption
	s	scattering
	PS	primary solar path (sun to scattering point)
	OP	line-of-sight optical path (scattering point to observer)

OTHER QUANTITIES:

K	monochromatic volumetric extinction, absorption, or scattering coefficient
$T = e^{-KL}$	monochromatic transmittance over a homogeneous path length L, due to extinction absorption, or scattering
$P(\gamma)$	scattering phase function of included angle γ
I^{SUN}	solar extraterrestrial intensity

Note that the dependence of most quantities on the spectral frequency ν will be shown by a subscript ν, although it will sometimes be suppressed for simplicity of notation when the concept is clear from context.

The monochromatic intensity (radiance) seen by an observer looking along a particular directional path is the sum of contributions from all sources lying along the line-of-sight. The sources are either primary sources

(infrared emission) or scattering sources. The scattering source function J for scattering points along the observer's line-of-sight can be expressed in terms of the local incoming intensity at each point $I_\nu(\hat{n}')$ by

$$J_\nu(\hat{n}) = \int I_\nu(\hat{n}')\left[P_\nu^A K_s^A + P_\nu^M K_s^M\right] d\Omega' \qquad (3.1)$$

where $\hat{n}$ is the unit vector directed toward the observer and $\hat{n}'$ (Ω') is to be summed over the solid angle denoted by Ω'. With only solar/lunar scattering included, the incident intensity $I_\nu(\hat{n}')$ is given by

$$I_\nu(\hat{n}') = I_\nu^{SUN} T_{e,ps}^{A+M} \qquad \delta(\hat{n}', \hat{n}_s') \qquad (3.2)$$

where $\hat{n}_s'$ is the direction of the incident solar/lunar radiation at the scattering point. A schematic of the scattering geometry for a particular sun/observer orientation is displayed in Figure 3.1. The path that the sunlight/moonlight takes in passing through the atmosphere prior to being scattered at any scattering point P will be called the 'primary solar' path. Other sources besides direct extraterrestrial illumination could of course contribute to the prescattered intensity $I_\nu(\hat{n}')$. One might include other direct sources such as gaseous emission and boundary surface radiation plus previously scattered radiation, but only unscattered sunlight/moonlight is included in the present scattering source function. The resulting source function is found by using [3.2] in [3.1] to obtain

$$J_\nu = I_\nu^{SUN} T_{e,\,ps}^{A+M} \qquad \left[(P_\nu^A(\gamma)K_s^A + P_\nu^M(\gamma)K_s^M)\right] \quad . \qquad (3.3)$$

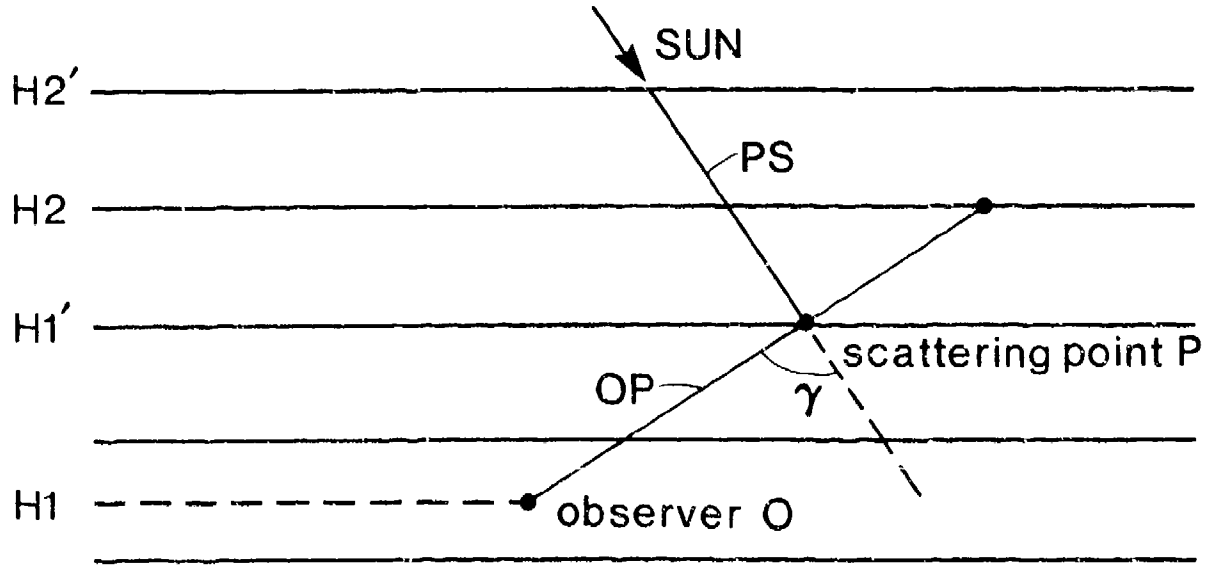

Figure 3.1 Schematic representation of the single scattering geometry. A scattering point at H1' is shown for an observer looking up from altitude H1. Both the optical paths and layer boundaries, which are shown to be straight lines, are slightly curved.

Note that P^A, P^M, K_s^M, and K_s^M vary with altitude (atmospheric density and composition) and are generally slowly varying functions of frequency. Note also that the included angle $\gamma = \arccos(\hat{n} \cdot \hat{n}_s')$ would be constant (independent of the particular scattering point) along a line-of-sight in the absense of refractive bending. Both the primary solar path and the line-of-sight optical path actually bend somewhat, so that γ can be expected to vary by as much as a few degrees along the line-of-sight. The primary solar transmittance $T_{e,ps}^{A+M}$ depends strongly on the optical path length of the primary solar path (prior to scattering), so that factor can be expected to vary considerably from one scattering point to the next.

The monochromatic intensity at the observer due to all of the single scattering sources within the line-of-sight is obtained by summing over the optical path the product of the source function and the transmission function which gives

$$I_\nu^{SCAT} = \int J_\nu \, T_{e,\,op}^{A+M} \, dL_{op}$$

$$= I_\nu^{SUN} \int T_{e,\,ps}^{A+M} \; T_{e,\,op}^{A+M} \; (P^A K_s^A + P^M K_s^M) \; dL_{op} \qquad (3.4)$$

The scattering optical depth increment $K_s \, dL_{op}$ can be expressed in terms of the incremental transmittance for both aerosol and molecular scattering as

$$K_s^X \, dL_{op} = \frac{dT_{s,\,op}^X}{T_{s,\,op}^X} \,, \qquad (3.5)$$

with X being either A or M. The intensity can therefore be written as

$$I_\nu^{SCAT} = I_\nu^{SUN} \int T_{e,\ ps+op}^{A+M} \left[p^A \frac{dT_{s,\ op}^{A}}{T_{s,\ op}^{A}} + p^M \frac{dT_{s,\ op}^{M}}{T_{s,\ op}^{M}} \right]. \quad (3.6)$$

which includes two separate integrals covering aerosol and molecular scattering effects. The above equation which provides for a monochromatic calculation at any frequency ν is now adapted for use with the molecular band transmission model used in LOWTRAN. The spectrally averaged intensity $\bar{I}$ is formally defined in terms of a convolution of the spectral intensity with a triangular spectral shape function $g(\nu)$ taken over a spectral width of approximately $\delta\nu = 20\ cm^{-1}$, that is,

$$\bar{I}_\nu = \frac{1}{\delta\nu} \int I_{\nu'}\, g(\nu-\nu')\, d\nu' \ . \quad (3.7)$$

The spectrally averaged, scattered intensity can be expressed in terms of known LOWTRAN quantities provided that only the molecular absorption transmittance is a rapidly varying function of frequency. All other quantities are assumed to be constant over the spectral interval $\delta\nu$. The result is

$$\bar{I}_\nu^{SCAT} = \bar{I}_\nu^{SUN} \int \bar{T}_{e,\ ps+op}^{A+M} \left[p^A \frac{dT_{s,\ op}^{A}}{T_{s,\ op}^{A}} + p^M \frac{dT_{s,\ op}^{M}}{T_{s,\ op}^{M}} \right]. \quad (3.8)$$

The quantity $\bar{T}_{ps+op}^{A+M}$ represents the spectrally averaged transmittance that is calculated in LOWTRAN. Therefore, the molecular band models and aerosol models of LOWTRAN provide a direct means of calculating the path transmittance required for each of the scattering points. In order to maintain compatibility

with the spherical shell atmosphere of LOWTRAN, the integral over the path of scattering sources is replaced by a layer-by-layer sum along the line-of-sight. For an optical path traversing N layers in an upward or downward direction this process gives

$$\bar{I}_{\nu}^{SCAT} = \bar{I}_{\nu}^{SUN} \sum_{j=1}^{N} \left[\left\langle \frac{\bar{T}_{e,\,ps+op}^{A+M}\; p_j^{A}}{T_{s,\,op}^{A}} \right\rangle_j \Delta T_{s,\,op,\,j}^{A} + \left\langle \frac{\bar{T}_{e,\,ps+op}^{A+M}\; p_j^{M}}{T_{s,\,op}^{M}} \right\rangle_j \Delta T_{s,\,op,\,j}^{M} \right] . \qquad (3.9)$$

The quantity ΔT_j is the change in molecular or aerosol scattering transmittance in passing through layer j and $\langle\ \rangle_j$ denotes an average value for that layer. The terms ΔT_j, $\bar{T}_{ps+op}$, and T_{op}^{X} are quantities available within LOWTRAN.

The layer-by-layer sum for the singly scattered solar or lunar intensity is computed simultaneously with the existing direct thermal radiance. The sum is evaluated starting with the point of lowest altitude along the line-of-sight and proceeding up through successive layers. Long paths which pass through a tangent or minimum height are handled with a special set of transmittances in the same way, again following the radiance calculation already in LOWTRAN. Equivalent absorber amounts are computed separately for the two path legs (primary solar and line-of-sight) corresponding to each scattering point by a modified geometry program which is described in the next section.

3.2 Single Scattering Geometry

The existing LOWTRAN geometry tracks a single optical line-of-sight from

an observer at altitude H1 to the path endpoint at H2, which can be above or below the observer. The path can be a short path directed up or down or a long slant path which passes through a minimum altitude point HMIN, lower than both H1 and H2. The optical path will generally be curved by refractive bending since the atmospheric index of refraction has a finite vertical gradient. Although curved, the optical path remains in the fixed vertical plane containing the two path endpoints and passing through the earth's center. The refracted optical path can be described in a spherical coordinate system in terms of two path variables, usually the altitude and local zenith angle. The azimuthal orientation of this vertical plane, which contains the line-of-sight, must be separately specified or found in each case.

The new single-scattering geometry involves tracking two optical paths for each scattering source point. One path leg leads from the observer at H1 to a scattering point at H1' along the line-of-sight. The other leg is traced from the scattering point toward the sun/moon and ends in space at H2' (presently taken to be 100 km). Note that each scattering source point defines two path legs and, therefore, two vertical planes, like the one described above (the new one contains the scattering point and the point where the sun's rays enter the atmosphere). With rather minor modifications to the existing geometry algorithm, LOWTRANSX tracks the altitude and zenith angle of both path legs for each scattering point. In addition, the path equivalent absorber amounts needed for transmittance, thermal radiance, and scattered radiance calculations are simultaneously summed by the same routines.

Aside from the in-plane tracking of each path leg, it is necessary to determine the angle of intersection of the two vertical planes, which is also the azimuthal angle separating the projections of the two path legs onto

the earth's surface. The projection of a path segment onto the earth forms part of a great circle on the earth, since a vertical plane always includes the earth center. The projected path segments for a typical geometrical configuration are shown in Figure 3.2 from a perspective above the earth's surface looking down. The relative azimuth angle ψ_r between the projected path legs at the projected scattering point is calculated in LOWTRANSX by a new set of geometry subroutines. The method of calculation involves first computing the absolute azimuth angle for the observer-to-subsolar-point projection OS. The absolute line-of-sight azimuth $\psi_{a,\,op}$ is required as an input to the code, where absolute azimuth angles are measured from the local east direction with positive angles indicating north-of-east in this discussion. The user should note that azimuths in the code input card deck are specified in the clockwise sense from north, that is, positive east-of-north. A conversion from one convention to the other occurs within the code. The relative azimuth angle at the observer $\psi_{r,\,0}$ is calculated next. A transformation which reparameterizes the optical path is then made to facilitate the calculation of relative azimuth angles ψ_r at each scattering point. This angle allows precise calculation of the scattering angle at each point.

The subsolar point and the projected observer position together define the great circle $\theta(\phi)$ which satisfies the condition

$$\tan \theta = A \cos \phi + B \sin \phi \ , \tag{3.10}$$

where θ and ϕ are the standard latitude and longitude angles shown in Figure 3.3 and A and B are constants to be found The case where the subsolar point and observer lie on the same longitude, $\tan \phi_s = \tan \phi_o$, is treated

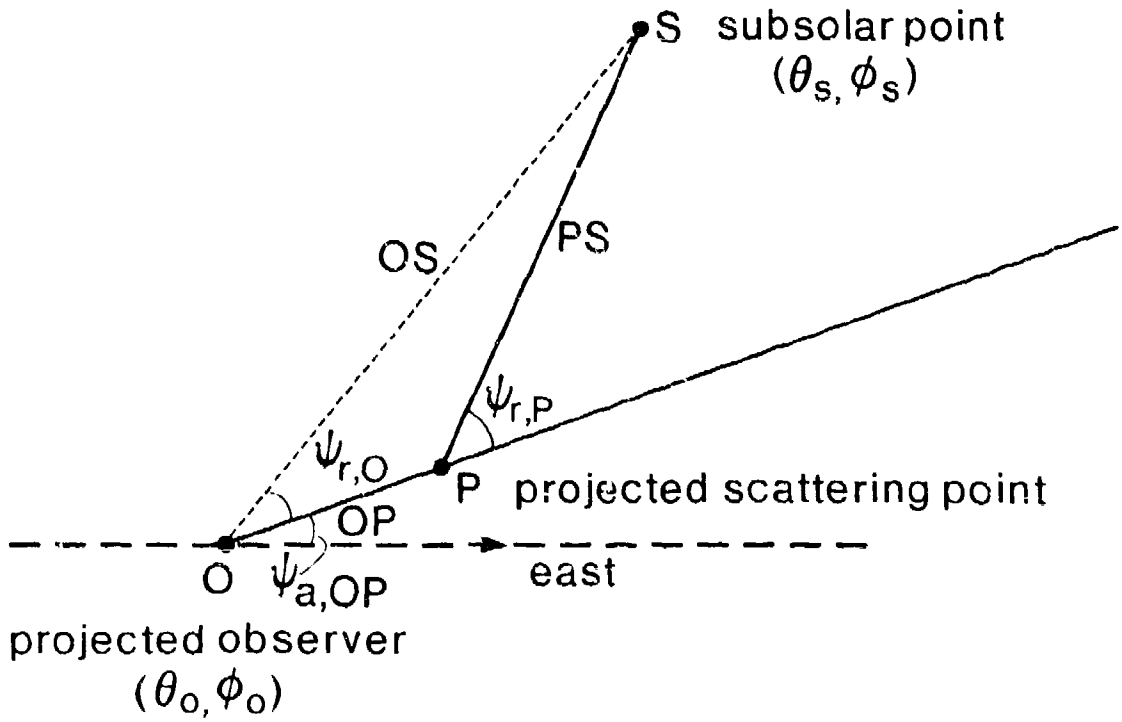

Figure 3.2 Looking down on the scattering path. All points are projected on the earth and all line segments are parts of great circles. The relative azimuth can be seen to vary as one moves the scattering point along OP.

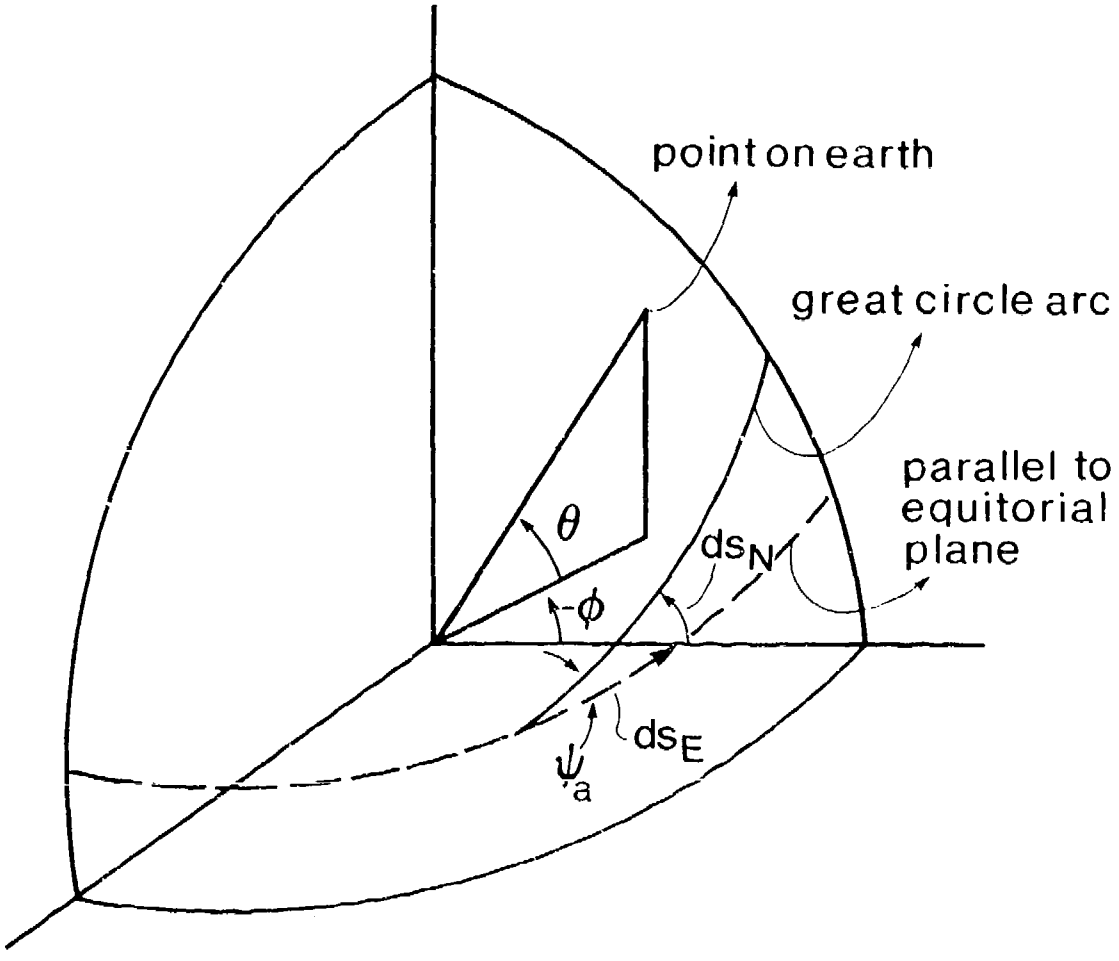

Figure 3.3 Latitude and longitude angles, where ϕ=0 passes through the Greenwich time base.

separately since ϕ is fixed in this case and θ (ϕ) is indeterminate. Except for this special case, A and B are determined for the particular great circle passing through these two points by using the angular surface locations of the subsolar (θ_s, ϕ_s) and observer (θ_o, ϕ_o) points to obtain

$$A = \frac{\tan\theta_s \sin\phi_o - \tan\theta_o \sin\phi_s}{\cos\phi_s \sin\phi_o - \cos\phi_o \sin\phi_s} \tag{3.11}$$

and

$$B = \frac{\tan\theta_o \cos\phi_s - \tan\theta_s \cos\phi_o}{\cos\phi_s \sin\phi_o - \cos\phi_o \sin\phi_s} \quad . \tag{3.12}$$

The absolute azimuth angle $\psi_{a,\,os}$ for the plane containing the great circle segment OS can be written as

$$\tan\psi_{a,\,os} = \frac{ds_N}{ds_E} = \frac{-1}{\cos\theta} \frac{d\theta}{d\phi} \quad , \tag{3.13}$$

where $d\theta/d\phi$ along this path is given by

$$\frac{d\theta}{d\phi} = \frac{B\cos\phi - A\sin\phi}{[1 + \tan^2\theta]} \quad . \tag{3.14}$$

The relations given in (3.13) can be derived from considerations based on Figure 3.3. Using the observer point location, the equations above are combined to obtain

$$\tan\psi_{a,os} = \frac{A \sin\phi_o - B \cos\phi_o}{[1 + \tan^2\theta_o] \cos\theta_o}$$

$$= \frac{\tan\theta_o \cos[\phi_s - \phi_o] - \tan\theta_s}{[1 + \tan^2\theta_o] \cos\theta_o \sin[\phi_s - \phi_o]} \qquad (3.15)$$

The relative azimuth between the line-of-sight OP plane and the OS plane is then given by

$$\psi_{r,o} = \psi_{a,os} - \psi_{a,op} \quad . \qquad (3.16)$$

Another useful angle to calculate is the angle Λ_o subtended at the earth center by radial lines from the sun and the observer. Using a dot product between position vectors on the unit sphere, it can be shown that

$$\cos\Lambda_o = \cos\theta_s \cos\phi_s \cos\theta_o \cos\phi_o +$$

$$+ \cos\theta_s \sin\phi_s \cos\theta_o \sin\phi_o +$$

$$+ \sin\theta_s \sin\theta_s$$

$$= \cos\theta_s \cos\theta_o \cos[\phi_s - \phi_o] + \sin\theta_s \sin\theta_o \quad . \qquad (3.17)$$

The two angles $\psi_{r,o}$ and Λ_o together with the multi-path altitude and zenith information specify the three dimensional single scattering geometry completely for any scattering source point. However, the angle $\psi_{r,p}$ between the PS and OP planes is yet to be obtained.

It proves convenient to make a coordinate transformation so that the line-of-sight optical path is more easily parameterized. In the original configuration, the longitude and latitude of each scattering point are not known and cumbersome to calculate. The transformation used moves the subsolar point and observer location on the sphere so that the line-of-sight runs east from an observer on the equator at ($\theta_o' = 0$, $\phi_o' = 0$). The angles ψ_o (short notation for $\psi_{r,o}$) and Λ_o are left invariant by the transformation so that the relative position of the sun in the sky is the same for the observer. No physical changes or approximations are introduced through this transformation. As one can see from Figure 3.4 by using (3.14) and (3.17) for the new coordinates, this transforation must satisfy the following equations for θ_s' and Δ_o:

$$\tan \theta_s' = \tan \psi_o \sin \phi_s' \tag{3.18}$$

and

$$\cos \Delta_o = \cos \theta_s' \cos \phi_s' \quad . \tag{3.19}$$

These conditions, when inverted, pinpoint the latitude θ_s' and longitude ϕ_s' of the new subsolar point in terms of the fixed angles ψ_o and Δ_o: that is

$$\tan \phi_s' = - \tan \Lambda_o \cos \psi_o \tag{3.20}$$

and

$$\sin \theta_s' = \sin \Lambda_o \sin \psi_o \quad . \tag{3.21}$$

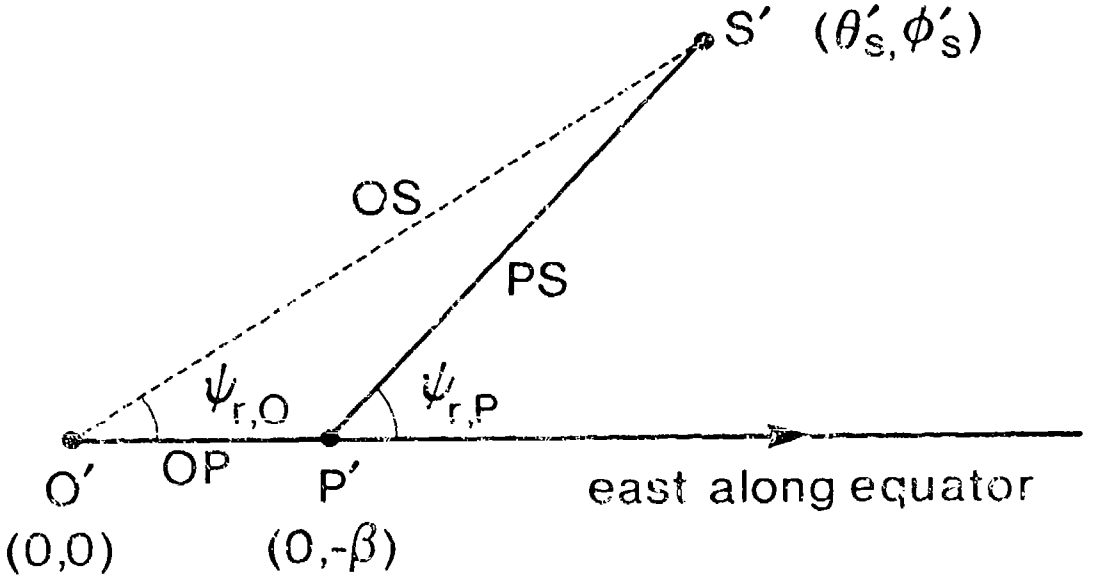

Figure 3.4 Looking down on the transformed scattering geometry. The line-of-sight lies on the equator. The sub-solar point at $(\theta_s' - \phi_s')$ has the same relative position as in Fig. 3.2.

A line-of-sight scattering point P now has the new latitude and longitude coordinates ($\theta'_p = 0$, $\phi'_p = -\beta$), where β is the angle subtended at earth center by radial lines to P and the observer O.

It is now possible to compute the relative azimuth angle between two path legs, that is, between the vertical plane containing PS and the vertical plane containing QP. The azimuth angle at $(0, -\beta)$ for the primary solar path connecting $(0, -\beta)$ and (θ'_s, ϕ'_s) is given by

$$\tan [\psi_p (\beta)] = \frac{\sin\Delta_o \sin\psi_o}{\cos\beta \sin\Delta_o \cos\psi_o - \sin\beta \cos\Delta_o} \quad . \tag{3.22}$$

It is also necessary to calculate the angle $\Delta(\beta)$ subtended at the earth center by radial lines to the sun and the scattering point $(0, -\beta)$. This is given by

$$\cos [\Lambda(\beta)] = \cos\Delta_o \cos\beta - \sin\beta \sin\Delta_o \cos\psi_o \quad , \tag{3.23}$$

where in the absence of refractive bending $\Delta(\beta)$ would be the zenith angle of the sun as viewed from the scattering point. In the presence of refraction $\Lambda(\beta)$ can be used as an initial guess for the actual zenith angle, and the primary solar path can be tracked iteratively to correct for refraction and obtain the correct zenith angle. The scattering point altitude $H1'(\beta)$ and approximate zenith angle $\Lambda(\beta)$ are used to specify the starting point of the primary solar path leg from P to space.

The set of angles which are discussed above is sufficient to track both legs of each L-shaped single scattering path. One additional angle, the included angle for single scattering $\gamma(\beta)$ is needed for the phase function in

the scattering source term. That angle is given by

$$\cos \gamma = \hat{n}_{ps} \cdot \hat{n}_{op} \quad , \tag{3.24}$$

where each path direction vector refers to the local direction at the scattering point. In terms of the two local zenith angles α_{ps} and α_{op} at the scattering point and the relative azimuth between vertical planes ψ_p (β), the included angle becomes

$$\cos [\gamma (\beta)] = \sin\alpha_{ps} \sin\alpha_{op} \cos [\psi_p (\beta)] +$$

$$+ \cos\alpha_{ps} \cos\alpha_{op} \quad . \tag{3.25}$$

The scattering angle γ and the cumulative absorber and scattering amounts are computed for each scattering point which contributes to the intensity in the sum given by [3.9]. LOWTRANSX specifically uses as scattering source points the intersections of the line-of-sight with the model atmosphere layer boundaries. Equation (3.9) leads to the following expression for the scattered radiance as it is computed in LOWTRANSX using this set of n single scattering source points.

$$\bar{I}_\nu^{SCAT} = \bar{I}_\nu^{SUN} \sum_{i=1}^{n-1} \sum_{X = (A, M)} \left[T^X_{s,\, op,\, i} - T^X_{s,\, op,\, i+1} \right]$$

$$\frac{1}{2} \left[\frac{\bar{T}^{A+M}_{e,\, ps+op,\, i}\, P^X_i}{T^X_{s,\, op,\, i}} + \frac{\bar{T}^{A+M}_{e,\, ps+op,\, i+1}\, P^X_{i+1}}{T^X_{s,\, op,\, i+1}} \right] . \tag{3.26}$$

The layer average $< >_j$ has been evaluated using the properties of only the two scattering points which bound each layer path segment. The sum is taken over scattering points labelled by i and this result applies to long slant paths as well as upward and downward trajectories. The observer position here coincides with i = 1 and the line-of-sight end point is i = n.

3.3 LOWTRANSX Verification

Verification of this newly developed single-scattering code was done in several stages. On the most basic level, the individual subroutines described in Appendix B were driven artificially during the developemental phase, hand calculations and common sense were used to evaluate intermediate results, and overall trends for various inputs were checked. Once the routines were performing correctly, they were linked with each other and LOWTRAN to form the complete program. Because of the code's overall complexity, verification becomes a difficult task. Simple cases involving two or three scattering layers were approximated by hand calculations. This was done for a number of configurations, and agreement was found in all cases. Unfortunately as the number of scattering layers increases the number of calculations and the possibility of human error increases to the point that this approach become impractical. There are, however, two special cases that cover the entire atmosphere (32 scattering layers) that reduce analytically to easy solutions. These occur when the optical-solar path configurations are such that all scattering path lengths, absorber amounts, and transmittances are equal. This happens when the observer (on the ground in both cases) is looking directly at the sun and when the observer is looking away from the sun (ψ = 180°) with a zenith angle of 45° and the solar

zenith at 45°. Examination of an expanded version of the standard output file for these cases confirmed that the scattering path lengths, absorber amounts, and L-path transmittances were the same. The total scattered radiance reaching the observer was also equal to that given by hand calculations in each case. While this certainly illustrates the internal consistency of the code and supports the verfication process, it does not establish the validity of the code in all modes of operation.

Further verification involving the entire atmosphere was made through comparisons with other single scattering codes. The unique band transmission functions and aerosol models found in LOWTRAN restricted such comparisons to other codes having similar data bases. Only one code called SPOT [Ref. 8] was found to have the necessary characteristics. It was developed by RRA of Fort Worth, Texas and used LOWTRAN 4 [Ref. 10] for its basic radiative transfer. Spot is a plane-parallel, single scattering code that calls LOWTRAN as a black box to find individual path transmittances. The L-path transmittances that arise in the calculation procedure are approximated as the product of the transmittances for each leg. This is incorrect since the LOWTRAN transmission functions do not obey Beer's law. The aerosol models and phase functions also differ from those found in LOWTRANSX. Since the SPOT code was no longer available on the AFGL computer system, comparisons were limited to existing output. One such comparison is illustrated in Figures 3.5 and 3.6. Figure 3.5 shows the single scattering radiance and emission at predicted by LOWTRANSX for an observer at 50 Km looking down at a zenith of 170°. The solar zenith angle is 60°, the relative azimuth angle is 10°, and a U.S. standard atmosphere with a rural aerosol model is used. Figure 3.6 shows the single scattering radiance and emission for a similar run of the SPOT code, i.e observer at 50 Km looking at 170° with a solar zenith

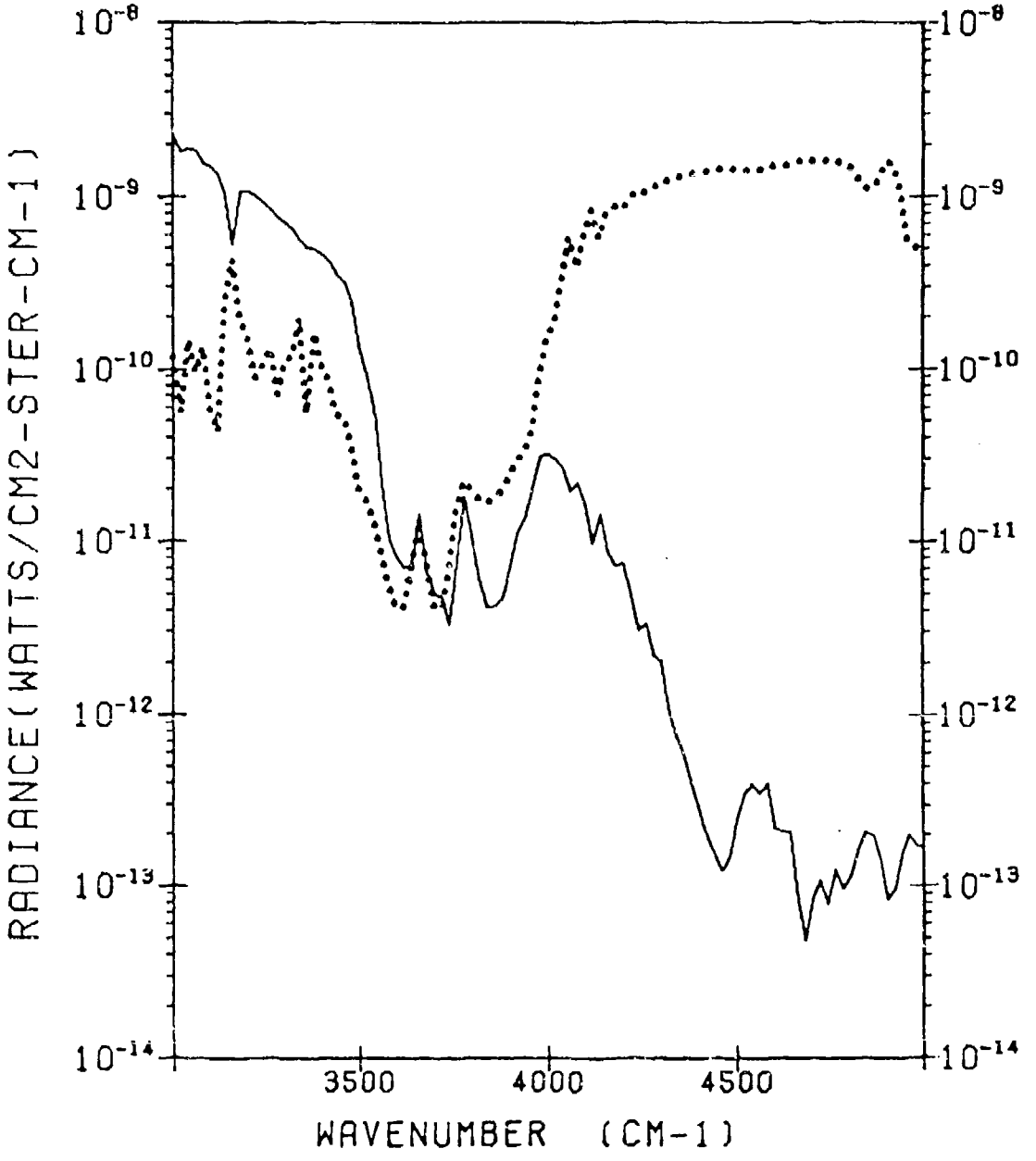

Figure 3.5 LOWTRANSX thermal emission — and single scattered radiance ... for 1962 standard atmosphere with default aerosol models at 50 Km looking down with $\mu = 10°$ and $\mu_o = 60°$.

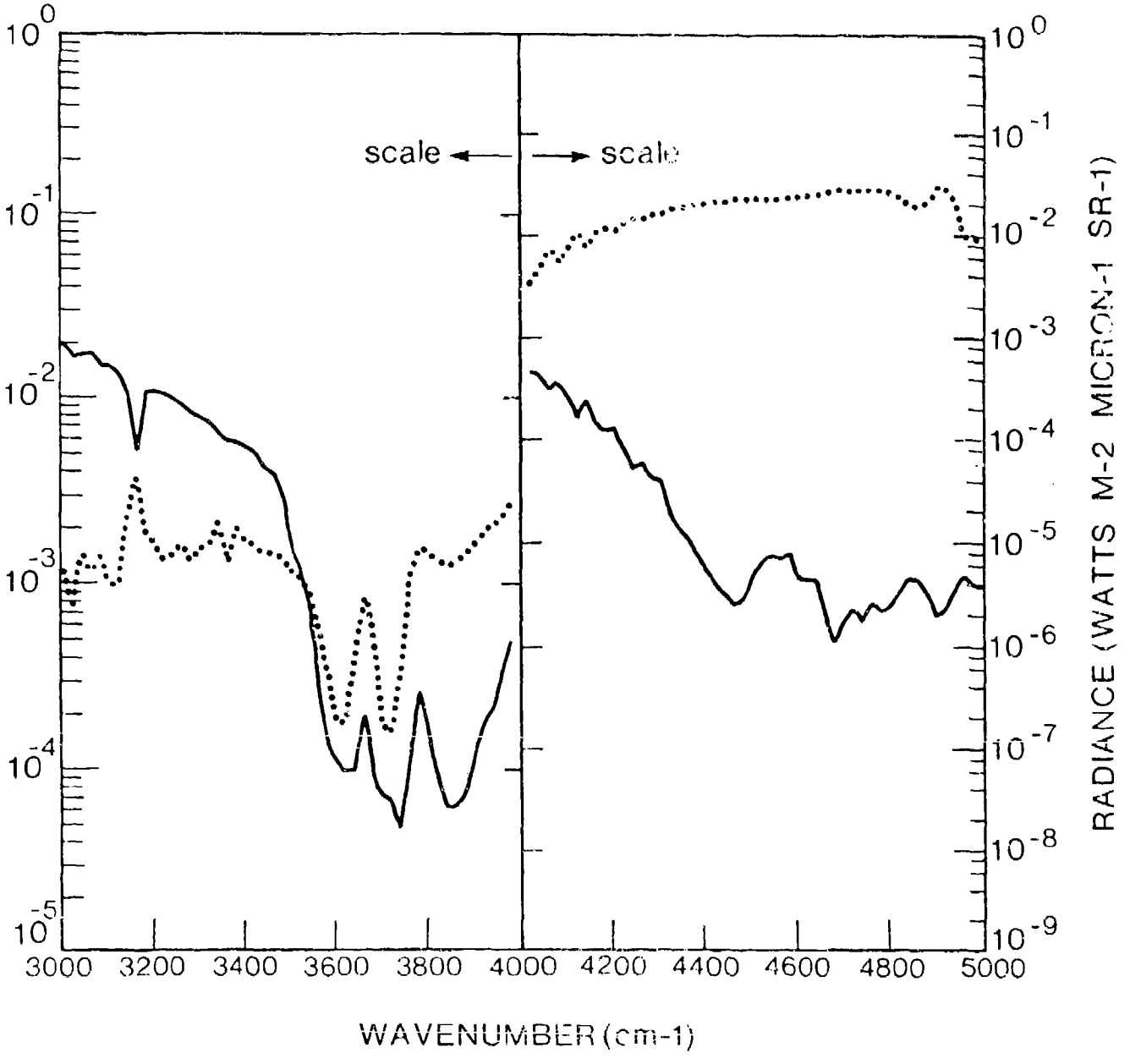

Figure 3.6 Plane-parallel, single scattering SPOT code at conditions equivalent to those in Fig. 3.5.

of 60°. The exact atmospheric and aerosol models for SPOT are not known, but they are similar. Take note that the vertical axes on these two figures have different units and the horizontal axes are scaled differently. Although comparison of these two figures indicates some slight differences in magnitude, they are well within the uncertainty of the atmosphere used in SPOT. Note that the spectral details in the single scattering and emission curves occur at identical wavenumbers in these two figures. While this is not a good comparison for checking details, it does serve to justify that the new algoritam is executing correctly.

A final verification of LOWTRANSX was made by using another single-scattering code developed under this contract and described in Chapter 4. Briefly, the code is based on a plane-parallel, monochromatic, multiple scattering code that requires optical depths, albedoes and phase functions for each layer. Since the LOWTRAN gaseous transmission functions do not obey Beer's law, the molecular band transmittances were "turned off" for this comparison. This was accomplished by setting the gaseous transmittances equal to one in the LOWTRANSX code. Statements were added to calculate and write total optical depths and albedoes based on the remaining attenuation mechanisms. This data was then used in the simple, plane-parallel single scattering code. Multiple runs of LOWTRANSX were made for comparison. Some of these results are presented in Table 3.1. The remainder of the results will be presented and discussed in Section 4 (Tables 4.9 and 4.10) where multiple scattering effects are examined. The numbers shown are the ratio of the single scattering radiance predicted by LOWTRANSX to that predicted by the single-scattering code for paths that are not effected by spherical geometry and refraction. The ratios are in good overall agreement and demonstrate that the LOWTRANSX code functions properly for these conditions. A discussion

Table 3.1 Ratio of LOWTRANSX To Single Scattering Plane-Parallel for Standard 1962 Atmosphere at 11 μm

Top (100 Km) ↑ g	0.0	0.8	azimuthal angle relative to the su
	1.0022	1.0023	0°
		1.0024	90°
		1.0020	180°

(a)

2 Km g	0.0	0.8	"
	1.0015 ↑	1.0014	0°
	1.000 ↓	1.000	
		↑ 1.0014	90°
		↓ .9962	
		↑ 1.0015	180°
		↓ .9907	

(b)

Bottom ↓ g	0.0	0.8	"
	1.0003	1.000	0°
		.9957	90°
		.9908	180°

(c)

All Zenith angles are 12.95°

↑ Radiation propagation

g = asymmetry factor

τ ≅ 0.183

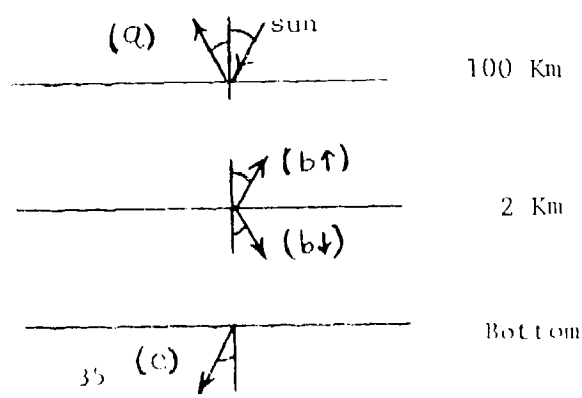

of the effects of spherical geometry and refraction, which are not included in the plane-parallel, single-scattering code, is presented in Chapter 4.

The versatility of the LOWTRANSX code leads to further verification problems. Various input combinations, path types, and unique geometric situations make the list of possible test cases exceedingly large. Briefly, the following situations are possible and have been addressed in the development of the code:

1. Optical path - up or down, short or long (through a tangent height)
2. Specification of the observer-solar orientation
   (a) θ_o, ϕ_o, θ_s, ϕ_s
   (b) θ_o, ϕ_o, time, day
   (c) α_s, ψ_s at observer
3. Unique Geometries
   (a) Arbitrary azimuth
   (b) Observer at pole (north or south)
   (c) Partially shaded path (end or center)
   (d) Long sun paths

The verification problem has been made more difficult by the parallel development of LOWTRAN6 at AFGL that required the continuous integration of the single-scattering algorithm. In some cases this involved only straightforward replacement of code, while others involved changes in coding logic, which opens the possibility for the introduction of errors.

Every attempt has been made to verify the code at each stage of development. All the situations listed above have been verified individually. Errors arising as a result of a rare combination of parameters occuring simultaneously

are unlikely, but still possible. The user should keep this in mind.

3.4 Concluding Remarks

The code constructed here (also see Appendices) using a recent LOWTRAN version and called LOWTRANSX is the one delivered to AFGL. The staff at AFGL is in the process of developing a LOWTRAN version (LOWTRAN6) that will contain the present single scattering model along with other modifications. Consequently, LOWTRANSX will not be available to the user in the form described here, although its capability will be. The reader should direct any inquiries concerning LOWTRANSX to the staff at AFGL.

4. MULTIPLE SCATTERING

The previous section discussed the procedure necessary to include the single scattering approximation in a LOWTRAN code [Ref. 1]. The spherical geometry and non-monochromatic (spectrally averaged) transmission functions found in LOWTRAN made single scattering difficult compared to the monochromatic, plane-parallel approach. These difficulties become insurmountable when multiple scattering is considered. At this time there is no multiple scattering formulation that can accept spherical geometry and LOWTRAN'S transmission functions. Monte Carlo codes are available [Refs.16 through 18] that calculate monochromatic multiple scattering in spherical atmospheres. Such codes have a reputation for being computationally slow (expensive). Several monochromatic multiple scattering formulations and highly developed codes are available for the plane-parallel geometry that are computationally fast [Refs. 19 and 20]. Unfortunately plane-parallel codes predict intensity fields that are totally wrong for low sun angles and long, horizontal observation paths.

To overcome the present impass, multiple scattering calculations must be developed that will accept spectrally averaged radiative properties (and therefore, spectrally averaged direct transmission functions) such that numerous monochromatic executions do not have to be made over the highly structured spectral domain caused by gaseous absorption and emission. The subject of how to deal with the spectral aspects of radiative transfer has always been an area of research in the field. Perhaps the most obvious and consequently the most common solution to this problem is to average or model the medium's spectral properties before the radiative transfer calculations are performed. This approach certainly has been useful, but has certain

unavoidable limitations. It is rare that one can determine (without approximations) how modeled or lumped photons are transported through the medium. That is, what is the governing equation? Consequently the errors involved are often unknown and uncontroilable. Furthermore, such calculations are limited to predicting spectrally averaged dependent variables, e.g., the intensity. In summary this approach lacks generality. The other approach to this spectral problem, and the one under research in this section, exploits the concept that monochromatic radiative transfer calculations over a highly structured spectral region are redundant. Therefore, only a relative few monochromatic calculations are necessary to represent the radiative transfer at all points in the spectral region. The research on this approach is neither as prodigious nor coherent as for the first approach and is associated with studies of the absorption or opacity distribution function, in homogeneous atmospheres in most cases. The work on exponential-sum fitting of the direct transmission function is also relatable to this latter approach.

To investigate spectral redundancy, a monochromatic multiple scattering code is required. Section 4.1 documents such a code [Refs. 5 through 7 and 20] for general plane-parallel media that is computationally fast. To check this code in a simple limit and to compare with LOWTRANSX, a plane-parallel, single-scattering code is described in section 4.2 that is compatible with the parametric inputs to the multiple-scattering code. Section 4.3 presents single versus multiple scattering results for a range of parameters to show when and by how much multiple scattering is important. The basic study of spectral redundancy or spectral degrading (averaging) in multiple scattering calculations is developed in section 4.4 along with some initial

results. Finally, section 4.5 is a discussion of further work that must be done to allow multiple scattering to be incorporated into codes like LOWTRAN and FASCODE.

4.1 Adding/Doubling, Multiple-Scattering Code

This multiple-scattering code was originally developed to handle internal, isotropic radiative sources (thermal radiation) for completely general media and boundary surfaces. Until now, Adding/Doubling (A/D) was used mostly for problems driven only by external, unidirectional (sun) sources. The formulation supporting the code is available in the open literature [Refs. 5 through 7] and the resulting code well documented in a Ph.D. thesis [Refs. 20]. The reader is assumed to be familiar with these references because only a brief discussion of the changes made will be presented here.

Because the present A/D code is general, well documented, and can handle thermal sources, all of which are of general interest to AFGL, it makes sense to modify the code to accept unidirectional, external illumination. This requires performing a Fourier decomposition (already inherent in the original development) of the radiative transfer process. That is, each monochromatic run is done for each Fourier component and the results are then recombined (inverse Fourier Tranform) to obtain the intensity fields. Note that each run contains all possible sun and observer angles. To retain as much computational speed as possible, a Fast Fourier Transform (FFT) code was used.

A natural starting point in an A/D computation is to find the Fourier coefficients P_n in the cosine Fourier expansion of the phase function P in the form (note that this report uses both t and τ for the optical depth)

$$P = \sum_{j=0}^{J} P_j(t, \mu, \mu') \cos j(\phi - \phi'), \qquad (4.1)$$

where P is normalized as

$$\int_{4\pi} P \, d\Omega' = 4\pi \quad . \tag{4.2}$$

Here θ ($\mu = \cos\theta$) and ϕ are the zenith and azimuthal angles, respectively, and $d\Omega'$ is the differential solid angle. Each P_j forms an n x n array or matrix, where n is the number of gaussian quadrature points used in the system (normally seven in the basic code). The P_j's each produce their own Fourier component for the dependent scattering functions which can be summed to obtain the final desired quantity. Note that if the radiative flux is wanted, the zeroth Fourier component is the only one required.

The P_j's in Eq. (4.1) are found by the FFT routine described in Appendix F. Due to the details of how FFT codes work, Fourier analysis (forward) and Fourier synthesis (inverse) must be done by compatible routines. As discussed in Appendix F, the externally driven A/D code is made up of three parts. The first part finds the Fourier coefficients for the given phase function and passes the results to the radiative transfer part. After each Fourier component has been processed through the radiative transfer code, these results are passed back to an FFT code for synthesis to obtain the radiative fields throughout the medium. The FFT code is rather straightforward, but the changes made to the existing A/D code will now be described.

The A/D code calculates several sets of diffuse scattering functions that represent intensity fields for Green's function type problems of different complexity. The functions of interest here are symbolized as $S_F^{j\pm}$ and $T_F^{j\pm}$ that represent how an internal fundamental source is diffusely transmitted to the boundaries. Through reciprocity, these functions are directly related

to the $\bar{S}_s^{\pm}$ and $\bar{T}_s^{\pm}$ functions that relate external sources to internal responses, the problem that is being solved. These functions of the two variables μ_o (illumination) and μ (response) appear as n x n matrices. Reciprocity [Ref. 21] says that

$$\tilde{T}_F \underline{j}^{\pm} = \bar{T}_s \underline{j}^{\mp}$$

$$\tilde{S}_F \underline{j}^{\pm} = \bar{T}_s \underline{j}^{\pm} \quad , \tag{4.3}$$

where ~ over a matrix means transpose. For a plane parallel medium with no boundary surfaces, the dimensionless (divided by driving intensity) diffuse radiative intensity I at any optical depth t is given by

$$I_D^{+}(t, \mu, \phi) = \frac{1}{4\pi\mu} \tilde{S}_F^{-}(\mu, \phi, t; \mu_o, \phi_o) \tag{4.4}$$

and

$$I_D^{-}(t, \mu, \phi) = \frac{1}{4\pi\mu} \tilde{T}_F^{+}(\mu, \phi, t; \mu_o, \phi_o), \tag{4.5}$$

where the $\tilde{S}_F^{-}$ and $\tilde{T}_F^{+}$ are Fourier synthesized from $\tilde{S}_F \underline{j}^{-}$ and $\tilde{T}_F \underline{j}^{+}$. The superscripts + and - on intensities denotes propagation up and down, respectively. The same superscripts on the scattering functions have a different meaning that need not be discussed here [see Refs. 5 and 20]. The angles μ and ϕ are those for the observer while subscript zero on these denote angles for the illumination.

Appendix E contains the original user's manual for the A/D code that was developed in Ref. 20. This plus a copy of Sharma's thesis [Ref. 20] will enable one to understand the basic A/D code. The surface scattering (or reflection), thermal sources, and heat transfer options in this code are turned off in the modified version by setting logical parameters. They could be

reactivated with some modification of control and input functions of the present code.

4.2 A Plane-Parallel Single Scattering Code

A simple plane-parallel, monochromatic, single scattering computer code is described in this section. This code is used to study the following items: (1) The Adding/Doubling multiple scattering code becomes single scattering in the limit of sufficiently small single scattering albedoes and can therefore be checked against the present independent and simple code. (2) Within the limitations imposed by the plane-parallel geometry, one can compare multiple and single scattering results to find the accuracy of the single scattering assumption for various parametric values. (3) LOWTRANSX can be verified by comparisons with the present simple code for appropriately chosen spectral regions (having no significant line structure) and geometric configurations (with vertical-like solar and observation paths). (4) By using other path configurations, the same comparison will show the effects of the spherical geometry on single scattering intensities.

The nomenclature used here, which is the same as that used in the adding/doubling code, is shown in Figure 4.1. In this context the radiative transfer equation is

$$\mu \frac{dI(\vartheta, \phi)}{d\tau} = 1 - J(0, \phi) \quad , \tag{4.6}$$

where 0 and ϕ are the zenith and azimuth angles respectively. The monochromatic intensity is given by I, the direction cosine is $\mu = \cos 0$, and the vertical optical depth parameter, as measured from the top surface and based on the extinction coefficient, is τ. Scattering sources are represented by

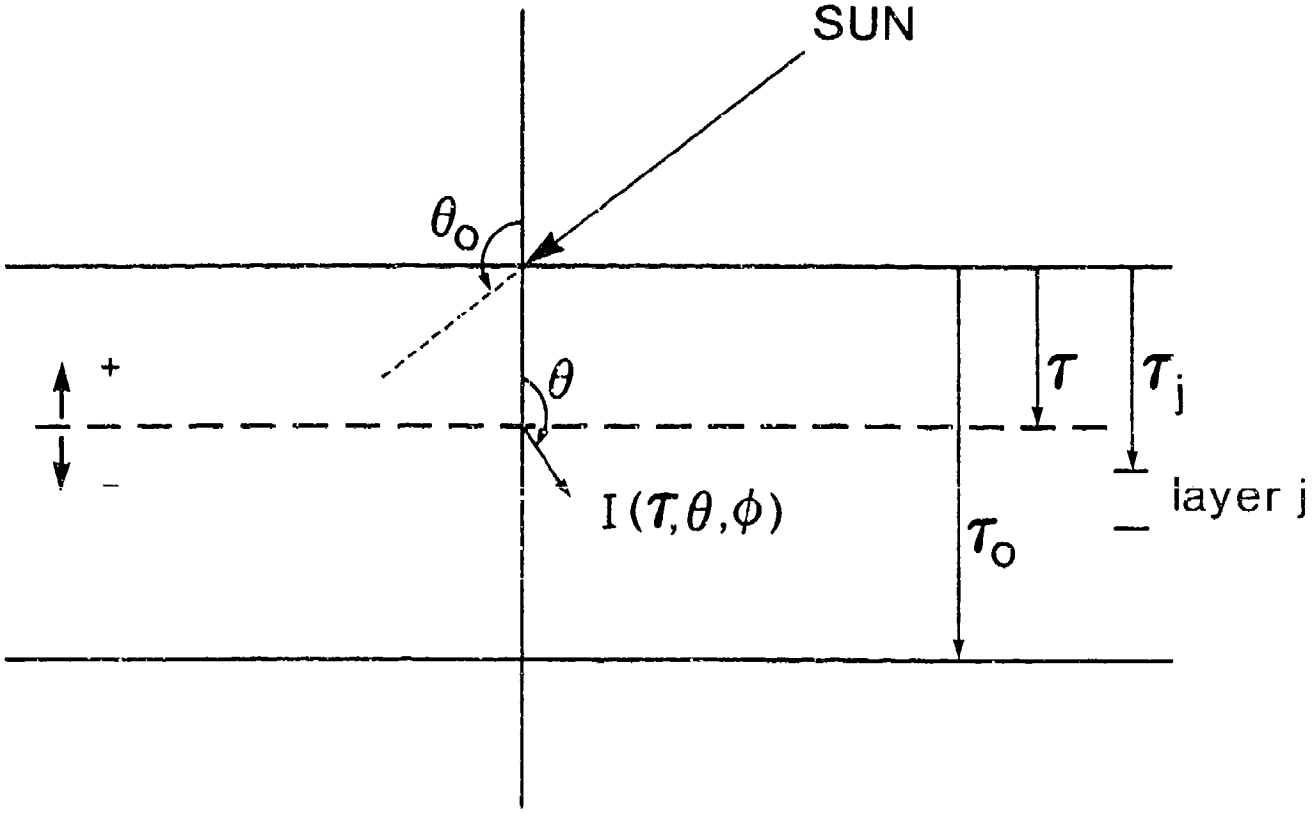

Figure 4.1 Plane-parallel geometry and nomenclature

the source function J defined by

$$J(0, \phi) = \frac{\omega}{4\pi} \int I(\theta', \phi')\ P(0, \theta', \phi - \phi')\ d\Omega' \ , \tag{4.7}$$

where ω is the single scattering albedo and Ω' measures solid angle. The phase function P is normalized according to

$$\int P(\theta, \theta', \phi - \phi')\ d\Omega' = 4\pi \tag{4.8}$$

To solve (4.6) for the solar driven problem, it is customary to break up the radiative intensity into direct and diffuse parts. With the direct solar intensity at any point τ given by (I_o^{SUN} being the solar intensity at the top of the atmosphere)

$$I^{SUN} = I_o^{SUN}\ e^{-\tau/\mu_o}\ \delta(\mu-\mu_o, \phi - \phi_o) \ , \tag{4.9}$$

the source function becomes

$$J(\theta, \phi) = \frac{\omega}{4\pi}\int I(\theta', \phi')\ P(\theta, \theta', \phi - \phi')\, d\Omega'$$

$$+ \frac{\omega}{4\pi}\ I_o^{SUN}\ e^{-\tau/\mu_o}\ P(\theta, \theta_o, \phi - \phi_o) \ . \tag{4.10}$$

where I now represents the diffuse radiative field (as obtained from (4.6) with boundary conditions of zero incident diffuse intensity) and δ is the Kroneker delta function. For single scattering, only the second term on the right hand side of (4.10) is retained in solving (4.6) and this gives

the downward (-) intensity

$$I^{-}(\tau, \theta, \theta_o, \phi - \phi_o) = \frac{1}{4\pi} \int_0^{\tau} \frac{\omega}{\mu} I_o^{SUN} P\, e^{-\tau'/\mu_o}\, e^{-(\tau - \tau')/\mu}\, d\tau' \tag{4.11}$$

and upward (+) intensity

$$I^{+}(\tau, \theta, \theta_o, \phi - \phi_o) = \frac{1}{4\pi} \int_{\tau}^{\tau_o} \frac{\omega}{\mu} I_o^{SUN} P\, e^{-\tau'/\mu_o}\, e^{-(\tau' - \tau)/\mu}\, d\tau', \tag{4.12}$$

where all values of μ and μ_o are now positive (angles measured from the normal in the appropriate hemisphere).

For inhomogeneous atmospheres, which are modelled with an atmosphere composed of N homogeneous layers, the above expressions can be integrated analytically. Let τ_j (j = 1, 2, ... N + 1) denote the optical depth from the top to any layer boundary ($\tau_1 = 0$) and ω_j and P_j the properties of the layer which lies below j. Equations (4.6) and (4.7) then take the form

$$\frac{I_j^{-}}{I_o^{SUN}} = \frac{1}{4\pi} \frac{\mu_o}{\mu - \mu_o} e^{-\tau_j/\mu} \sum_{i=1}^{j-1} \omega_i P_i \left[e^{-\tau_i \left(\frac{1}{\mu_o} - \frac{1}{\mu}\right)} - e^{\tau_{i+1} \left(\frac{1}{\mu_o} - \frac{1}{\mu}\right)} \right] \tag{4.13}$$

for $j > 1$ and

$$\frac{I_j^+}{I_o^{SUN}} = \frac{1}{4\pi} \frac{\mu_o}{\mu+\mu_o} e^{-\tau_j/\mu} \sum_{i=j}^{N} \omega_i P_i \left[e^{-\tau_i (\frac{1}{\mu} + \frac{1}{\mu_o})} - e^{-\tau_{i+1} (\frac{1}{\mu} + \frac{1}{\mu_o})} \right] \tag{4.14}$$

for $j < N + 1$.

One can get a somewhat more physical understanding of (4.13) and (4.14) by rearranging terms slightly. Let $P^{\pm}(\mu, \mu_o, \phi)$ denote backward scattering upward (+) and forward scattering downward (-) phase functions, that is for 0 less (+) or greater (-) than 90 degrees. Both the upward and downward intensities contain similar expressions for what might be called the single layer "discrete source" terms defined by

$$S_i^{\pm}(\mu, \mu_o, \phi) = \frac{\mu_o I_o^{SUN}}{\mu \pm \mu_o} \omega_i P_i^{\pm} e^{-\tau_i/\mu_o} \left[1 - \exp\left[-(\tau_{i+1} - \tau_i)(\frac{1}{\mu_o} \pm \frac{1}{\mu}) \right] \right] , \tag{4.15}$$

except for the forward scattering case $\mu = \mu_o$ where

$$S_i^{-}(\mu = \mu_o, \phi) = \frac{I_o^{SUN}}{\mu_o} e^{-\tau_i/\mu_o} P_i^{-} [\tau_{i+1} - \tau] . \tag{4.16}$$

Using these "discrete sources," the complete downward and upward intensities at level j are

$$I_j^{-}(\tau_j, \mu, \mu_o, \phi) = \sum_{i=1}^{j-1} S_i^{-}(\mu, \mu_o, \phi) e^{-(\tau_j - \tau_i)/\mu} \tag{4.17}$$

and

$$I_j^+(\tau_j, \mu, \mu_o, \phi) = \sum_{i=j}^{N} S_i^+(\mu, \mu_o, \phi) \; e^{-(\tau_i - \tau_j)/\mu} \qquad (4.18)$$

Physically, the sums include contributions from all of the scattering layers, which in the case of the downward intensity I_j^- includes all layers above level j, while all layers below j contribute to I_j^+. The upward single layer "discrete source" S_i^+ represents all of the singly scattered intensity at level i due to scattering in the layer immediately below it. Similarly,

$$S_i^- \; e^{-(\tau_{i+1} - \tau_i)/\mu}$$

represents the intensity at level i+1 due to scattering in the layer just above this level (the i'th layer).

The code takes the following steps in calculating the single scattering intensities at each observer level (layer boundary) for each set of angles:

(1) The upward and downward "discrete source" terms $S^{\pm}$ are first computed for the top layer, for all pairs of zenith quadrature points and a single azimuth angle.

(2) The contribution to the intensity at each level which comes from these terms is computed and added to the total intensity for that level.

(3) This process is repeated for each successive scattering layer, producing upward and downward intensities for all possible zenith angles at all levels.

(4) The entire calculation is repeated for each new azimuth angle if the scattering is anisotropic.

This algorithm allows a completely different phase function to be specified for each layer. The phase function, expressed in terms of the quadrature zenith angles and azimuth, is computed from the phase function of the included angle of scattering by ADNGFFT. The Fourier transform is not required and is therefore bypassed within ADNGFFT in the case of single scattering (user sets INOFT=1). All other code input data are identical in content and format with that for Adding/Doubling code, and the reader is referred to Appendix F for these details.

4.3 Intercomparison of Radiative Transfer Results

Since LOWTRANSX only includes single-scattering, it is important to know how the error produced by this approximation varies parametrically, Unfortunately, multiple scattering results are not available for refracting and spherical atmospheres. To investigate this error question, a comparison is made between results for single and multiple scattering in homogeneous, plane-parallel atmospheres. Such information gives a good deal of insight for the same problems when the geometry is spherical. To further bridge the conceptual differences between these two situations, comparisons are made for single scattering results from LOWTRANSX (spherical and refracting atmospheres) and the plane parallel formulation of Section 4.2 for a realistic example atmosphere.

The first intercomparison to be discussed is that between plane-parallel single and multiple scattering. For simplicity only homogeneous* model atmospheres are used. The parameters involved, namely τ_o (optical depth), ω (single scattering albedo), g (phase function asymmetry factor), τ (position of observer), and $\phi-\phi_o$ (azimuthal angle between observer and sun), are quite numerous. The only parameter that is functionally well understood is ω, since order of scattering expansions go asymptotically in powers of ω

*Radiative parameters are constant throughout the atmosphere.

(everything else held fixed). The affect of the other parameters will be found numerically.

The first set of data is for isotropic scattering (g = 0) and consequently $\phi-\phi_o$ is no longer a parameter. The data is presented as a ratio of multiple scattering over single scattering intensities (ratio is always greater than one) in 7 x 7 arrays representing combinations of sun and observer zenith angles.* The optical depth and single scattering albedo are varied as well as the observer location. To understand these results one should note that the top layers in the atmosphere will have scattering source functions that are closer (than those in deeper layers) to those predicted by the single scattering approximation, and as the sun approaches grazing angles such single scattering type layers will be found only at the very top of the atmosphere. The overall view, therefore, is one of scattering source functions becoming more effected by multiple scattering as one goes from the top to the bottom of the atmosphere.

With the above discussion in hand, the data in Table 4.1 for τ_o = 1.0 and ω = 0.3 makes physical sense. At the top of the atmospere the intensity ratio for θ_o = 12.95° decreases from 1.21 to 1.13 as the observer angle varies from 12.95° to 88.54°. The improvement is caused by the fact that the scattering source function is more single scattering in the top most layers seen by the more grazing view angles. Still looking at up intensities, the ratio gets larger (more multiple scattering) as τ increases, again because these intensities see source functions deeper in the medium. In all cases, except for the top of the atmosphere, the ratios get larger (note that all ratios greater than 10^3 are printed as 10^3) as the sun angle goes towards grazing (read from left to right on the tables). The intensities out of the top are unique since the ratios become smaller as the sun angle

*See the last page of this section for a list of the angles used.

increases, for any observer angle. This must be caused by the fact that at grazing sun angles less flux is entering the atmosphere and, therefore, less backscattering flux from the larger τ's is available to cause multiple scattering effects in the top most portion of the atmosphere. The angle and τ effects discussed above also hold as other parameters are varied.

Table 4.2 is also for $\tau_o = 1.0$ (as is Table 4.1) but now $\omega = 0.6$. Since these intensity ratios vary from unity approximately linearly with the single scattering albedo (for $\omega < 1$), the multiple scattering effects are about doubled by going from Table 4.1 to Table 4.2. The effect of total optical depth is not as simple and can be seen by comparing Table 4.1 with Table 4.3, the latter table is for $\tau_o = 2.0$. This comparison keeps ω constant and doubles the optical depth. The ratios in Table 4.3 are all larger than those of Table 4.1 and this becomes much more pronounced as both sun and observer angles increase. Note again the rather unique properties of the intensities exiting the top. Comparing 4.2 with 4.4, where τ_o goes from 1.0 to 0.5 while ω remains constant at 0.6, shows that for the smaller view and sun angles the multiple scattering effect is almost linear in τ_o and would become more so as τ_o decreases further. However, this is not true for the larger view and sun angles of 82° and 88°.

The influence of changing the asymmetry parameter is shown in Tables 4.5 through 4.8 where the cases of Tables 4.1 through 4.4 are repeated for $g = 0.8$ (forward scattering peak). The results are now given for $\phi-\phi_o$ of 0°, 90°, and 180°. The most important overall effect is that the corresponding ratios are now larger for forward scattering and, therefore, multiple scattering is stronger. However, this is not true for intensities that view or depend mostly on only the top of the medium. These portions now become closer to the single scattering results because the forward scattering reduces the

backscattering that leads to less diffuse flux up into the top of the medium to cause multiple scattering effects. The multiple scattering effects are slightly larger (larger ratios) for out of plane ($\phi-\phi_o$ of 90° and 180°) viewing than when $\phi-\phi_o$ is 0. Also note that the linearity in ω observed previously for g = 0 does not hold as well in the present cases for g = 0.8. However, theory says that as ω goes to zero this linear effect must again hold.

To use the plane-parallel multiple over single scattering ratios discussed above to evaluate the accuracy of the single scattering approximation in LOWTRANSX, the influence of spherical geometry and refraction must be understood. To accomplish this a comparison has been made between LOWTRANSX and compariable plane-parallel, single-scattering results. LOWTRANSX was executed for a vertical path with all gaseous band transmittances set equal to one. It then returned the layer-by-layer absorption and scattering coefficients for the remaining mechanisms. This data was then used in the single-scattering, plane-parallel code and the results compared with runs made by LOWTRANSX for specified observer locations and view angles. The sun angle was also varied, and the Henyey-Greenstein phase function asymmetry factors were either 0 (isotropic) or 0.8. Each run with LOWTRANSX is for only one set of sun and observer angles and observer location, while a plane-parallel run produces results for all sun angles, observer angles, and observer locations. Therefore, these comparisons were restricted to a few angle and location choices. Table 4.9 presents the ratio of LOWTRANSX to plane-parallel intensities (both single scattering) for sun (view) angles of 12.95°, 82.57° and 88.54° for g = 0.0 at three locations (top, bottom and 2 Km). The first thing to note is that the view angles of 82° and 88° at the top of the atmosphere represents tangent paths for LOWTRANSX and the ratios are extremely small. Plane-parallel results are completely erroneous for such cases. However, at 2 Km and the bottom the

upper 2 x 2 part of the arrays show that geometry effects are 10% or less. In general (keeping away from tangent paths), geometry and refraction effects are weak until view and or sun angles are greater than 82°. The same comparison is repeated in Table 4.10 for g = 0.8 where the azimuthal angle is now present and also shown. The discussion for Table 4.9 also holds here and the only effect of changing the asymmetry factor was to increase the ratios slightly (geometry and refraction effects are slightly stronger for forward scattering aerosols).

The above two comparisons are of general interest in radiative transfer, but the important conclusion for present purposes is that the plane-parallel multiple versus single scattering study can be used to estimate the accuracy of the LOWTRANSX results for sun and view angles of 82° or less as long as tangent paths are not allowed.

The zenith angles used in Tables 4.1 through 4.10 are fixed by the Gaussian quadrature used in the Adding/Doubling code. For the present results, seven quadrature angles were used and the angles are as follows:

12.95°

29.45°

45.34°

60.00°

72.72°

82.57°

88.54°

Table 4.1 through 4.8 are ratios of multiple to single scattering intensities in plane parallel media for the conditions shown. The solar and observer zenith angles are 12.95°, 29.45°, 45.34°, 60.00°, 72.72°, 82.57° and 88.54°.

TABLE 4.1 TOT. OPT. DEPTH = 1.0 ALBEDO = 0.3 G = 0.0

[SOLAR ZENITH ANGLE INCREASING ---->]

Observer Zenith Angle Increasing

RATIO OF INTENSITIES UP OBSERVER TAU = 0.000

1.21246	1.21117	1.20830	1.20249	1.19036	1.16624	1.13334
1.21117	1.20977	1.20669	1.20049	1.18778	1.16308	1.12998
1.20830	1.20669	1.20316	1.19620	1.18232	1.15654	1.12310
1.20249	1.20049	1.19620	1.18793	1.17219	1.14485	1.11101
1.19036	1.18778	1.18232	1.17220	1.15412	1.12521	1.09121
1.16624	1.16308	1.15654	1.14486	1.12520	1.09588	1.06246
1.13334	1.12998	1.12310	1.11101	1.09120	1.06246	1.03001

RATIO OF INTENSITIES DOWN OBSERVER TAU = 0.000

0.0	0.0	0.0	0.0	0.0	0.0	0.0
0.0	0.0	0.0	0.0	0.0	0.0	0.0
0.0	0.0	0.0	0.0	0.0	0.0	0.0
0.0	0.0	0.0	0.0	0.0	0.0	0.0
0.0	0.0	0.0	0.0	0.0	0.0	0.0
0.0	0.0	0.0	0.0	0.0	0.0	0.0
0.0	0.0	0.0	0.0	0.0	0.0	0.0

RATIO OF INTENSITIES UP OBSERVER TAU = 0.250

1.24906	1.25125	1.25654	1.26963	1.31292	1.63736	1000 ++++
1.24871	1.25081	1.25590	1.26855	1.31065	1.62781	1000 ++++
1.24792	1.24982	1.25449	1.26619	1.30575	1.60771	1000 ++++
1.24624	1.24777	1.25159	1.26148	1.29633	1.57065	928.04468
1.24231	1.24312	1.24535	1.25187	1.27830	1.50489	739.32300
1.23249	1.23208	1.23165	1.23287	1.24652	1.40144	460.22192
1.21708	1.21564	1.21297	1.20958	1.21156	1.29634	186.51082

RATIO OF INTENSITIES DOWN OBSERVER TAU = 0.250

1.17355	1.17038	1.16427	1.15355	1.13626	1.11398	1.10015
1.17357	1.17061	1.16451	1.15381	1.13657	1.11442	1.10110
1.17407	1.17111	1.16504	1.15438	1.13723	1.11540	1.10332
1.17511	1.17216	1.16616	1.15566	1.13865	1.11752	1.10830
1.17756	1.17468	1.16877	1.15845	1.14204	1.12273	1.12177
1.18476	1.19206	1.17656	1.16706	1.15261	1.14078	1.16776
1.20484	1.20284	1.19891	1.19280	1.18739	1.22495	11.89555

TABLE 4.1 (CONT.) TOT. OPT. DEPTH = 1.0 ALBEDO = 0.3 G = 0.0

[SOLAR ZENITH ANGLE INCREASING ---->]

RATIO OF INTENSITIES UP OBSERVER TAU = 0.500

1.26442	1.27002	1.28377	1.31894	1.44982	3.26738	1000 ++++
1.26447	1.27003	1.28366	1.31854	1.44829	3.24503	1000 ++++
1.26458	1.27003	1.28341	1.31764	1.44491	3.19679	1000 ++++
1.26477	1.27000	1.28286	1.31578	1.43814	3.10316	1000 ++++
1.26502	1.26978	1.28150	1.31164	1.42385	2.91902	1000 ++++
1.26448	1.26814	1.27728	1.30130	1.39243	2.56610	1000 ++++
1.25935	1.26153	1.26726	1.28332	1.34778	2.13791	1000 ++++

RATIO OF INTENSITIES DOWN OBSERVER TAU = 0.500

1.20482	1.20273	1.19845	1.19101	1.17962	1.16814	1.15600
1.20547	1.20341	1.19919	1.19188	1.18079	1.17016	1.15936
1.20692	1.20492	1.20084	1.19384	1.18343	1.17483	1.16735
1.20992	1.20807	1.20431	1.19795	1.18911	1.18538	1.18645
1.21667	1.21517	1.21220	1.20754	1.20295	1.21443	1.24781
1.23315	1.23272	1.23223	1.23318	1.24482	1.34559	1.80176
1.25291	1.25425	1.25798	1.26922	1.31673	1.85566	1000 ++++

RATIO OF INTENSITIES UP OBSERVER TAU = 0.750

1.26073	1.26939	1.29104	1.34890	1.59461	8.22163	1000 ++++
1.26083	1.26949	1.29110	1.34887	1.59412	8.19781	1000 ++++
1.26106	1.26969	1.29124	1.34881	1.59303	8.14506	1000 ++++
1.26154	1.27011	1.29152	1.34867	1.59077	8.03689	1000 ++++
1.26263	1.27107	1.29215	1.34833	1.58557	7.79660	1000 ++++
1.26559	1.27364	1.29371	1.34713	1.57077	7.16768	1000 ++++
1.27171	1.27858	1.29575	1.34139	1.52923	5.72404	1000 ++++

RATIO OF INTENSITIES DOWN OBSERVER TAU = 0.750

1.22566	1.22489	1.22355	1.22085	1.21770	1.21508	1.19945
1.22674	1.22605	1.22470	1.22260	1.22036	1.21985	1.20607
1.22915	1.22864	1.22772	1.22654	1.22647	1.23127	1.22234
1.23399	1.23392	1.23397	1.23487	1.23996	1.25889	1.26411
1.24422	1.24517	1.24760	1.25398	1.27440	1.34820	1.42458
1.26265	1.26626	1.27485	1.29689	1.37494	1.96403	2.39497
1.27256	1.27625	1.29286	1.33172	1.48810	4.50042	1000 ++++

TABLE 4.1 (CONT.)   TOT. OPT. DEPTH = 1.0   ALBEDO = 0.3   G = 0.0

[SOLAR ZENITH ANGLE INCREASING ---->]

RATIO OF INTENSITIES UP   OBSERVER   TAU = 1.000

0.0	0.0	0.0	0.0	0.0	0.0	0.0
0.0	0.0	0.0	0.0	0.0	0.0	0.0
0.0	0.0	0.0	0.0	0.0	0.0	0.0
0.0	0.0	0.0	0.0	0.0	0.0	0.0
0.0	0.0	0.0	0.0	0.0	0.0	0.0
0.0	0.0	0.0	0.0	0.0	0.0	0.0
0.0	0.0	0.0	0.0	0.0	0.0	0.0

RATIO OF INTENSITIES DOWN   OBSERVER   TAU = 1.000

1.23397	1.23512	1.23761	1.24234	1.25035	1.25449	1.23530
1.23512	1.23646	1.23936	1.24498	1.25504	1.26288	1.24584
1.23761	1.23936	1.24323	1.25096	1.26601	1.28361	1.27250
1.24234	1.24498	1.25096	1.26353	1.29115	1.33750	1.34595
1.25035	1.25504	1.26601	1.29115	1.35899	1.54708	1.68678
1.25449	1.26289	1.28360	1.33750	1.54707	4.05412	15.87399
1.23530	1.24584	1.27250	1.34595	1.68678	15.87399	1000 ++++

TABLE 4.2 TOT. OPT. DEPTH = 1.0 ALBEDO = 0.6 G = 0.0

[SOLAR ZENITH ANGLE INCREASING ---->]

RATIO OF INTENSITIES UP OBSERVER TAU = 0.000

1.54692	1.54325	1.53512	1.51872	1.48474	1.41840	1.33196
1.54324	1.53927	1.53054	1.51305	1.47741	1.40950	1.32270
1.53512	1.53054	1.52054	1.50087	1.46196	1.39113	1.30378
1.51872	1.51305	1.50087	1.47750	1.43343	1.35852	1.27079
1.48474	1.47741	1.46196	1.43342	1.38298	1.30442	1.21765
1.41839	1.40950	1.39113	1.35852	1.30442	1.22639	1.14352
1.33196	1.32270	1.30378	1.27079	1.21765	1.14352	1.06594

RATIO OF INTENSITIES DOWN OBSERVER TAU = 0.000

0.0	0.0	0.0	0.0	0.0	0.0	0.0
0.0	0.0	0.0	0.0	0.0	0.0	0.0
0.0	0.0	0.0	0.0	0.0	0.0	0.0
0.0	0.0	0.0	0.0	0.0	0.0	0.0
0.0	0.0	0.0	0.0	0.0	0.0	0.0
0.0	0.0	0.0	0.0	0.0	0.0	0.0
0.0	0.0	0.0	0.0	0.0	0.0	0.0

RATIO OF INTENSITIES UP OBSERVER TAU = 0.250

1.64987	1.65603	1.67093	1.70771	1.82897	2.73415	1000 ++++
1.64880	1.65469	1.66901	1.70448	1.82220	2.70590	1000 ++++
1.64637	1.65170	1.66474	1.69743	1.80767	2.64648	1000 ++++
1.64122	1.64546	1.65603	1.68341	1.77973	2.53708	1000 ++++
1.62933	1.63144	1.63729	1.65481	1.72635	2.34371	1000 ++++
1.60011	1.59866	1.59678	1.59871	1.63288	2.04296	1000 ++++
1.55540	1.55098	1.54261	1.53132	1.53249	1.74691	482.81714

RATIO OF INTENSITIES DOWN OBSERVER TAU = 0.250

1.43629	1.42781	1.41045	1.38011	1.33162	1.27046	1.23446
1.43688	1.42842	1.41108	1.38078	1.33239	1.27156	1.23683
1.43820	1.42977	1.41249	1.38229	1.33413	1.27404	1.24231
1.44099	1.43261	1.41544	1.38547	1.33781	1.27938	1.25454
1.44747	1.43923	1.42234	1.39295	1.34656	1.29251	1.28775
1.46667	1.45839	1.44300	1.41567	1.37401	1.33819	1.45123
1.52102	1.51505	1.50323	1.48454	1.46586	1.55497	28.60285

TABLE 4.2 (CONT.) TOT. OPT. DEPTH = 1.0 ALBEDO = 0.6 G = 0.0

[SOLAR ZENITH ANGLE INCREASING ---->]

RATIO OF INTENSITIES UP OBSERVER TAU = 0.500

1.69644	1.71272	1.75265	1.85485	2.23588	7.56126	1000 ++++
1.69655	1.71269	1.75228	1.85361	2.23126	7.49381	1000 ++++
1.69677	1.71260	1.75144	1.85087	2.22112	7.34820	1000 ++++
1.69712	1.71232	1.74963	1.84519	2.20072	7.06560	1000 ++++
1.69740	1.71121	1.74519	1.83253	2.15766	6.50983	1000 ++++
1.69491	1.70548	1.73185	1.80100	2.06281	5.44547	1000 ++++
1.67881	1.68500	1.70119	1.74647	1.92808	4.16254	1000 ++++

RATIO OF INTENSITIES DOWN OBSERVER TAU = 0.500

1.52359	1.51752	1.50510	1.48352	1.45039	1.41679	1.38530
1.52538	1.51939	1.50714	1.48591	1.45357	1.42219	1.39417
1.52938	1.52358	1.51172	1.49130	1.46079	1.43474	1.41528
1.53771	1.53229	1.52130	1.50266	1.47632	1.46311	1.46594
1.55646	1.55202	1.54321	1.52919	1.51430	1.54161	1.62959
1.60268	1.60123	1.59929	1.60080	1.63041	1.89995	3.13059
1.65952	1.66318	1.67340	1.70435	1.83574	3.33537	1000 ++++

RATIO OF INTENSITIES UP OBSERVER TAU = 0.750

1.68856	1.71381	1.77700	1.94651	2.67205	22.54845	1000 ++++
1.68884	1.71406	1.77716	1.94642	2.67062	22.47699	1000 ++++
1.68947	1.71462	1.77752	1.94623	2.66744	22.31868	1000 ++++
1.69077	1.71576	1.77826	1.94579	2.66081	21.99399	1000 ++++
1.69372	1.71834	1.77990	1.94472	2.64557	21.27216	1000 ++++
1.70174	1.72528	1.78405	1.94098	2.60201	19.37981	1000 ++++
1.71818	1.73840	1.78889	1.92327	2.47813	15.00966	1000 ++++

RATIO OF INTENSITIES DOWN OBSERVER TAU = 0.750

1.58351	1.58130	1.57688	1.56965	1.56040	1.55283	1.51194
1.58658	1.58461	1.58073	1.57462	1.56794	1.56628	1.53038
1.59337	1.59196	1.58951	1.58583	1.58529	1.59848	1.57572
1.60721	1.60700	1.60711	1.60958	1.62373	1.67661	1.69265
1.63643	1.63917	1.64616	1.66436	1.72228	1.93116	2.14648
1.69039	1.70047	1.72533	1.78913	2.01446	3.71771	10.74888
1.71933	1.73657	1.77961	1.89362	2.35317	11.28338	1000 ++++

TABLE 4.2 (CONT.)   TOT. OPT. DEPTH = 1.0   ALBEDO = 0.6   G = 0.0

[SOLAR ZENITH ANGLE INCREASING ---->]

RATIO OF INTENSITIES UP   OBSERVER   TAU = 1.000

0.0	0.0	0.0	0.0	0.0	0.0	0.0
0.0	0.0	0.0	0.0	0.0	0.0	0.0
0.0	0.0	0.0	0.0	0.0	0.0	0.0
0.0	0.0	0.0	0.0	0.0	0.0	0.0
0.0	0.0	0.0	0.0	0.0	0.0	0.0
0.0	0.0	0.0	0.0	0.0	0.0	0.0
0.0	0.0	0.0	0.0	0.0	0.0	0.0

RATIO OF INTENSITIES DOWN   OBSERVER   TAU = 1.000

1.60855	1.61189	1.61911	1.63291	1.65668	1.67096	1.61977
1.61189	1.61576	1.62418	1.64055	1.67022	1.69524	1.64995
1.61911	1.62418	1.63536	1.65782	1.70198	1.75532	1.72651
1.63290	1.64055	1.65782	1.69429	1.77494	1.91225	1.93867
1.65668	1.67022	1.70198	1.77494	1.97295	2.52762	2.93449
1.67096	1.69524	1.75532	1.91225	2.52761	9.99790	45.22081
1.61977	1.64996	1.72651	1.93867	2.93449	45.22086	1000 ++++

TABLE 4.3 TOT. OPT. DEPTH = 2.0 ALBEDO = 0.3 G = 0.0

[SOLAR ZENITH ANGLE INCREASING ---->]

RATIO OF INTENSITIES UP OBSERVER TAU = 0.000

1.25644	1.25278	1.24514	1.23153	1.20921	1.17739	1.14159
1.25277	1.24897	1.24110	1.22720	1.20467	1.17284	1.13712
1.24514	1.24110	1.23283	1.21846	1.19563	1.16382	1.12830
1.23153	1.22720	1.21845	1.20359	1.18054	1.14892	1.11377
1.20921	1.20467	1.19563	1.18054	1.15761	1.12649	1.09199
1.17739	1.17284	1.16382	1.14892	1.12649	1.09618	1.06260
1.14158	1.13712	1.12830	1.11377	1.09199	1.06260	1.03005

RATIO OF INTENSITIES DOWN OBSERVER TAU = 0.000

0.0	0.0	0.0	0.0	0.0	0.0	0.0
0.0	0.0	0.0	0.0	0.0	0.0	0.0
0.0	0.0	0.0	0.0	0.0	0.0	0.0
0.0	0.0	0.0	0.0	0.0	0.0	0.0
0.0	0.0	0.0	0.0	0.0	0.0	0.0
0.0	0.0	0.0	0.0	0.0	0.0	0.0
0.0	0.0	0.0	0.0	0.0	0.0	0.0

RATIO OF INTENSITIES UP OBSERVER TAU = 0.500

1.34676	1.35221	1.36645	1.40665	1.57471	4.08499	1000 ++++
1.34518	1.35036	1.36397	1.40271	1.56576	4.00010	1000 ++++
1.34179	1.34642	1.35876	1.39460	1.54769	3.83087	1000 ++++
1.33540	1.33908	1.34952	1.38035	1.51697	3.54961	1000 ++++
1.32394	1.32628	1.33347	1.35755	1.46998	3.13157	1000 ++++
1.30686	1.30772	1.31149	1.32744	1.41023	2.61103	1000 ++++
1.29064	1.29035	1.29139	1.30051	1.35752	2.15376	1000 ++++

RATIO OF INTENSITIES DOWN OBSERVER TAU = 0.500

1.22101	1.21715	1.20960	1.19772	1.18211	1.16899	1.15674
1.22176	1.21791	1.21042	1.19865	1.18330	1.17103	1.16013
1.22345	1.21964	1.21227	1.20074	1.18602	1.17574	1.16817
1.22695	1.22326	1.21614	1.20516	1.19185	1.18629	1.18742
1.23489	1.23147	1.22500	1.21546	1.20609	1.21572	1.24929
1.25465	1.25212	1.24776	1.24323	1.24928	1.34827	1.80842
1.28019	1.27921	1.27858	1.28347	1.32425	1.86542	1000 ++++

TABLE 4.3 (CONT.) TOT. OPT. DEPTH = 2.0 ALBEDO = 0.3 G = 0.0

[SOLAR ZENITH ANGLE INCREASING -----]

RATIO OF INTENSITIES UP OBSERVER TAU = 1.000

1.39538	1.41174	1.45533	1.58894	2.36425	63.04080	1000 ++++
1.39509	1.41122	1.45424	1.58605	2.34916	61.58226	1000 ++++
1.39442	1.41008	1.45186	1.57985	2.31751	58.58670	1000 ++++
1.39296	1.40772	1.44718	1.56813	2.25982	53.32828	1000 ++++
1.38953	1.40267	1.43799	1.54664	2.16068	44.82637	1000 ++++
1.38173	1.39250	1.42180	1.51275	2.01737	33.36525	1000 ++++
1.37180	1.38062	1.40485	1.48044	1.88814	23.32350	1000 ++++

RATIO OF INTENSITIES DOWN OBSERVER TAU = 1.000

1.27554	1.27334	1.26933	1.26406	1.26039	1.25877	1.23913
1.27779	1.27573	1.27205	1.26750	1.26558	1.26747	1.25001
1.28278	1.28106	1.27816	1.27535	1.27777	1.28897	1.27755
1.29289	1.29193	1.29083	1.29218	1.30586	1.34505	1.35364
1.31350	1.31443	1.31795	1.33094	1.38285	1.56429	1.70874
1.34615	1.35105	1.36486	1.40780	1.60678	4.22724	16.73137
1.36506	1.37276	1.39406	1.46051	1.80965	17.24490	1000 ++++

RATIO OF INTENSITIES UP OBSERVER TAU = 1.500

1.40637	1.43342	1.50871	1.76818	3.98176	1000 ++++	1000 ++++
1.40661	1.43358	1.50867	1.76730	3.96992	1000 ++++	1000 ++++
1.40712	1.43394	1.50857	1.76535	3.94396	1000 ++++	1000 ++++
1.40814	1.43464	1.50833	1.76134	3.89196	1000 ++++	1000 ++++
1.41021	1.43600	1.50764	1.75254	3.78304	935.90674	1000 ++++
1.41402	1.43813	1.50494	1.73146	3.54821	741.11255	1000 ++++
1.41540	1.43709	1.49708	1.69807	3.23234	512.16797	1000 ++++

RATIO OF INTENSITIES DOWN OBSERVER TAU = 1.500

1.31551	1.31598	1.31742	1.32146	1.32978	1.32876	1.30348
1.31951	1.32041	1.32288	1.32915	1.34229	1.34745	1.32469
1.32828	1.33022	1.33515	1.34705	1.37329	1.39683	1.38194
1.34530	1.34959	1.36032	1.38667	1.45303	1.54720	1.56592
1.37485	1.38439	1.40909	1.47692	1.71925	2.44265	2.87778
1.40391	1.42057	1.46586	1.60969	2.30142	47.99670	359.95140
1.41347	1.43371	1.48950	1.67444	2.02942	369.72021	1000 ++++

TABLE 4.3 (CONT.) TOT. OPT. DEPTH = 2.0 ALBEDO = 0.3 G = 0.0

[SOLAR ZENITH ANGLE INCREASING ---->]

RATIO OF INTENSITIES UP OBSERVER TAU = 2.000

0.0	0.0	0.0	0.0	0.0	0.0	0.0
0.0	0.0	0.0	0.0	0.0	0.0	0.0
0.0	0.0	0.0	0.0	0.0	0.0	0.0
0.0	0.0	0.0	0.0	0.0	0.0	0.0
0.0	0.0	0.0	0.0	0.0	0.0	0.0
0.0	0.0	0.0	0.0	0.0	0.0	0.0
0.0	0.0	0.0	0.0	0.0	0.0	0.0

RATIO OF INTENSITIES DOWN OBSERVER TAU = 2.000

1.33711	1.34196	1.35215	1.36968	1.38957	1.38567	1.35665
1.34196	1.34780	1.36033	1.38298	1.41231	1.41659	1.39028
1.35215	1.36033	1.37862	1.41475	1.47221	1.50379	1.48706
1.36968	1.38298	1.41475	1.48777	1.64861	1.81487	1.85118
1.38957	1.41231	1.47221	1.64861	2.41293	4.74680	5.98568
1.38567	1.41659	1.50379	1.81487	4.74679	816.32739	1000 ++++
1.35665	1.39028	1.48706	1.85116	5.98568	1000 ++++	1000 ++++

TABLE 4.4 TOT. OPT. DEPTH = 0.5 ALBEDO = 0.6 G = 0.0

[SOLAR ZENITH ANGLE INCREASING ---->]

RATIO OF INTENSITIES UP OBSERVER TAU = 0.000

1.35725	1.35655	1.35495	1.35155	1.34340	1.31960	1.26214
1.35654	1.35577	1.35402	1.35030	1.34151	1.31638	1.25774
1.35495	1.35402	1.35193	1.34753	1.33734	1.30943	1.24837
1.35155	1.35030	1.34754	1.34180	1.32888	1.29586	1.23068
1.34340	1.34151	1.33734	1.32889	1.31074	1.26881	1.19758
1.31960	1.31638	1.30943	1.29585	1.26881	1.21493	1.13883
1.26214	1.25774	1.24837	1.23068	1.19758	1.13883	1.06491

RATIO OF INTENSITIES DOWN OBSERVER TAU = 0.000

0.0	0.0	0.0	0.0	0.0	0.0	0.0
0.0	0.0	0.0	0.0	0.0	0.0	0.0
0.0	0.0	0.0	0.0	0.0	0.0	0.0
0.0	0.0	0.0	0.0	0.0	0.0	0.0
0.0	0.0	0.0	0.0	0.0	0.0	0.0
0.0	0.0	0.0	0.0	0.0	0.0	0.0
0.0	0.0	0.0	0.0	0.0	0.0	0.0

RATIO OF INTENSITIES UP OBSERVER TAU = 0.125

1.39006	1.39211	1.39689	1.40780	1.43862	1.59817	21.49704
1.38997	1.39197	1.39665	1.40733	1.43757	1.59461	21.19501
1.38976	1.39166	1.39610	1.40627	1.4	1.58680	20.34475
1.38927	1.39096	1.39492	1.40406	1.43041	1.57119	19.28813
1.38794	1.38916	1.39205	1.39891	1.41965	1.53835	16.82693
1.38266	1.38266	1.38285	1.38411	1.39186	1.46440	12.04416
1.36096	1.35890	1.35460	1.34694	1.33533	1.34516	5.72190

RATIO OF INTENSITIES DOWN OBSERVER TAU = 0.125

1.29946	1.29553	1.28716	1.27127	1.24139	1.18880	1.13889
1.29960	1.29568	1.28731	1.27143	1.24158	1.18904	1.13943
1.29995	1.29601	1.28765	1.27180	1.24199	1.18957	1.14065
1.30061	1.29670	1.28837	1.27257	1.24236	1.19069	1.14526
1.30221	1.29833	1.29006	1.27438	1.24492	1.19337	1.14984
1.30718	1.30340	1.29534	1.28007	1.25143	1.20208	1.17436
1.33107	1.32787	1.32107	1.30832	1.28522	1.25373	1.59501

TABLE 4.4 (CONT.) TOT. OPT. DEPTH = 0.5 ALBEDO = 0.6 G = 0.0

[SOLAR ZENITH ANGLE INCREASING ----->]

RATIO OF INTENSITIES UP OBSERVER TAU = 0.250

1.39985	1.40450	1.41543	1.44084	1.51650	2.00947	1000 ++++
1.39996	1.40459	1.41547	1.44076	1.51608	2.00653	1000 ++++
1.40020	1.40478	1.41555	1.44059	1.51513	2.00000	1000 ++++
1.40069	1.40518	1.41571	1.44021	1.51315	1.98661	1000 ++++
1.40177	1.40602	1.41601	1.43927	1.50858	1.95679	1000 ++++
1.40436	1.40793	1.41633	1.43602	1.49523	1.87819	1000 ++++
1.40530	1.40690	1.41086	1.42085	1.45439	1.69245	451.25439

RATIO OF INTENSITIES DOWN OBSERVER TAU = 0.250

1.33860	1.33579	1.32977	1.31827	1.29646	1.25882	1.22743
1.33901	1.33621	1.33022	1.31879	1.29711	1.25985	1.22970
1.33991	1.33715	1.33123	1.31995	1.29858	1.26217	1.23495
1.34180	1.33911	1.33335	1.32237	1.30168	1.26716	1.24666
1.34619	1.34367	1.33828	1.32806	1.30904	1.27943	1.27845
1.35896	1.35699	1.35283	1.34514	1.33198	1.32203	1.43463
1.39211	1.39211	1.39240	1.39438	1.40649	1.52199	27.15179

RATIO OF INTENSITIES UP OBSERVER TAU = 0.375

1.38782	1.39477	1.41123	1.45027	1.57268	2.57024	1000 ++++
1.38790	1.39485	1.41129	1.45030	1.57261	2.56905	1000 ++++
1.38809	1.39503	1.41145	1.45039	1.57248	2.56639	1000 ++++
1.38849	1.39540	1.41177	1.45057	1.57220	2.56083	1000 ++++
1.38942	1.39627	1.41251	1.45106	1.57152	2.54787	1000 ++++
1.39223	1.39892	1.41474	1.45222	1.56934	2.50863	1000 ++++
1.40422	1.41000	1.42369	1.45611	1.55693	2.33580	1000 ++++

RATIO OF INTENSITIES DOWN OBSERVER TAU = 0.375

1.36219	1.36088	1.35806	1.35266	1.34239	1.32511	1.30085
1.36287	1.36155	1.35882	1.35361	1.34376	1.32764	1.30571
1.36424	1.36300	1.36055	1.35574	1.34684	1.33341	1.31712
1.36710	1.36617	1.36408	1.36019	1.35339	1.34609	1.33335
1.37372	1.37321	1.37217	1.37051	1.36904	1.37883	1.42155
1.39049	1.39141	1.39366	1.39921	1.41661	1.50567	1.93628
1.41115	1.41522	1.42490	1.44788	1.51690	2.02228	1000 ++++

TABLE 4.4 (CONT.) TOT. OPT. DEPTH = 0.5 ALBEDO = 0.6 G = 0.0

[SOLAR ZENITH ANGLE INCREASING ---->]

RATIO OF INTENSITIES UP OBSERVER TAU = 0.500

0.0	0.0	0.0	0.0	0.0	0.0	0.0
0.0	0.0	0.0	0.0	0.0	0.0	0.0
0.0	0.0	0.0	0.0	0.0	0.0	0.0
0.0	0.0	0.0	0.0	0.0	0.0	0.0
0.0	0.0	0.0	0.0	0.0	0.0	0.0
0.0	0.0	0.0	0.0	0.0	0.0	0.0
0.0	0.0	0.0	0.0	0.0	0.0	0.0

RATIO OF INTENSITIES DOWN OBSERVER TAU = 0.500

1.36824	1.36883	1.37011	1.37266	1.37776	1.38520	1.36282
1.36883	1.36950	1.37097	1.37391	1.37993	1.38989	1.37088
1.37011	1.37097	1.37286	1.37669	1.38485	1.40075	1.39005
1.37266	1.37391	1.37669	1.38246	1.39534	1.42524	1.43593
1.37776	1.37993	1.38485	1.39534	1.42048	1.49257	1.58342
1.38520	1.38989	1.40074	1.42524	1.49256	1.79418	2.91582
1.36282	1.37088	1.39005	1.43593	1.58342	2.91582	1000 ++++

TABLE 4.5 TOT. OPT. DEPTH = 1.0 ALBEDO = 0.3 G = 0.8

[SOLAR ZENITH ANGLE INCREASING ---->]

RATIO OF INTENSITIES UP OBSERVER AZIMUTH = 0 TAU = 0.000

1.36877	1.38241	1.40435	1.42460	1.40998	1.31607	1.17614
1.38240	1.39630	1.41731	1.43397	1.41051	1.30700	1.16061
1.40435	1.41731	1.43512	1.44459	1.41001	1.29346	1.14232
1.42460	1.43397	1.44459	1.44254	1.39404	1.26768	1.11842
1.40998	1.41051	1.41001	1.39404	1.33076	1.21270	1.08689
1.31607	1.30700	1.29346	1.26768	1.21270	1.12799	1.05381
1.17614	1.16061	1.14232	1.11842	1.08689	1.05381	1.02885

RATIO OF INTENSITIES DOWN OBSERVER AZIMUTH = 0 TAU = 0.000

0.0	0.0	0.0	0.0	0.0	0.0	0.0
0.0	0.0	0.0	0.0	0.0	0.0	0.0
0.0	0.0	0.0	0.0	0.0	0.0	0.0
0.0	0.0	0.0	0.0	0.0	0.0	0.0
0.0	0.0	0.0	0.0	0.0	0.0	0.0
0.0	0.0	0.0	0.0	0.0	0.0	0.0
0.0	0.0	0.0	0.0	0.0	0.0	0.0

RATIO OF INTENSITIES UP OBSERVER AZIMUTH = 90 TAU = 0.000

1.36833	1.38137	1.40347	1.42527	1.41456	1.32688	1.18899
1.38137	1.39403	1.41543	1.43677	1.42577	1.33676	1.19643
1.40347	1.41543	1.43606	1.45618	1.44471	1.35498	1.20987
1.42527	1.43677	1.45618	1.47623	1.46608	1.37967	1.22826
1.41456	1.42577	1.44470	1.46608	1.46532	1.39382	1.24395
1.32688	1.33676	1.35498	1.37967	1.39382	1.35384	1.22600
1.18899	1.19643	1.20987	1.22826	1.24392	1.22604	1.13325

RATIO OF INTENSITIES DOWN OBSERVER AZIMUTH = 90 TAU = 0.000

0.0	0.0	0.0	0.0	0.0	0.0	0.0
0.0	0.0	0.0	0.0	0.0	0.0	0.0
0.0	0.0	0.0	0.0	0.0	0.0	0.0
0.0	0.0	0.0	0.0	0.0	0.0	0.0
0.0	0.0	0.0	0.0	0.0	0.0	0.0
0.0	0.0	0.0	0.0	0.0	0.0	0.0
0.0	0.0	0.0	0.0	0.0	0.0	0.0

TABLE 4.5 (CONT.)   TOT. OPT. DEPTH = 1.0   ALBEDO = 0.3   G = 0.8

[SOLAR ZENITH ANGLE INCREASING ---->]

RATIO OF INTENSITIES UP   OBSERVER   AZIMUTH = 180   TAU = 0.000

1.36785	1.38011	1.40207	1.42482	1.41712	1.33330	1.19848
1.38011	1.39147	1.41218	1.43480	1.42921	1.34786	1.21262
1.40207	1.41218	1.43196	1.45350	1.44755	1.36649	1.22786
1.42482	1.43480	1.45349	1.47374	1.46774	1.38746	1.24279
1.41712	1.42920	1.44755	1.46773	1.46656	1.39602	1.24990
1.33330	1.34785	1.36649	1.38743	1.39601	1.34696	1.21731
1.19848	1.21262	1.22785	1.24278	1.24992	1.21730	1.11973

RATIO OF INTENSITIES DOWN   OBSERVER   AZIMUTH = 180   TAU = 0.000

0.0	0.0	0.0	0.0	0.0	0.0	0.0
0.0	0.0	0.0	0.0	0.0	0.0	0.0
0.0	0.0	0.0	0.0	0.0	0.0	0.0
0.0	0.0	0.0	0.0	0.0	0.0	0.0
0.0	0.0	0.0	0.0	0.0	0.0	0.0
0.0	0.0	0.0	0.0	0.0	0.0	0.0
0.0	0.0	0.0	0.0	0.0	0.0	0.0

RATIO OF INTENSITIES UP   OBSERVER   AZIMUTH = 0   TAU = 0.250

1.43295	1.45716	1.50113	1.56170	1.62470	1.84575	696.93286
1.45045	1.47523	1.51813	1.57297	1.61736	1.77865	563.28076
1.48207	1.50674	1.54663	1.59150	1.61248	1.70089	424.70215
1.52419	1.54656	1.57926	1.60765	1.59582	1.60411	284.12109
1.55316	1.56728	1.56711	1.59123	1.53269	1.47354	161.54990
1.52023	1.52355	1.52353	1.49974	1.41407	1.32058	82.14607
1.44038	1.43373	1.42231	1.38319	1.29036	1.21031	42.08784

RATIO OF INTENSITIES DOWN   OBSERVER   AZIMUTH = 0   TAU = 0.250

1.01304	1.03121	1.06934	1.11019	1.16654	1.23667	1.29022
1.03122	1.01459	1.05629	1.08502	1.14889	1.22554	1.29278
1.06945	1.03651	1.01818	1.04647	1.11521	1.20652	1.29527
1.11104	1.08536	1.04655	1.02602	1.06475	1.16144	1.26694
1.17213	1.15233	1.11673	1.06517	1.04404	1.09618	1.19129
1.26527	[illegible]	1.22013	1.16841	1.09875	1.08148	1.14200
1.38670	1.36835	1.35288	1.30832	1.21497	[illegible]	4.36268

TABLE 4.5 (CONT.) TOT. OPT. DEPTH = 1.0 ALBEDO = 0.3 G = 0.8

|SOLAR ZENITH ANGLE INCREASING ----> |

RATIO OF INTENSITIES UP OBSERVER AZIMUTH = 90 TAU = 0.250

1.43249	1.45611	1.50080	1.56505	1.63917	1.90782	807.93384
1.44929	1.47288	1.51758	1.58292	1.66028	1.94409	853.28931
1.48083	1.50434	1.54974	1.61654	1.69933	2.01290	934.06079
1.52405	1.54811	1.59427	1.66489	1.75627	2.11448	1000 ++++
1.55649	1.58148	1.62938	1.70464	1.81087	2.21443	1000 ++++
1.53080	1.55516	1.60399	1.68495	1.80438	2.21495	930.60815
1.45414	1.47731	1.52350	1.60056	1.71773	2.04965	484.45239

RATIO OF INTENSITIES DOWN OBSERVER AZIMUTH = 90 TAU = 0.250

1.03561	1.06128	1.09020	1.12684	1.18156	1.24795	1.29302
1.06130	1.07758	1.10227	1.13941	1.19553	1.26186	1.30783
1.09040	1.10249	1.12586	1.16452	1.22304	1.29019	1.33836
1.12829	1.14104	1.16616	1.20728	1.27002	1.33952	1.39277
1.18962	1.20444	1.23308	1.27967	1.34097	1.41253	1.48448
1.28299	1.29952	1.33228	1.38583	1.45347	1.52737	1.72861
1.39535	1.41627	1.45782	1.52672	1.62756	1.84991	34.18654

RATIO OF INTENSITIES UP OBSERVER AZIMUTH = 180 TAU = 0.250

1.43197	1.45479	1.49978	1.56660	1.64935	1.95270	899.20972
1.44785	1.47011	1.51491	1.58460	1.67812	2.02967	1000 ++++
1.47898	1.50030	1.54580	1.61813	1.72021	2.11878	1000 ++++
1.52262	1.54424	1.59062	1.66591	1.77659	2.21899	1000 ++++
1.55748	1.58179	1.62964	1.70826	1.82817	2.29895	1000 ++++
1.53541	1.56262	1.61180	1.69178	1.81547	2.25312	1000 ++++
1.46308	1.49045	1.53729	1.61140	1.72138	2.03916	510.88330

RATIO OF INTENSITIES DOWN OBSERVER AZIMUTH = 180 TAU = 0.250

1.04676	1.07413	1.10049	1.13654	1.19090	1.25354	1.29376
1.07419	1.09462	1.11927	1.15622	1.21084	1.27086	1.30685
1.10082	1.11967	1.14520	1.18442	1.24040	1.29866	1.33487
1.13855	1.15896	1.18725	1.22507	1.28520	1.34433	1.38691
1.20093	1.22364	1.25525	1.29900	1.34389	1.40730	1.47361
1.29362	1.31837	1.35290	1.40210	1.45557	1.50149	1.69627
1.40527	1.43198	1.47423	1.53946	1.62953	1.82405	34.81050

TABLE 4.5 (CONT.) TOT. OPT. DEPTH = 1.0 ALBEDO = 0.3 G = 0.8

[SOLAR ZENITH ANGLE INCREASING ---->]

RATIO OF INTENSITIES UP OBSERVER AZIMUTH = 0 TAU = 0.500

1.47247	1.50456	1.56541	1.65993	1.81904	3.18484	1000 ++++
1.49113	1.52376	1.58299	1.66925	1.79798	2.92530	1000 ++++
1.52719	1.56018	1.61633	1.69008	1.78265	2.64622	1000 ++++
1.58297	1.61487	1.66421	1.71807	1.76060	2.34106	1000 ++++
1.64681	1.67176	1.70782	1.72978	1.69637	2.00254	1000 ++++
1.67149	1.68484	1.69492	1.67133	1.57354	1.66878	1000 ++++
1.62713	1.62729	1.61957	1.56531	1.43425	1.45179	1000 ++++

RATIO OF INTENSITIES DOWN OBSERVER AZIMUTH = 0 TAU = 0.500

1.02633	1.06314	1.13997	1.21796	1.31492	1.43194	1.48897
1.06314	1.02944	1.07319	1.16964	1.28664	1.42024	1.49594
1.14006	1.07320	1.03656	1.09265	1.22383	1.38824	1.49809
1.21882	1.16998	1.09273	1.05148	1.12498	1.30580	1.45029
1.32084	1.29018	1.22542	1.12542	1.08316	1.17955	1.32379
1.46165	1.44243	1.40279	1.31135	1.18237	1.16721	1.33911
1.58465	1.57692	1.56302	1.49606	1.35029	1.33555	1000 ++++

RATIO OF INTENSITIES UP OBSERVER AZIMUTH = 90 TAU = 0.500

1.47213	1.50389	1.56634	1.66718	1.84769	3.42161	1000 ++++
1.49023	1.52229	1.58551	1.68934	1.87926	3.54493	1000 ++++
1.52620	1.55881	1.62432	1.73323	1.94026	3.78542	1000 ++++
1.58278	1.61709	1.68592	1.80464	2.03852	4.16224	1000 ++++
1.64968	1.68675	1.76117	1.89253	2.16476	4.60153	1000 ++++
1.68282	1.72125	1.80101	1.94596	2.24585	4.76392	1000 ++++
1.64301	1.68159	1.76107	1.90444	2.19628	4.31122	1000 ++++

RATIO OF INTENSITIES DOWN OBSERVER AZIMUTH = 90 TAU = 0.500

1.07212	1.12420	1.18117	1.24796	1.33919	1.44865	1.49416
1.12422	1.15669	1.20404	1.27061	1.36404	1.47393	1.52373
1.18136	1.20426	1.24721	1.31495	1.41277	1.53201	1.58585
1.24941	1.27227	1.31662	1.38735	1.49495	1.63246	1.70210
1.34739	1.37315	1.42315	1.50508	1.61838	1.80217	1.94826
1.48512	1.51521	1.57657	1.68278	1.84887	2.28532	3.55055
1.60192	1.63887	1.71488	1.85141	2.11894	3.76148	1000 ++++

TABLE 4.5 (CONT.) TOT. OPT. DEPTH = 1.0 ALBEDO = 0.3 G = 0.8

|SOLAR ZENITH ANGLE INCREASING ---->]

RATIO OF INTENSITIES UP OBSERVER AZIMUTH = 180 TAU = 0.500

1.47173	1.50291	1.56637	1.67192	1.86936	3.60532	1000 ++++
1.48901	1.52020	1.58495	1.69734	1.91998	3.91206	1000 ++++
1.52448	1.55537	1.62289	1.74313	1.99196	4.27342	1000 ++++
1.58111	1.61310	1.68432	1.81461	2.09461	4.70392	1000 ++++
1.64988	1.68586	1.76246	1.90515	2.22020	5.12912	1000 ++++
1.68664	1.72761	1.81007	1.96176	2.29313	5.15985	1000 ++++
1.65244	1.69485	1.77693	1.92353	2.22638	4.50857	1000 ++++

RATIO OF INTENSITIES DOWN OBSERVER AZIMUTH = 180 TAU = 0.500

1.09471	1.15002	1.20042	1.26408	1.35296	1.45613	1.49571
1.15005	1.18929	1.23398	1.29715	1.38566	1.48762	1.52343
1.20075	1.23442	1.27835	1.34469	1.43698	1.54371	1.58412
1.26610	1.29991	1.34763	1.41052	1.51582	1.64119	1.70178
1.36312	1.39865	1.45220	1.53022	1.61861	1.79949	1.95243
1.49746	1.53674	1.60063	1.70265	1.85491	2.26467	3.62358
1.61262	1.65527	1.73338	1.87110	2.15978	3.85289	1000 ++++

RATIO OF INTENSITIES UP OBSERVER AZIMUTH = 0 TAU = 0.750

1.48528	1.52222	1.59396	1.71373	1.97905	6.51300	1000 ++++
1.50193	1.53899	1.60814	1.71682	1.93829	5.70869	1000 ++++
1.53589	1.57339	1.63906	1.73302	1.90584	4.88796	1000 ++++
1.59417	1.63169	1.69137	1.76421	1.87434	4.05989	1000 ++++
1.67932	1.71253	1.76117	1.80066	1.81672	3.24477	1000 ++++
1.76204	1.78582	1.80760	1.79177	1.71376	2.52394	1000 ++++
1.77888	1.78655	1.78344	1.71908	1.57383	2.03428	1000 ++++

RATIO OF INTENSITIES DOWN OBSERVER AZIMUTH = 0 TAU = 0.750

1.03994	1.09610	1.21388	1.38141	1.47064	1.62463	1.66800
1.09610	1.04465	1.11127	1.25794	1.43064	1.61098	1.67698
1.21395	1.11129	1.05556	1.14018	1.33646	1.50661	1.67777
1.38211	1.25822	1.14024	1.07747	1.18679	1.44397	1.60924
1.47564	1.43369	1.30767	1.18719	1.12400	1.26997	1.45072
1.65060	1.63095	1.58009	1.45125	1.27263	1.31887	1.76584
1.75595	1.75289	1.74025	1.65469	1.47841	1.81034	1000 ++++

TABLE 4.5 (CONT.) TOT. OPT. DEPTH = 1.0 ALBEDO = 0.3 G = 0.8

[SOLAR ZENITH ANGLE INCREASING ---->]

RATIO OF INTENSITIES UP OBSERVER AZIMUTH = 90 TAU = 0.750

1.48521	1.52228	1.59667	1.72561	2.02509	7.25996	1000 ++++
1.50163	1.53921	1.61497	1.74861	2.06525	7.64139	1000 ++++
1.53563	1.57423	1.65351	1.79563	2.14491	8.41006	1000 ++++
1.59438	1.63551	1.72027	1.87833	2.28180	9.71070	1000 ++++
1.68156	1.72706	1.82146	2.00277	2.49103	11.58723	1000 ++++
1.77270	1.82282	1.93026	2.14345	2.72614	13.36678	1000 ++++
1.79631	1.85008	1.96439	2.18881	2.79028	12.53097	1000 ++++

RATIO OF INTENSITIES DOWN OBSERVER AZIMUTH = 90 TAU = 0.750

1.10985	1.19003	1.27730	1.37615	1.50522	1.64892	1.67779
1.19005	1.24003	1.31198	1.41001	1.54302	1.69254	1.72355
1.27746	1.31215	1.37646	1.47592	1.61784	1.78507	1.82177
1.37733	1.41135	1.47730	1.58232	1.74629	1.96136	2.01768
1.51207	1.55069	1.62671	1.75521	1.95436	2.33790	2.54480
1.68058	1.72711	1.82502	2.00826	2.38568	4.26739	10.07781
1.77600	1.82927	1.94232	2.16259	2.72923	10.55128	1000 ++++

RATIO OF INTENSITIES UP OBSERVER AZIMUTH = 180 TAU = 0.750

1.48505	1.52196	1.59829	1.73431	2.06137	7.86334	1000 ++++
1.50094	1.53855	1.61772	1.76474	2.13589	8.88495	1000 ++++
1.53454	1.57250	1.65632	1.81649	2.23807	10.13985	1000 ++++
1.59299	1.63267	1.72267	1.90041	2.38790	11.77456	1000 ++++
1.68109	1.72560	1.82505	2.02737	2.60365	13.85881	1000 ++++
1.77510	1.82730	1.94066	2.17218	2.83927	15.56407	1000 ++++
1.80579	1.86330	1.98380	2.22312	2.88347	14.10306	1000 ++++

RATIO OF INTENSITIES DOWN OBSERVER AZIMUTH = 180 TAU = 0.750

1.14469	1.22998	1.30652	1.39943	1.52414	1.65913	1.68180
1.23001	1.28994	1.35648	1.44765	1.57260	1.70982	1.72770
1.30678	1.35681	1.42109	1.51755	1.65195	1.80556	1.82832
1.40105	1.44985	1.52006	1.61405	1.77817	1.98421	2.03506
1.53256	1.58335	1.66469	1.79063	1.96174	2.36296	2.60153
1.69492	1.75238	1.85542	2.04132	2.41909	4.41179	11.03944
1.78756	1.84707	1.96355	2.19739	2.80465	11.58812	1000 ++++

TABLE 4.5 (CONT.) TOT. OPT. DEPTH = 1.0 ALBEDO = 0.3 G = 0.8

[SOLAR ZENITH ANGLE INCREASING ---->]

RATIO OF INTENSITIES UP OBSERVER AZIMUTH = 0 TAU = 1.000

0.0	0.0	0.0	0.0	0.0	0.0	0.0
0.0	0.0	0.0	0.0	0.0	0.0	0.0
0.0	0.0	0.0	0.0	0.0	0.0	0.0
0.0	0.0	0.0	0.0	0.0	0.0	0.0
0.0	0.0	0.0	0.0	0.0	0.0	0.0
0.0	0.0	0.0	0.0	0.0	0.0	0.0
0.0	0.0	0.0	0.0	0.0	0.0	0.0

RATIO OF INTENSITIES DOWN OBSERVER AZIMUTH = 0 TAU = 1.000

1.05387	1.13013	1.29128	1.45121	1.63418	1.81334	1.84177
1.13013	1.06024	1.15063	1.35032	1.58125	1.79647	1.85077
1.29128	1.15063	1.07470	1.18933	1.45361	1.73901	1.84844
1.45121	1.35032	1.18933	1.10423	1.25128	1.58107	1.76131
1.63418	1.58125	1.45361	1.25128	1.16845	1.37277	1.59282
1.81334	1.79647	1.73901	1.58107	1.37277	1.65568	3.09888
1.84176	1.85077	1.84844	1.76130	1.59282	3.09888	1000 ++++

RATIO OF INTENSITIES UP OBSERVER AZIMUTH = 90 TAU = 1.000

0.0	0.0	0.0	0.0	0.0	0.0	0.0
0.0	0.0	0.0	0.0	0.0	0.0	0.0
0.0	0.0	0.0	0.0	0.0	0.0	0.0
0.0	0.0	0.0	0.0	0.0	0.0	0.0
0.0	0.0	0.0	0.0	0.0	0.0	0.0
0.0	0.0	0.0	0.0	0.0	0.0	0.0
0.0	0.0	0.0	0.0	0.0	0.0	0.0

RATIO OF INTENSITIES DOWN OBSERVER AZIMUTH = 90 TAU = 1.000

1.14865	1.25895	1.37899	1.51240	1.68082	1.84709	1.85817
1.25895	1.32767	1.42066	1.55897	1.73435	1.91020	1.92209
1.37899	1.42066	1.51463	1.64966	1.84207	2.04782	2.06272
1.51241	1.55897	1.64966	1.79619	2.03402	2.33064	2.36454
1.68082	1.73436	1.84207	2.03403	2.38069	3.10657	3.39183
1.84709	1.91020	2.04781	2.33064	3.10658	10.38308	36.47739
1.85817	1.92209	2.06272	2.36454	3.39177	36.47745	1000 ++++

TABLE 4.5 (CONT.) TOT. OPT. DEPTH = 1.0 ALBEDO = 0.3 G = 0.8

[SOLAR ZENITH ANGLE INCREASING ---->]

RATIO OF INTENSITIES UP OBSERVER AZIMUTH = 180 TAU = 1.000

0.0	0.0	0.0	0.0	0.0	0.0	0.0
0.0	0.0	0.0	0.0	0.0	0.0	0.0
0.0	0.0	0.0	0.0	0.0	0.0	0.0
0.0	0.0	0.0	0.0	0.0	0.0	0.0
0.0	0.0	0.0	0.0	0.0	0.0	0.0
0.0	0.0	0.0	0.0	0.0	0.0	0.0
0.0	0.0	0.0	0.0	0.0	0.0	0.0

RATIO OF INTENSITIES DOWN OBSERVER AZIMUTH = 180 TAU = 1.000

1.19672	1.31429	1.41931	1.54378	1.70599	1.86177	1.86618
1.31428	1.39700	1.48752	1.60942	1.77418	1.93655	1.93416
1.41931	1.48750	1.57475	1.70552	1.89012	2.08313	2.08395
1.54378	1.60941	1.70562	1.83961	2.08400	2.38088	2.41395
1.70599	1.77419	1.89009	2.08402	2.41086	3.20768	3.56681
1.86177	1.93656	2.08313	2.38076	3.20738	11.40927	42.77612
1.86618	1.93415	2.08397	2.41391	3.56696	42.77678	1000 ++++

TABLE 4.6 TOT. OPT. DEPTH = 1.0 ALBEDO = 0.6 G = 0.8

[SOLAR ZENITH ANGLE INCREASING ---->]

RATIO OF INTENSITIES UP OBSERVER AZIMUTH = 0 TAU = 0.000

2.04127	2.09175	2.17422	2.25155	2.20131	1.88806	1.48245
2.09175	2.14250	2.21995	2.28017	2.19307	1.84723	1.42989
2.17422	2.21995	2.28279	2.31086	2.17658	1.79035	1.36937
2.25155	2.28018	2.31086	2.28856	2.10033	1.69428	1.29404
2.20131	2.19307	2.17659	2.10033	1.87474	1.52192	1.20363
1.88806	1.84723	1.79035	1.69427	1.52191	1.29535	1.11917
1.48245	1.42989	1.36937	1.29403	1.20363	1.11918	1.06118

RATIO OF INTENSITIES DOWN OBSERVER AZIMUTH = 0 TAU = 0.000

0.0	0.0	0.0	0.0	0.0	0.0	0.0
0.0	0.0	0.0	0.0	0.0	0.0	0.0
0.0	0.0	0.0	0.0	0.0	0.0	0.0
0.0	0.0	0.0	0.0	0.0	0.0	0.0
0.0	0.0	0.0	0.0	0.0	0.0	0.0
0.0	0.0	0.0	0.0	0.0	0.0	0.0
0.0	0.0	0.0	0.0	0.0	0.0	0.0

RATIO OF INTENSITIES UP OBSERVER AZIMUTH = 90 TAU = 0.000

2.03999	2.08906	2.17352	2.25945	2.22679	1.93299	1.52730
2.08906	2.13786	2.22169	2.30788	2.27419	1.97178	1.55384
2.17352	2.22169	2.30584	2.39140	2.35608	2.04314	1.60173
2.25945	2.30788	2.39140	2.48051	2.44927	2.13598	1.66367
2.22679	2.27419	2.35608	2.44927	2.44639	2.17384	1.69914
1.93299	1.97178	2.04314	2.13599	2.17383	2.00507	1.60422
1.52730	1.55384	1.60173	1.66367	1.69913	1.60423	1.32128

RATIO OF INTENSITIES DOWN OBSERVER AZIMUTH = 90 TAU = 0.000

0.0	0.0	0.0	0.0	0.0	0.0	0.0
0.0	0.0	0.0	0.0	0.0	0.0	0.0
0.0	0.0	0.0	0.0	0.0	0.0	0.0
0.0	0.0	0.0	0.0	0.0	0.0	0.0
0.0	0.0	0.0	0.0	0.0	0.0	0.0
0.0	0.0	0.0	0.0	0.0	0.0	0.0
0.0	0.0	0.0	0.0	0.0	0.0	0.0

TABLE 4.6 (CONT.)   TOT. OPT. DEPTH = 1.0   ALBEDO = 0.6   G = 0.8

[SOLAR ZENITH ANGLE INCREASING ---->]

RATIO OF INTENSITIES UP   OBSERVER   AZIMUTH = 180   TAU = 0.000

2.03852	2.08545	2.17049	2.26202	2.24286	1.96208	1.56126
2.08545	2.13075	2.21444	2.30978	2.30110	2.02497	1.61463
2.17049	2.21444	2.29913	2.39626	2.38881	2.10596	1.67425
2.26201	2.30978	2.39625	2.49441	2.48644	2.19340	1.73016
2.24285	2.30111	2.38880	2.48644	2.48830	2.21436	1.73891
1.96208	2.02497	2.10594	2.19340	2.21441	2.01178	1.59792
1.56127	1.61463	1.67425	1.73024	1.73896	1.59756	1.29567

RATIO OF INTENSITIES DOWN   OBSERVER   AZIMUTH = 180   TAU = 0.000

0.0	0.0	0.0	0.0	0.0	0.0	0.0
0.0	0.0	0.0	0.0	0.0	0.0	0.0
0.0	0.0	0.0	0.0	0.0	0.0	0.0
0.0	0.0	0.0	0.0	0.0	0.0	0.0
0.0	0.0	0.0	0.0	0.0	0.0	0.0
0.0	0.0	0.0	0.0	0.0	0.0	0.0
0.0	0.0	0.0	0.0	0.0	0.0	0.0

RATIO OF INTENSITIES UP   OBSERVER   AZIMUTH = 0   TAU = 0.250

2.20061	2.28363	2.43626	2.64909	2.87585	3.70832	1000 ++++
2.26344	2.34835	2.49649	2.68602	2.84174	3.45265	1000 ++++
2.37812	2.46168	2.59743	2.74677	2.81174	3.15948	1000 ++++
2.53077	2.60238	2.70693	2.78817	2.72909	2.79392	1000 ++++
2.62745	2.66199	2.70927	2.69351	2.47992	2.32080	543.49829
2.48882	2.47789	2.45128	2.34629	2.07296	1.82469	246.22598
2.20143	2.15958	2.10145	1.96729	1.70671	1.50710	112.67081

RATIO OF INTENSITIES DOWN   OBSERVER   AZIMUTH = 0   TAU = 0.250

1.02654	1.06417	1.14597	1.24127	1.38101	1.55610	1.68525
1.06419	1.02979	1.07517	1.18195	1.33377	1.52497	1.68576
1.14629	1.07523	1.03744	1.09777	1.25271	1.47091	1.68021
1.24467	1.18332	1.09809	1.05461	1.13982	1.36168	1.61068
1.40310	1.34817	1.25914	1.14137	1.09551	1.21317	1.45185
1.66871	1.60762	1.52383	1.38797	[illegible]	1.18240	[illegible]
2.00822	[illegible]	[illegible]	[illegible]	[illegible]	[illegible]	[illegible]

TABLE 4.6 (CONT.) TOT. OPT. DEPTH = 1.0 ALBEDO = 0.6 G = 0.8

[SOLAR ZENITH ANGLE INCREASING ---->]

RATIO OF INTENSITIES UP OBSERVER AZIMUTH = 90 TAU = 0.250

2.19915	2.28074	2.43719	2.66621	2.93842	3.95554	1000 ++++
2.26015	2.34305	2.50235	2.73926	3.02821	4.11894	1000 ++++
2.37594	2.46134	2.62822	2.87874	3.19813	4.43419	1000 ++++
2.55595	2.62703	2.80455	3.08080	3.44783	4.90092	1000 ++++
2.65107	2.74835	2.93820	3.24105	3.67218	5.31704	1000 ++++
2.54080	2.63354	2.82115	3.13346	3.59047	5.16674	1000 ++++
2.26169	2.34370	2.50891	2.78492	3.19521	4.35255	1000 ++++

RATIO OF INTENSITIES DOWN OBSERVER AZIMUTH = 90 TAU = 0.250

1.07308	1.12786	1.19372	1.28401	1.42398	1.59008	1.69752
1.12792	1.16446	1.22308	1.31680	1.46236	1.62928	1.73889
1.19446	1.22388	1.28295	1.38461	1.54026	1.71080	1.82563
1.28976	1.32345	1.39168	1.50717	1.67964	1.85777	1.98514
1.45770	1.50050	1.58498	1.72448	1.90631	2.09094	2.26968
1.72984	1.78255	1.88803	2.06037	2.27195	2.47891	3.06545
2.06812	2.13925	2.28165	2.51796	2.85262	3.57085	112.33289

RATIO OF INTENSITIES UP OBSERVER AZIMUTH = 180 TAU = 0.250

2.19747	2.27680	2.43516	2.67555	2.98286	4.13771	1000 ++++
2.25581	2.33487	2.49647	2.75357	3.10976	4.47467	1000 ++++
2.37112	2.45086	2.62134	2.89879	3.30261	4.89700	1000 ++++
2.53507	2.62225	2.80612	3.10988	3.56704	5.39908	1000 ++++
2.66325	2.76740	2.96683	3.29556	3.79156	5.77106	1000 ++++
2.56953	2.68552	2.88723	3.21090	3.70183	5.44336	1000 ++++
2.30328	2.41365	2.59417	2.87305	3.27408	4.43791	1000 ++++

RATIO OF INTENSITIES DOWN OBSERVER AZIMUTH = 180 TAU = 0.250

1.09653	1.15665	1.21955	1.31107	1.45221	1.60879	1.70317
1.15077	1.20526	1.26837	1.36679	1.51186	1.66138	1.74253
1.22052	1.27002	1.33953	1.44933	1.60140	1.74567	1.82614
1.31904	1.37601	1.46147	1.57608	1.74314	1.88737	1.98161
1.49429	1.56690	1.66815	1.80727	1.95177	2.10359	2.25941
1.76995	1.85774	1.97852	2.14677	2.32316	2.45705	3.03614
2.11079	2.21869	2.37103	2.60638	2.91716	3.58172	117.50253

TABLE 4.6 (CONT.) TOT. OPT. DEPTH = 1.0 ALBEDO = 0.6 G = 0.8

[SOLAR ZENITH ANGLE INCREASING -----]

RATIO OF INTENSITIES UP OBSERVER AZIMUTH = 0 TAU = 0.500

2.29294	2.40049	2.60843	2.94229	3.54015	8.96948	1000 ++++
2.35883	2.46860	2.67110	2.97417	3.45844	7.93765	1000 ++++
2.48756	2.59861	2.79045	3.04720	3.39615	6.84723	1000 ++++
2.68846	2.79359	2.95850	3.13814	3.30032	5.64349	1000 ++++
2.91372	2.98761	3.09495	3.14892	3.04276	4.29324	1000 ++++
2.98040	3.00197	3.00775	2.90074	2.59113	3.01524	1000 ++++
2.79380	2.76636	2.71037	2.51702	2.13478	2.24945	1000 ++++

RATIO OF INTENSITIES DOWN OBSERVER AZIMUTH = 0 TAU = 0.500

1.05435	1.13243	1.30341	1.49615	1.75941	2.09161	2.25928
1.13245	1.06107	1.15513	1.37595	1.67515	2.04535	2.26541
1.30376	1.15520	1.07675	1.20066	1.51329	1.94658	2.25505
1.49993	1.37750	1.20103	1.11088	1.28030	1.72246	2.11328
1.78609	1.69129	1.52060	1.28232	1.18705	1.42054	1.78927
2.21848	2.14003	2.00849	1.75386	1.43149	1.40308	1.87354
2.63073	2.57903	2.50537	2.28556	1.88341	1.93511	1000 ++++

RATIO OF INTENSITIES UP OBSERVER AZIMUTH = 90 TAU = 0.500

2.29181	2.39870	2.61330	2.97285	3.65747	9.96792	1000 ++++
2.35618	2.46573	2.68655	3.06274	3.79489	10.58372	1000 ++++
2.48568	2.69065	2.83638	3.24406	4.06820	11.82195	1000 ++++
2.69259	2.81897	3.07877	3.54455	4.52048	13.83895	1000 ++++
2.92567	3.07864	3.37396	3.91607	5.10177	16.22261	1000 ++++
3.03901	3.19032	3.51126	4.11442	5.42182	16.86662	1000 ++++
2.86995	3.01595	3.32365	3.89637	5.10379	14.18124	1000 ++++

RATIO OF INTENSITIES DOWN OBSERVER AZIMUTH = 90 TAU = 0.500

1.15086	1.26607	1.40228	1.57807	1.83500	2.15156	2.28630
1.20014	1.34240	1.47126	1.64164	1.91012	2.23818	2.38152
1.40310	1.46216	1.57916	1.77119	2.06293	2.42207	2.58394
1.58446	1.64905	1.77915	1.99830	2.33543	2.76598	2.95596
1.87221	1.97253	2.11339	2.38719	2.78295	3.39391	3.89094
2.30853	2.41215	2.62811	3.01142	3.63155	5.25757	10.11590
2.71016	2.84571	3.15067	3.65715	4.71952	11.42239	1000 ++++

TABLE 4.6 (CONT.) TOT. OPT. DEPTH = 1.0 ALBEDO = 0.6 G = 0.8

[SOLAR ZENITH ANGLE INCREASING -----]

RATIO OF INTENSITIES UP OBSERVER AZIMUTH = 180 TAU = 0.500

2.29044	2.39572	2.61457	2.99312	3.74615	10.74912	1000 ++++
2.35233	2.45941	2.68715	3.09881	3.96578	12.17384	1000 ++++
2.48088	2.59130	2.83677	3.29304	4.29671	14.01805	1000 ++++
2.69015	2.81225	3.08548	3.60607	4.79282	16.43787	1000 ++++
2.94459	3.09258	3.40578	4.00879	5.41172	18.98248	1000 ++++
3.06730	3.24263	3.58916	4.24268	5.73121	19.15028	1000 ++++
2.91887	3.09719	3.43257	4.04199	5.34765	15.51361	1000 ++++

RATIO OF INTENSITIES DOWN OBSERVER AZIMUTH = 180 TAU = 0.500

1.20046	1.32643	1.45270	1.62627	1.88154	2.18209	2.29919
1.32654	1.42448	1.54541	1.72668	1.98948	2.29125	2.39693
1.45400	1.54718	1.67566	1.87672	2.16113	2.48452	2.60401
1.63505	1.73907	1.89023	2.10443	2.43988	2.83220	3.01790
1.92779	2.05024	2.23583	2.51338	2.86137	3.46106	3.97112
2.36210	2.51186	2.75283	3.14495	3.75137	5.38682	10.70323
2.76289	2.93689	3.24796	3.80207	4.91960	12.21088	1000 ++++

RATIO OF INTENSITIES UP OBSERVER AZIMUTH = 0 TAU = 0.750

2.30718	2.42806	2.66880	3.08954	4.09576	22.71381	1000 ++++
2.36455	2.48626	2.71842	3.09922	3.94177	19.38222	1000 ++++
2.48289	2.60644	2.82757	3.15663	3.82100	16.06749	1000 ++++
2.68895	2.81175	3.01155	3.26389	3.70081	12.73545	1000 ++++
2.99124	3.09486	3.24914	3.37516	3.47889	9.39260	1000 ++++
3.27599	3.33567	3.38534	3.31167	3.09296	6.39704	1000 ++++
3.31282	3.30845	3.26438	3.03168	2.60790	4.39111	1000 ++++

RATIO OF INTENSITIES DOWN OBSERVER AZIMUTH = 0 TAU = 0.750

1.08360	1.20596	1.47866	1.78845	2.20143	2.69635	2.85381
1.20597	1.09420	1.34182	1.59391	2.00995	2.62955	2.85897
1.47916	1.34188	1.11877	1.31320	1.80884	2.47546	2.83426
1.79166	1.59527	1.51552	1.17159	1.43617	2.12146	2.61572
2.22476	2.08436	1.81555	1.43810	1.29046	1.67257	2.18646
2.61224	2.71854	2.55557	2.15339	1.66468	1.85481	2.37284
3.20965	3.16696	3.06830	2.79606	2.29469	3.50089	1000 ++++

TABLE 4.6 (CONT.) TOT. OPT. DEPTH = 1.0 ALBEDO = 0.6 G = 0.8

[SOLAR ZENITH ANGLE INCREASING -- ->]

RATIO OF INTENSITIES UP OBSERVER AZIMUTH = 90 TAU = 0.750

2.30692	2.42869	2.67956	3.13605	4.28019	25.98068	1000 ++++
2.36381	2.48889	2.74789	3.22762	4.45463	27.92700	1000 ++++
2.48316	2.61511	2.89340	3.41872	4.81199	31.98566	1000 ++++
2.69348	2.84018	3.15169	3.76342	5.45035	39.22368	1000 ++++
3.00956	3.18137	3.54987	4.29651	6.46029	50.28783	1000 ++++
3.33304	3.53249	3.97275	4.89194	7.58933	60.97853	1000 ++++
3.40060	3.61473	4.08448	5.05426	7.82464	56.12442	1000 ++++

RATIO OF INTENSITIES DOWN OBSERVER AZIMUTH = 90 TAU = 0.750

1.23453	1.41910	1.63980	1.91990	2.32022	2.79399	2.90578
1.41915	1.54308	1.73552	2.02291	2.44602	2.94991	3.07074
1.64049	1.73628	1.92310	2.23254	2.70525	3.29035	3.43592
1.92529	2.02923	2.23944	2.59873	3.17848	3.97198	4.20436
2.35249	2.48312	2.75021	3.22621	4.01989	5.54360	6.42849
2.93592	3.10937	3.48431	4.21604	5.81502	14.07995	40.93022
3.30796	3.51665	3.97304	4.90560	7.45059	44.93736	1000 ++++

RATIO OF INTENSITIES UP OBSERVER AZIMUTH = 180 TAU = 0.750

2.30639	2.42800	2.68620	3.17021	4.42572	28.63690	1000 ++++
2.36176	2.48739	2.75973	3.29247	4.74354	33.48718	1000 ++++
2.48033	2.61139	2.90800	3.50666	5.20784	39.96437	1000 ++++
2.69144	2.83638	3.17087	3.86831	5.93316	49.26445	1000 ++++
3.01507	3.19102	3.58729	4.43475	7.03356	62.25243	1000 ++++
3.35632	3.57791	4.05717	5.08150	8.24531	73.63420	1000 ++++
3.45317	3.70230	4.21814	5.28718	8.43915	65.80807	1000 ++++

RATIO OF INTENSITIES DOWN OBSERVER AZIMUTH = 180 TAU = 0.750

1.31405	1.51741	1.72147	1.99528	2.39147	2.84360	2.95304
1.51751	1.67040	1.86930	2.15393	2.56776	3.03987	3.11320
1.72256	1.87078	2.07426	2.39364	2.86056	3.40901	3.50106
2.00267	2.16433	2.40509	2.76118	3.35629	4.12952	4.33825
2.43127	2.62010	2.92586	3.42256	4.19037	5.80974	6.80530
3.06521	3.23650	3.65681	4.47595	6.14209	15.51075	48.67416
3.36932	3.62348	4.12505	5.16349	7.96591	51.56225	1000 ++++

TABLE 4.6 (CONT.)   TOT. OPT. DEPTH = 1.0   ALBEDO = 0.6   G = 0.8

[SOLAR ZENITH ANGLE INCREASING ---->]

RATIO OF INTENSITIES UP   OBSERVER AZIMUTH = 0   TAU = 1.000

0.0	0.0	0.0	0.0	0.0	0.0	0.0
0.0	0.0	0.0	0.0	0.0	0.0	0.0
0.0	0.0	0.0	0.0	0.0	0.0	0.0
0.0	0.0	0.0	0.0	0.0	0.0	0.0
0.0	0.0	0.0	0.0	0.0	0.0	0.0
0.0	0.0	0.0	0.0	0.0	0.0	0.0
0.0	0.0	0.0	0.0	0.0	0.0	0.0

RATIO OF INTENSITIES DOWN   OBSERVER AZIMUTH = 0   TAU = 1.000

1.11461	1.28517	1.67417	2.12295	2.71467	3.36470	3.50010
1.28517	1.12931	1.33587	1.83858	2.52368	3.26920	3.49699
1.67417	1.33587	1.16363	1.43665	2.14358	3.04928	3.45073
2.12294	1.83858	1.43665	1.23758	1.61162	2.55821	3.15216
2.71467	2.52368	2.14358	1.61162	1.41227	1.99421	2.69258
3.36470	3.26920	3.04928	2.55821	1.99421	3.00766	8.49616
3.50016	3.49699	3.45073	3.15216	2.69259	8.49618	1000 ++++

RATIO OF INTENSITIES UP   OBSERVER AZIMUTH = 90   TAU = 1.000

0.0	0.0	0.0	0.0	0.0	0.0	0.0
0.0	0.0	0.0	0.0	0.0	0.0	0.0
0.0	0.0	0.0	0.0	0.0	0.0	0.0
0.0	0.0	0.0	0.0	0.0	0.0	0.0
0.0	0.0	0.0	0.0	0.0	0.0	0.0
0.0	0.0	0.0	0.0	0.0	0.0	0.0
0.0	0.0	0.0	0.0	0.0	0.0	0.0

RATIO OF INTENSITIES DOWN   OBSERVER AZIMUTH = 90   TAU = 1.000

1.32457	1.58856	1.90970	2.31639	2.89023	3.51416	3.58886
1.58856	1.76676	2.05050	2.46954	3.08490	3.76310	3.84357
1.90970	2.05050	2.32538	2.78235	3.49578	4.32588	4.42437
2.31638	2.46954	2.78234	3.33136	4.27034	5.54076	5.74853
2.89023	3.08490	3.49377	4.27031	5.80311	9.13982	10.61940
3.51416	3.76311	4.32388	5.54075	9.13984	47.32498	183.64839
3.58886	3.84355	4.42436	5.74850	10.61939	183.64854	1000 ++++

TABLE 4.6 (CONT.) TOT. OPT. DEPTH = 1.0 ALBEDO = 0.6 G = 0.8

[SOLAR ZENITH ANGLE INCREASING ---->]

RATIO OF INTENSITIES UP OBSERVER AZIMUTH = 180 TAU = 1.000

0.0	0.0	0.0	0.0	0.0	0.0	0.0
0.0	0.0	0.0	0.0	0.0	0.0	0.0
0.0	0.0	0.0	0.0	0.0	0.0	0.0
0.0	0.0	0.0	0.0	0.0	0.0	0.0
0.0	0.0	0.0	0.0	0.0	0.0	0.0
0.0	0.0	0.0	0.0	0.0	0.0	0.0
0.0	0.0	0.0	0.0	0.0	0.0	0.0

RATIO OF INTENSITIES DOWN OBSERVER AZIMUTH = 180 TAU = 1.000

1.43812	1.73191	2.03015	2.42637	2.99471	3.59219	3.63904
1.73190	1.96499	2.24662	2.66003	3.26599	3.91097	3.93213
2.03015	2.24656	2.54465	3.01744	3.73417	4.53828	4.57440
2.42637	2.66002	3.01744	3.57382	4.56960	5.87496	6.06440
2.99472	3.26600	3.73414	4.56934	6.16732	9.91749	11.71553
3.59219	3.91097	4.53825	5.87493	9.91757	52.30151	222.37546
3.63904	3.93212	4.57439	6.06441	11.71555	222.37550	1000 ++++

TABLE 4.7 TOT. OPT. DEPTH = 2.0 ALBEDO = 0.3 G = 0.8

[SOLAR ZENITH ANGLE INCREASING ---->]

RATIO OF INTENSITIES UP OBSERVER AZIMUTH = 0 TAU = 0.000

1.51672	1.52263	1.52599	1.50959	1.44567	1.32435	1.17958
1.52263	1.52784	1.52951	1.51004	1.44041	1.31296	1.16284
1.52599	1.52951	1.52820	1.50485	1.43173	1.29696	1.14345
1.50958	1.51004	1.50485	1.47891	1.40564	1.26909	1.11879
1.44567	1.44041	1.43173	1.40564	1.33377	1.21295	1.08694
1.32435	1.31296	1.29696	1.26909	1.21295	1.12800	1.05382
1.17958	1.16284	1.14345	1.11878	1.08694	1.05381	1.02885

RATIO OF INTENSITIES DOWN OBSERVER AZIMUTH = 0 TAU = 0.000

0.0	0.0	0.0	0.0	0.0	0.0	0.0
0.0	0.0	0.0	0.0	0.0	0.0	0.0
0.0	0.0	0.0	0.0	0.0	0.0	0.0
0.0	0.0	0.0	0.0	0.0	0.0	0.0
0.0	0.0	0.0	0.0	0.0	0.0	0.0
0.0	0.0	0.0	0.0	0.0	0.0	0.0
0.0	0.0	0.0	0.0	0.0	0.0	0.0

RATIO OF INTENSITIES UP OBSERVER AZIMUTH = 90 TAU = 0.000

1.51682	1.52283	1.52729	1.51321	1.45291	1.33667	1.19330
1.52283	1.52859	1.53292	1.52009	1.46213	1.34609	1.20058
1.52729	1.53292	1.53834	1.52841	1.47615	1.36309	1.21350
1.51321	1.52009	1.52841	1.52701	1.48795	1.38520	1.23071
1.45291	1.46213	1.47615	1.48795	1.47429	1.39584	1.24477
1.33667	1.34609	1.36309	1.38520	1.39584	1.35416	1.22610
1.19330	1.20058	1.21350	1.23071	1.24476	1.22611	1.13327

RATIO OF INTENSITIES DOWN OBSERVER AZIMUTH = 90 TAU = 0.000

0.0	0.0	0.0	0.0	0.0	0.0	0.0
0.0	0.0	0.0	0.0	0.0	0.0	0.0
0.0	0.0	0.0	0.0	0.0	0.0	0.0
0.0	0.0	0.0	0.0	0.0	0.0	0.0
0.0	0.0	0.0	0.0	0.0	0.0	0.0
0.0	0.0	0.0	0.0	0.0	0.0	0.0
0.0	0.0	0.0	0.0	0.0	0.0	0.0

TABLE 4.7 (CONT.)   TOT. OPT. DEPTH = 2.0   ALBEDO = 0.3   G = 0.8

[SOLAR ZENITH ANGLE INCREASING ---->]

RATIO OF INTENSITIES UP   OBSERVER AZIMUTH = 180   TAU = 0.000

1.51682	1.52260	1.52766	1.51513	1.45767	1.34438	1.20360
1.52260	1.52836	1.53327	1.52265	1.46971	1.35968	1.21832
1.52766	1.53327	1.53938	1.53160	1.48387	1.37745	1.23327
1.51513	1.52265	1.53160	1.53029	1.49368	1.39515	1.24655
1.45767	1.46970	1.48387	1.49366	1.47772	1.39893	1.25121
1.34438	1.35967	1.37745	1.39513	1.39891	1.34744	1.21750
1.20360	1.21833	1.23327	1.24654	1.25124	1.21749	1.11981

RATIO OF INTENSITIES DOWN   OBSERVER AZIMUTH = 180   TAU = 0.000

0.0	0.0	0.0	0.0	0.0	0.0	0.0
0.0	0.0	0.0	0.0	0.0	0.0	0.0
0.0	0.0	0.0	0.0	0.0	0.0	0.0
0.0	0.0	0.0	0.0	0.0	0.0	0.0
0.0	0.0	0.0	0.0	0.0	0.0	0.0
0.0	0.0	0.0	0.0	0.0	0.0	0.0
0.0	0.0	0.0	0.0	0.0	0.0	0.0

RATIO OF INTENSITIES UP   OBSERVER AZIMUTH = 0   TAU = 0.500

1.73770	1.76904	1.82341	1.89500	2.02113	3.71949	1000 ++++
1.75437	1.78399	1.83300	1.89045	1.97518	3.33024	1000 ++++
1.78029	1.80698	1.84790	1.88652	1.92681	2.91477	1000 ++++
1.80101	1.82268	1.85211	1.86823	1.85894	2.48076	1000 ++++
1.78517	1.79786	1.81524	1.80819	1.73965	2.04587	1000 ++++
1.71879	1.72388	1.72387	1.68880	1.58072	1.67259	1000 ++++
1.64427	1.63979	1.62738	1.56897	1.43527	1.45206	1000 ++++

RATIO OF INTENSITIES DOWN   OBSERVER AZIMUTH = 0   TAU = 0.500

1.02654	1.06516	1.14006	1.21819	1.31515	1.45200	1.46901
1.06317	1.02945	1.07321	1.16975	1.28676	1.42028	1.49597
1.14021	1.07524	1.05657	1.09266	1.22588	1.38827	1.49810
1.21951	1.17920	1.09278	1.07150	1.12509	1.29361	[illegible]
1.32369	1.29112	1.22576	1.12549	1.08318	1.17956	1.32580
1.46067	[illegible]	1.40430	1.31387	1.18245	1.16722	1.37914
1.59577	1.58457	1.56746	1.49790	1.35071	1.35565	1000 ++++

TABLE 4.7 (CONT.) TOT. OPT. DEPTH = 2.0 ALBEDO = 0.3 G = 0.8

[SOLAR ZENITH ANGLE INCREASING ----]

RATIO OF INTENSITIES UP OBSERVER AZIMUTH = 90 TAU = 0.500

1.73821	1.77047	1.82875	1.91054	2.06594	4.05373	1000 ++++
1.75549	1.78782	1.84659	1.93163	2.09721	4.17977	1000 ++++
1.78319	1.81577	1.87690	1.96770	2.15189	4.40592	1000 ++++
1.80708	1.84152	1.90664	2.01029	2.22417	4.70224	1000 ++++
1.79566	1.83335	1.90604	2.02781	2.28461	4.92335	1000 ++++
1.73602	1.77495	1.85436	1.99499	2.28389	4.83225	1000 ++++
1.66373	1.70270	1.78220	1.92349	2.20931	4.32585	1000 ++++

RATIO OF INTENSITIES DOWN OBSERVER AZIMUTH = 90 TAU = 0.500

1.07215	1.12430	1.18143	1.24837	1.33951	1.44894	1.49422
1.12403	1.15690	1.20443	1.27115	1.36442	1.47604	1.52380
1.18175	1.20476	1.24795	1.31578	1.41329	1.53216	1.58595
1.25047	1.27348	1.31808	1.38881	1.49579	1.63268	1.70226
1.35013	1.37609	1.42628	1.50793	1.61988	1.80263	1.94862
1.49184	1.52215	1.58361	1.68894	1.85235	2.28476	3.55303
1.61578	1.65507	1.72915	1.86416	2.12721	3.76884	1000 ++++

RATIO OF INTENSITIES UP OBSERVER AZIMUTH = 180 TAU = 0.500

1.73857	1.77122	1.83231	1.92193	2.10112	4.32133	1000 ++++
1.75591	1.78976	1.85347	1.95291	2.16470	4.71660	1000 ++++
1.78453	1.81898	1.88682	1.99616	2.23823	5.11032	1000 ++++
1.81021	1.84722	1.91989	2.04118	2.31496	5.44678	1000 ++++
1.80181	1.84407	1.92304	2.05911	2.36445	5.57083	1000 ++++
1.74451	1.79048	1.87502	2.02238	2.34137	5.25768	1000 ++++
1.67625	1.72205	1.80579	1.94994	2.24470	4.53224	1000 ++++

RATIO OF INTENSITIES DOWN OBSERVER AZIMUTH = 180 TAU = 0.500

1.09477	1.13022	1.20085	1.26469	1.35536	1.45625	1.49579
1.13027	1.16977	1.23468	1.29818	1.38630	1.48779	1.52554
1.20113	1.23511	1.27992	1.34641	1.43796	1.54397	1.58429
1.30764	1.33225	1.36056	1.41359	1.51755	1.64166	1.70207
1.46674	1.48545	1.49776	1.53523	1.62131	1.80033	1.95310
1.59571	1.59667	1.61167	1.71338	1.86021	2.26717	3.62817
1.62693	1.62436	1.72387	1.88983	2.15197	3.86532	1000 ++++

TABLE 4.7 (CONT.) TOT. OPT. DEPTH = 2.0 ALBEDO = 0.3 G = 0.8

[SOLAR ZENITH ANGLE INCREASING -----]

RATIO OF INTENSITIES UP OBSERVER AZIMUTH = 0 TAU = 1.000

1.90842	1.96458	2.07456	2.27349	2.95679	37.39584	1000 ++++
1.93352	1.98640	2.08637	2.25522	2.80632	30.02631	1000 ++++
1.97983	2.02829	2.11454	2.24515	2.65640	22.73589	1000 ++++
2.04001	2.08105	2.14698	2.22859	2.48297	15.83120	1000 ++++
2.08143	2.10770	2.14762	2.17055	2.24392	9.67307	1000 ++++
2.05884	2.07137	2.07681	2.03483	1.97183	5.77702	1000 ++++
2.00432	2.00263	1.98611	1.89652	1.74841	3.86343	1000 ++++

RATIO OF INTENSITIES DOWN OBSERVER AZIMUTH = 0 TAU = 1.000

1.05388	1.13021	1.29167	1.45224	1.63545	1.81381	1.84208
1.13022	1.06026	1.15074	1.35060	1.58206	1.79681	1.85102
1.29183	1.15077	1.07475	1.18050	1.45406	1.73926	1.84864
1.45366	1.35135	1.18961	1.10 34	1.25152	1.58125	1.76149
1.64422	1.58718	1.45628	1.25211	1.16877	1.37300	1.59312
1.85458	1.82678	1.75854	1.59102	1.37668	1.65853	3.10825
1.96812	1.95652	1.93211	1.81933	1.62736	3.16472	1000 ++++

RATIO OF INTENSITIES UP OBSERVER AZIMUTH = 90 TAU = 1.000

1.90972	1.96835	2.08650	2.30906	3.09776	43.95659	1000 ++++
1.93653	1.99606	2.11666	2.34816	3.17799	46.25937	1000 ++++
1.98593	2.04716	2.17396	2.42116	3.32542	50.46678	1000 ++++
2.05110	2.11637	2.25200	2.52627	3.53825	56.07448	1000 ++++
2.09980	2.17064	2.31890	2.62485	3.74751	60.05214	1000 ++++
2.08827	2.16200	2.32167	2.65789	3.85014	57.30388	1000 ++++
2.03747	2.11327	2.27693	2.61843	3.78163	47.92648	1000 ++++

RATIO OF INTENSITIES DOWN OBSERVER AZIMUTH = 90 TAU = 1.000

1.14891	1.25925	1.57991	1.51420	1.66265	1.84774	1.85859
1.25928	1.32855	1.42809	1.56156	1.73866	1.91103	1.92262
1.38025	1.42648	1.51752	1.65370	1.84528	2.04900	2.06555
1.51662	1.56411	1.65642	1.80447	2.04078	2.33224	2.36640
1.69502	1.75039	1.86114	2.05574	2.39933	3.11657	3.40071
1.89620	1.96595	2.11199	2.40562	3.19070	10.56656	37.11110
2.00220	2.07726	2.23951	2.57650	3.66011	25.97644	1000 ++++

TABLE 4.7 (CONT.) TOT. OPT. DEPTH = 2.0 ALBEDO = 0.3 G = 0.8

[SOLAR ZENITH ANGLE INCREASING ----->]

RATIO OF INTENSITIES UP OBSERVER AZIMUTH = 180 TAU = 1.000

1.91082	1.97115	2.09570	2.33732	3.21515	49.60272	1000 ++++
1.93855	2.00265	2.13567	2.40471	3.41707	58.21622	1000 ++++
1.98974	2.05723	2.20170	2.50086	3.65557	67.36661	1000 ++++
2.05774	2.13123	2.28853	2.62134	3.92559	75.88985	1000 ++++
2.11115	2.19393	2.36460	2.72995	4.15387	79.69389	1000 ++++
2.10346	2.19306	2.37418	2.75837	4.19475	72.75104	1000 ++++
2.05850	2.14926	2.33221	2.71261	4.05431	58.27740	1000 ++++

RATIO OF INTENSITIES DOWN OBSERVER AZIMUTH = 180 TAU = 1.000

1.19689	1.31490	1.42080	1.54632	1.70834	1.86257	1.86671
1.31496	1.39860	1.49052	1.61370	1.77771	1.93776	1.93495
1.42140	1.49129	1.58066	1.71292	1.89579	2.08515	2.08532
1.54975	1.61842	1.71790	1.85356	2.09455	2.38518	2.41712
1.72389	1.79788	1.91933	2.11651	2.43756	3.22331	3.58150
1.92073	2.00812	2.16827	2.47869	3.31603	11.67786	43.76620
2.02396	2.11551	2.29480	2.66484	3.90993	46.19073	1000 ++++

RATIO OF INTENSITIES UP OBSERVER AZIMUTH = 0 TAU = 1.500

1.99967	2.07604	2.23791	2.59566	4.50987	544.06421	1000 ++++
2.02687	2.09833	2.24579	2.55573	4.14793	422.65186	1000 ++++
2.08307	2.14933	2.27960	2.53413	3.80725	309.24243	1000 ++++
2.17390	2.23282	2.33931	2.52544	3.46037	207.32935	1000 ++++
2.28786	2.33059	2.40336	2.50109	3.05093	122.37816	1000 ++++
2.36409	2.38554	2.40407	2.38873	2.60586	63.40099	1000 ++++
2.35214	2.35062	2.33113	2.23190	2.23118	35.21785	1000 ++++

RATIO OF INTENSITIES DOWN OBSERVER AZIMUTH = 0 TAU = 1.500

1.08276	1.20156	1.45862	1.71521	1.98796	2.18962	2.19256
1.29186	1.09269	1.25386	1.55029	1.90253	2.16100	2.19662
1.44907	1.2339	1.11518	1.29408	1.70317	2.07477	2.16606
1.51567	1.57027	1.29426	1.16144	1.39272	1.85663	2.07416
1.99689	1.90883	1.70554	1.39338	1.27849	1.64827	1.99022
2.2922	2.19501	2.09595	1.86782	1.65317	2.32046	24.75546
2.32569	2.3127	2.27937	2.14096	2.03593	25.36105	1000 ++++

TABLE 4.7 (CONT.) TOT. OPT. DEPTH = 2.0 ALBEDO = 0.3 G = 0.8

[SOLAR ZENITH ANGLE INCREASING --->]

RATIO OF INTENSITIES UP OBSERVER AZIMUTH = 90 TAU = 1.500

2.00194	2.08260	2.25742	2.65645	4.85356	658.58325	1000 ++++
2.03214	2.11475	2.29488	2.71285	5.03923	704.07007	1000 ++++
2.09264	2.17908	2.37139	2.82497	5.40067	793.11401	1000 ++++
2.18976	2.28407	2.49531	3.01044	5.98722	931.81250	1000 ++++
2.31349	2.41949	2.65903	3.25605	6.76826	1000 ++++	1000 ++++
2.40765	2.52329	2.79164	3.47054	7.38029	1000 ++++	1000 ++++
2.40408	2.52576	2.80629	3.50529	7.36733	926.93848	1000 ++++

RATIO OF INTENSITIES DOWN OBSERVER AZIMUTH = 90 TAU = 1.500

1.23100	1.40752	1.60365	1.81828	2.06744	2.24960	2.22855
1.40755	1.52049	1.68360	1.89889	2.16504	2.36123	2.33685
1.60401	1.68397	1.83231	2.05992	2.37282	2.62013	2.58962
1.82066	1.90160	2.06269	2.33519	2.79547	3.25007	3.22896
2.07995	2.17913	2.38929	2.81229	3.83630	6.09566	6.70981
2.30224	2.41940	2.68905	3.33603	6.21574	118.25345	706.19702
2.38296	2.50543	2.78764	3.48517	7.18899	738.39185	1000 ++++

RATIO OF INTENSITIES UP OBSERVER AZIMUTH = 180 TAU = 1.500

2.00397	2.08796	2.27337	2.70678	5.15036	760.95312	1000 ++++
2.03618	2.12707	2.32855	2.81683	5.66626	929.26221	1000 ++++
2.09940	2.19738	2.42069	2.97544	6.31098	1000 ++++	1000 ++++
2.20008	2.30926	2.55998	3.19900	7.14059	1000 ++++	1000 ++++
2.32990	2.45663	2.74149	3.48125	8.10560	1000 ++++	1000 ++++
2.43120	2.57547	2.89352	3.71470	8.74290	1000 ++++	1000 ++++
2.43749	2.58643	2.91743	3.74668	8.56195	1000 ++++	1000 ++++

RATIO OF INTENSITIES DOWN OBSERVER AZIMUTH = 180 TAU = 1.500

1.30776	1.49880	1.67196	1.87199	2.11131	2.27881	2.24952
1.49886	1.63720	1.78857	1.98790	2.23911	2.41885	2.37650
1.67253	1.78902	1.94615	2.16337	2.43736	2.71177	2.66444
1.87333	1.99254	2.17026	2.43640	2.93256	3.42224	3.40995
2.12696	2.25861	2.49863	2.95712	4.05573	6.75520	7.64957
2.33926	2.49277	2.80255	3.53458	6.91496	147.79265	952.57764
2.41608	2.57252	2.89993	3.71698	8.37504	978.86230	1000 ++++

TABLE 4.7 (CONT.)   TOT. OPT. DEPTH = 2.0   ALBEDO = 0.3   G = 0.8

[SOLAR ZENITH ANGLE INCREASING ---->]

RATIO OF INTENSITIES UP   OBSERVER AZIMUTH = 0 TAU = 2.000

0.0	0.0	0.0	0.0	0.0	0.0	0.0
0.0	0.0	0.0	0.0	0.0	0.0	0.0
0.0	0.0	0.0	0.0	0.0	0.0	0.0
0.0	0.0	0.0	0.0	0.0	0.0	0.0
0.0	0.0	0.0	0.0	0.0	0.0	0.0
0.0	0.0	0.0	0.0	0.0	0.0	0.0
0.0	0.0	0.0	0.0	0.0	0.0	0.0

RATIO OF INTENSITIES DOWN   OBSERVER AZIMUTH = 0 TAU = 2.000

1.11313	1.27848	1.64255	2.00965	2.36890	2.57660	2.55873
1.27848	1.12687	1.32328	1.76967	2.24704	2.53024	2.55380
1.64254	1.32328	1.15826	1.40815	1.97053	2.41437	2.53638
2.00965	1.76967	1.40815	1.22467	1.55539	2.15582	2.42820
2.36890	2.24704	1.97053	1.55539	1.43708	2.11130	2.71006
2.57659	2.53024	2.41437	2.15582	2.11130	45.95488	370.30493
2.55875	2.55380	2.53638	2.42820	2.71006	370.30469	1000 ++++

RATIO OF INTENSITIES UP   OBSERVER AZIMUTH = 90 TAU = 2.000

0.0	0.0	0.0	0.0	0.0	0.0	0.0
0.0	0.0	0.0	0.0	0.0	0.0	0.0
0.0	0.0	0.0	0.0	0.0	0.0	0.0
0.0	0.0	0.0	0.0	0.0	0.0	0.0
0.0	0.0	0.0	0.0	0.0	0.0	0.0
0.0	0.0	0.0	0.0	0.0	0.0	0.0
0.0	0.0	0.0	0.0	0.0	0.0	0.0

RATIO OF INTENSITIES DOWN   OBSERVER AZIMUTH = 90 TAU = 2.000

1.31880	1.57046	1.85602	2.16562	2.49212	2.67245	2.62254
1.57046	1.73530	1.97646	2.29281	2.65192	2.84697	2.78848
1.85602	1.97647	2.20310	2.55585	3.01595	3.27888	3.20168
2.16562	2.29281	2.55584	3.03681	3.88341	4.52628	4.44113
2.49213	2.65193	3.01592	3.88344	6.82344	13.64949	15.24861
2.67242	2.84697	3.27888	4.52629	13.64949	1000 ++++	1000 ++++
2.62254	2.78848	3.20169	4.44112	15.24857	1000 ++++	1000 ++++

TABLE 4.7 (CONT.) TOT. OPT. DEPTH = 2.0 ALBEDO = 0.3 G = 0.8

[SOLAR ZENITH ANGLE INCREASING ---->]

RATIO OF INTENSITIES UP OBSERVER AZIMUTH = 180 TAU = 2.000

0.0	0.0	0.0	0.0	0.0	0.0	0.0
0.0	0.0	0.0	0.0	0.0	0.0	0.0
0.0	0.0	0.0	0.0	0.0	0.0	0.0
0.0	0.0	0.0	0.0	0.0	0.0	0.0
0.0	0.0	0.0	0.0	0.0	0.0	0.0
0.0	0.0	0.0	0.0	0.0	0.0	0.0
0.0	0.0	0.0	0.0	0.0	0.0	0.0

RATIO OF INTENSITIES DOWN OBSERVER AZIMUTH = 180 TAU = 2.000

1.42813	1.70413	1.95906	2.24859	2.56244	2.72353	2.66301
1.70413	1.91008	2.13746	2.43433	2.77792	2.95403	2.87194
1.95906	2.15746	2.37391	2.73374	3.20586	3.46771	3.36810
2.24859	2.43432	2.73374	3.23604	4.20305	4.95874	4.89413
2.56244	2.77791	3.20587	4.20297	7.66876	16.47729	19.02090
2.72353	2.95403	3.46769	4.95872	16.47685	1000 ++++	1000 ++++
2.66301	2.87194	3.36810	4.89415	19.02110	1000 ++++	1000 ++++

TABLE 4.8 TOT. OPT. DEPTH = 0.5 ALBEDO = 0.6 G = 0.8

[SOLAR ZENITH ANGLE INCREASING ----->]

RATIO OF INTENSITIES UP OBSERVER AZIMUTH = 0 TAU = 0.000

1.55089	1.58593	1.65119	1.74452	1.81821	1.72960	1.42130
1.58593	1.62379	1.69053	1.78002	1.83438	1.71388	1.38413
1.65119	1.69053	1.75542	1.83351	1.85831	1.68859	1.33964
1.74452	1.78002	1.83351	1.86500	1.85932	1.63151	1.27956
1.81821	1.83439	1.85831	1.85933	1.75493	1.49826	1.19973
1.72960	1.71387	1.68859	1.63150	1.49826	1.29235	1.11885
1.42130	1.38414	1.33964	1.27956	1.19973	1.11885	1.06116

RATIO OF INTENSITIES DOWN OBSERVER AZIMUTH = 0 TAU = 0.000

0.0	0.0	0.0	0.0	0.0	0.0	0.0
0.0	0.0	0.0	0.0	0.0	0.0	0.0
0.0	0.0	0.0	0.0	0.0	0.0	0.0
0.0	0.0	0.0	0.0	0.0	0.0	0.0
0.0	0.0	0.0	0.0	0.0	0.0	0.0
0.0	0.0	0.0	0.0	0.0	0.0	0.0
0.0	0.0	0.0	0.0	0.0	0.0	0.0

RATIO OF INTENSITIES UP OBSERVER AZIMUTH = 90 TAU = 0.000

1.54928	1.58211	1.64629	1.74154	1.82440	1.75492	1.45370
1.58211	1.61502	1.67937	1.77587	1.86044	1.78767	1.47679
1.64628	1.67937	1.74497	1.84302	1.92978	1.85203	1.52063
1.74154	1.77587	1.84302	1.94549	2.03537	1.95119	1.58563
1.82440	1.86044	1.92979	2.03538	2.13164	2.04155	1.64690
1.75492	1.78767	1.85203	1.95118	2.04151	1.96083	1.59104
1.45370	1.47679	1.52063	1.58563	1.64691	1.59105	1.31925

RATIO OF INTENSITIES DOWN OBSERVER AZIMUTH = 90 TAU = 0.000

0.0	0.0	0.0	0.0	0.0	0.0	0.0
0.0	0.0	0.0	0.0	0.0	0.0	0.0
0.0	0.0	0.0	0.0	0.0	0.0	0.0
0.0	0.0	0.0	0.0	0.0	0.0	0.0
0.0	0.0	0.0	0.0	0.0	0.0	0.0
0.0	0.0	0.0	0.0	0.0	0.0	0.0
0.0	0.0	0.0	0.0	0.0	0.0	0.0

TABLE 4.8 (CONT.)   TOT. OPT. DEPTH = 0.5   ALBEDO = 0.6   G = 0.8

[SOLAR ZENITH ANGLE INCREASING ---->]

RATIO OF INTENSITIES UP   OBSERVER AZIMUTH = 180   TAU = 0.000

1.54762	1.57803	1.64074	1.73673	1.82618	1.76886	1.47708
1.57803	1.60617	1.66669	1.76342	1.85976	1.81088	1.51657
1.64074	1.66669	1.72694	1.82491	1.92468	1.87559	1.56557
1.73673	1.76342	1.82492	1.92540	2.02735	1.96784	1.62439
1.82617	1.85977	1.92468	2.02735	2.12865	2.05098	1.66826
1.76885	1.81087	1.87560	1.96784	2.05105	1.95386	1.57907
1.47708	1.51657	1.56558	1.62444	1.66828	1.57866	1.29243

RATIO OF INTENSITIES DOWN   OBSERVER AZIMUTH = 180   TAU = 0.000

0.0	0.0	0.0	0.0	0.0	0.0	0.0
0.0	0.0	0.0	0.0	0.0	0.0	0.0
0.0	0.0	0.0	0.0	0.0	0.0	0.0
0.0	0.0	0.0	0.0	0.0	0.0	0.0
0.0	0.0	0.0	0.0	0.0	0.0	0.0
0.0	0.0	0.0	0.0	0.0	0.0	0.0
0.0	0.0	0.0	0.0	0.0	0.0	0.0

RATIO OF INTENSITIES UP   OBSERVER AZIMUTH = 0   TAU = 0.125

1.58501	1.62935	1.71447	1.84607	1.99751	2.17483	22.72131
1.62084	1.66858	1.75564	1.88266	2.00863	2.12302	19.41878
1.69033	1.74113	1.82803	1.94394	2.03394	2.05953	15.81057
1.80055	1.85091	1.93012	2.02054	2.04921	1.96104	11.74555
1.92804	1.96414	2.01862	2.05618	1.97754	1.78004	7.66330
1.95949	1.96551	1.96620	1.92355	1.76127	1.51846	4.59384
1.78337	1.75753	1.72171	1.64121	1.47787	1.30630	2.87021

RATIO OF INTENSITIES DOWN   OBSERVER AZIMUTH = 0   TAU = 0.125

1.01313	1.03170	1.07240	1.12305	1.20663	1.31567	1.38106
1.03170	1.01475	1.03724	1.09157	1.17702	1.29178	1.37725
1.07251	1.03727	1.01660	1.04906	1.13189	1.25679	1.37059
1.12443	1.09217	1.04921	1.02760	1.07309	1.19653	1.33362
1.21874	1.18460	1.13551	1.07417	1.05148	1.11932	1.24077
1.38312	1.34475	1.29216	1.21755	1.12656	1.10502	1.16486
1.60340	1.56514	1.52105	1.43920	1.50048	1.19556	1.55594

TABLE 4.8 (CONT.) TOT. OPT. DEPTH = 0.5 ALBEDO = 0.6 G = 0.8

|SOLAR ZENITH ANGLE INCREASING ----> |

RATIO OF INTENSITIES UP OBSERVER AZIMUTH = 90 TAU = 0.125

1.58330	1.62533	1.70970	1.84481	2.01133	2.23656	25.55476
1.61670	1.65918	1.74456	1.88295	2.05654	2.29755	27.21570
1.68452	1.72791	1.81638	1.96046	2.14674	2.42095	30.42851
1.79526	1.84136	1.93474	2.09090	2.29802	2.62726	35.35097
1.92971	1.98039	2.08231	2.25447	2.49450	2.88839	40.52437
1.98100	2.03323	2.14073	2.32528	2.58226	2.98535	37.96236
1.81781	1.86452	1.95877	2.11742	2.33727	2.60799	20.36819

RATIO OF INTENSITIES DOWN OBSERVER AZIMUTH = 90 TAU = 0.125

1.03606	1.06310	1.09677	1.14704	1.23390	1.33921	1.38902
1.06312	1.08151	1.11232	1.16538	1.25638	1.36145	1.40874
1.09703	1.11260	1.14491	1.20390	1.30215	1.40731	1.44946
1.14933	1.16808	1.20686	1.27562	1.38513	1.48986	1.52259
1.25036	1.27506	1.32440	1.40849	1.52531	1.62195	1.64228
1.42345	1.45362	1.51415	1.61490	1.74155	1.80806	1.83306
1.63990	1.67805	1.75402	1.87924	2.04270	2.16129	3.75628

RATIO OF INTENSITIES UP OBSERVER AZIMUTH = 180 TAU = 0.125

1.58154	1.62106	1.70419	1.84124	2.01878	2.27608	27.74509
1.61230	1.64973	1.73164	1.87242	2.06599	2.36862	31.26591
1.67810	1.71647	1.79674	1.94235	2.15287	2.50289	35.49341
1.78851	1.82459	1.91177	2.06847	2.29903	2.70188	40.53488
1.92730	1.97125	2.06697	2.23859	2.49583	2.94874	44.89142
1.98974	2.04574	2.15078	2.32983	2.59109	3.00800	40.33838
1.84044	1.89923	1.99530	2.14642	2.34913	2.57966	20.63806

RATIO OF INTENSITIES DOWN OBSERVER AZIMUTH = 180 TAU = 0.125

1.04760	1.07752	1.11051	1.16305	1.25256	1.35317	1.39305
1.07755	1.10286	1.13775	1.19560	1.28957	1.38558	1.41249
1.11093	1.13810	1.17890	1.24328	1.34268	1.43316	1.44954
1.16614	1.19982	1.24803	1.31791	1.42586	1.51052	1.51722
1.27261	1.31520	1.37367	1.45686	1.55322	1.62811	1.62635
1.44556	1.49903	1.56047	1.66347	1.76569	1.76535	1.76704
1.66526	1.72036	1.80049	1.91807	2.03973	2.12653	3.06071

TABLE 4.8 (CONT.) TOT. OPT. DEPTH = 0.5 ALBEDO = 0.6 G = 0.8

[SOLAR ZENITH ANGLE INCREASING ---->]

RATIO OF INTENSITIES UP OBSERVER AZIMUTH = 0 TAU = 0.250

1.59878	1.64940	1.74790	1.90538	2.11948	2.70942	1000 ++++
1.63229	1.68630	1.78633	1.93747	2.11949	2.59880	1000 ++++
1.69932	1.75716	1.85764	1.99699	2.13720	2.47536	948.18433
1.81338	1.87337	1.96903	2.08412	2.15644	2.31832	675.69604
1.97281	2.02404	2.10086	2.16470	2.11370	2.08320	415.78223
2.09752	2.12408	2.14880	2.12067	1.94686	1.76773	225.65625
2.04021	2.03007	2.00690	1.91097	1.68383	1.50124	111.65099

RATIO OF INTENSITIES DOWN OBSERVER AZIMUTH = 0 TAU = 0.250

1.02649	1.06396	1.14475	1.23753	1.37498	1.55294	1.68378
1.06396	1.02973	1.07485	1.18032	1.33019	1.52276	1.68472
1.14486	1.07487	1.03732	1.09725	1.25098	1.46956	1.67949
1.23889	1.18091	1.09740	1.05435	1.13914	1.36096	1.61023
1.38659	1.33754	1.25451	1.14021	1.09501	1.21280	1.43157
1.62001	1.57429	1.50464	1.37992	1.22002	1.18195	1.32325
1.90523	1.87511	1.83540	1.72243	1.49656	1.35873	9.49570

RATIO OF INTENSITIES UP OBSERVER AZIMUTH = 90 TAU = 0.250

1.59718	1.64572	1.74416	1.90719	2.14293	2.82795	1000 ++++
1.62836	1.67757	1.77761	1.94552	2.19348	2.92734	1000 ++++
1.69547	1.74407	1.84847	2.02535	2.29643	3.13221	1000 ++++
1.80692	1.86121	1.97298	2.16816	2.47885	3.49241	1000 ++++
1.97080	2.03183	2.15731	2.38049	2.75729	4.02792	1000 ++++
2.11397	2.18161	2.32420	2.58350	3.02719	4.50715	1000 ++++
2.07323	2.14159	2.28343	2.53660	2.96110	4.17139	1000 ++++

RATIO OF INTENSITIES DOWN OBSERVER AZIMUTH = 90 TAU = 0.250

1.07285	1.12695	1.19081	1.27745	1.41512	1.58582	1.69560
1.12697	1.16246	1.21867	1.30821	1.45166	1.62434	1.73663
1.19106	1.21891	1.27454	1.37123	1.52542	1.70428	1.82266
1.27907	1.31082	1.37409	1.48336	1.65625	1.84797	1.98055
1.43084	1.46956	1.54683	1.67893	1.86553	2.07429	2.26108
1.66677	1.71534	1.80849	1.97207	2.19686	2.44024	2.64116
1.94577	2.00500	2.13100	2.35246	2.70362	3.47885	109.38150

TABLE 4.8 (CONT.) TOT. OPT. DEPTH = 0.5 ALBEDO = 0.6 G = 0.8

[SOLAR ZENITH ANGLE INCREASING ---->]

RATIO OF INTENSITIES UP OBSERVER AZIMUTH = 180 TAU = 0.250

1.59553	1.64175	1.73955	1.90617	2.15803	2.90968	1000 ++++
1.62415	1.66869	1.76641	1.93985	2.21757	3.08031	1000 ++++
1.68698	1.72976	1.83029	2.01373	2.32064	3.31970	1000 ++++
1.79894	1.84267	1.94920	2.14913	2.49773	3.68150	1000 ++++
1.96516	2.01665	2.13581	2.36284	2.77293	4.20435	1000 ++++
2.11729	2.18368	2.32250	2.58063	3.04687	4.63489	1000 ++++
2.09272	2.16814	2.30997	2.55882	2.97898	4.19695	1000 ++++

RATIO OF INTENSITIES DOWN OBSERVER AZIMUTH = 180 TAU = 0.250

1.09609	1.15485	1.21456	1.30169	1.44070	1.60354	1.70080
1.15488	1.20061	1.25895	1.35132	1.49508	1.65415	1.74025
1.21495	1.25955	1.32221	1.42415	1.57667	1.73541	1.82137
1.30468	1.35544	1.42867	1.53423	1.70532	1.87192	1.97405
1.45977	1.51944	1.60618	1.73472	1.89015	2.07828	2.24548
1.69476	1.76277	1.86403	2.02030	2.21787	2.40985	2.99813
1.96848	2.04351	2.17135	2.38681	2.72166	3.45517	113.08446

RATIO OF INTENSITIES UP OBSERVER AZIMUTH = 0 TAU = 0.375

1.59146	1.64511	1.74999	1.92000	2.17706	3.30253	1000 ++++
1.61945	1.67583	1.78094	1.94188	2.15980	3.10540	1000 ++++
1.67696	1.73702	1.84199	1.98934	2.15997	2.89535	1000 ++++
1.78073	1.84450	1.94634	2.07055	2.17074	2.86154	1000 ++++
1.94505	2.00865	2.09829	2.17795	2.15204	2.37719	1000 ++++
2.13754	2.18202	2.22767	2.21525	2.04982	2.04201	1000 ++++
2.21748	2.22792	2.22275	2.12069	1.85443	1.76538	1000 ++++

RATIO OF INTENSITIES DOWN OBSERVER AZIMUTH = 0 TAU = 0.375

1.04020	1.09739	1.22090	1.35906	1.53362	1.80856	1.97012
1.09739	1.04513	1.11390	1.27380	1.49266	1.77205	1.97499
1.22096	1.11392	1.05001	1.14752	1.37617	1.69842	1.96895
1.36806	1.27424	1.14744	1.08185	1.20729	1.53541	1.86506
1.56227	1.49821	1.27890	1.20813	1.13932	1.31168	1.60959
1.68926	1.61254	1.32667	1.25117	1.11795	1.27566	1.54065
2.15061	2.13566	2.10270	1.96475	1.67026	1.52956	393.94159

TABLE 4.8 (CONT.) TOT. OPT. DEPTH = 0.5 ALBEDO = 0.6 G = 0.8

|SOLAR ZENITH ANGLE INCREASING -----> |

RATIO OF INTENSITIES UP OBSERVER AZIMUTH = 90 TAU = 0.375

1.59019	1.64230	1.74818	1.92612	2.21151	3.49994	1000 ++++
1.61626	1.66911	1.77684	1.96057	2.26219	3.64313	1000 ++++
1.67195	1.72635	1.83896	2.03349	2.36633	3.94113	1000 ++++
1.77433	1.83266	1.95362	2.16987	2.55720	4.48182	1000 ++++
1.94321	2.00917	2.14642	2.39823	2.88103	5.37782	1000 ++++
2.14735	2.22344	2.38636	2.69475	3.30640	6.55009	1000 ++++
2.24460	2.33049	2.51252	2.85407	3.53326	6.87737	1000 ++++

RATIO OF INTENSITIES DOWN OBSERVER AZIMUTH = 90 TAU = 0.375

1.11096	1.19400	1.29068	1.41632	1.60755	1.85232	1.98769
1.19401	1.24815	1.33191	1.46061	1.65992	1.91132	2.05336
1.29086	1.35212	1.41308	1.55028	1.76537	2.03480	2.19271
1.41794	1.46253	1.55241	1.70589	1.95061	2.25920	2.45560
1.61917	1.67317	1.78132	1.96771	2.24174	2.62910	2.97841
1.91417	1.97961	2.11555	2.35734	2.73074	3.42366	5.30756
2.18780	2.27090	2.44581	2.76935	3.37863	5.83665	1000 ++++

RATIO OF INTENSITIES UP OBSERVER AZIMUTH = 180 TAU = 0.375

1.58885	1.63916	1.74535	1.92886	2.23582	3.64296	1000 ++++
1.61274	1.66200	1.76935	1.96259	2.30467	3.91818	1000 ++++
1.66627	1.71414	1.82537	2.03169	2.41448	4.29103	1000 ++++
1.76651	1.81512	1.93328	2.16006	2.60146	4.85485	1000 ++++
1.93544	1.99065	2.12302	2.38458	2.91881	5.75156	1000 ++++
2.14501	2.21536	2.37445	2.68788	3.34428	6.89004	1000 ++++
2.25785	2.34426	2.52507	2.86891	3.56838	7.09288	1000 ++++

RATIO OF INTENSITIES DOWN OBSERVER AZIMUTH = 180 TAU = 0.375

1.14672	1.23665	1.32547	1.44939	1.64037	1.87449	1.99530
1.23668	1.30489	1.38885	1.51750	1.71416	1.94834	2.05966
1.32573	1.38921	1.47670	1.61767	1.82847	2.07411	2.19517
1.45157	1.52049	1.62092	1.76638	2.00981	2.29195	2.45754
1.65436	1.73195	1.85008	2.03172	2.26671	2.64132	2.98368
1.94365	2.03647	2.17197	2.40715	2.75537	3.39930	5.36586
2.20925	2.30145	2.47675	2.79918	3.40928	5.92455	1000 ++++

TABLE 4.8 (CONT.) TOT. OPT. DEPTH = 0.5 ALBEDO = 0.6 G = 0.8

[SOLAR ZENITH ANGLE INCREASING ---->]

RATIO OF INTENSITIES UP OBSERVER AZIMUTH = 0 TAU = 0.500

0.0	0.0	0.0	0.0	0.0	0.0	0.0
0.0	0.0	0.0	0.0	0.0	0.0	0.0
0.0	0.0	0.0	0.0	0.0	0.0	0.0
0.0	0.0	0.0	0.0	0.0	0.0	0.0
0.0	0.0	0.0	0.0	0.0	0.0	0.0
0.0	0.0	0.0	0.0	0.0	0.0	0.0
0.0	0.0	0.0	0.0	0.0	0.0	0.0

RATIO OF INTENSITIES DOWN OBSERVER AZIMUTH = 0 TAU = 0.500

1.05427	1.13203	1.30098	1.48795	1.74357	2.08035	2.25332
1.13202	1.06095	1.15447	1.37223	1.66525	2.03713	2.26087
1.30098	1.15447	1.07649	1.19940	1.50809	1.94093	2.25160
1.48795	1.37223	1.19940	1.11019	1.27803	1.71890	2.11068
1.74357	1.66525	1.50809	1.27803	1.18498	1.41806	1.78699
2.08035	2.03713	1.94093	1.71890	1.41806	1.39685	1.86567
2.25332	2.26087	2.25160	2.11068	1.78699	1.86567	1000 ++++

RATIO OF INTENSITIES UP OBSERVER AZIMUTH = 90 TAU = 0.500

0.0	0.0	0.0	0.0	0.0	0.0	0.0
0.0	0.0	0.0	0.0	0.0	0.0	0.0
0.0	0.0	0.0	0.0	0.0	0.0	0.0
0.0	0.0	0.0	0.0	0.0	0.0	0.0
0.0	0.0	0.0	0.0	0.0	0.0	0.0
0.0	0.0	0.0	0.0	0.0	0.0	0.0
0.0	0.0	0.0	0.0	0.0	0.0	0.0

RATIO OF INTENSITIES DOWN OBSERVER AZIMUTH = 90 TAU = 0.500

1.15044	1.26436	1.39660	1.56402	1.81236	2.13684	2.27665
1.26436	1.33872	1.45243	1.62300	1.88245	2.22077	2.37218
1.39660	1.45241	1.56078	1.74135	2.02353	2.39817	2.57305
1.56402	1.62300	1.74137	1.94269	2.27000	2.72666	2.96345
1.81237	1.88246	2.02352	2.26999	2.65474	3.31247	3.83461
2.13684	2.22077	2.39818	2.72685	3.31247	4.96719	9.67315
2.27665	2.37218	2.57305	2.96345	3.83460	9.67315	1000 ++++

TABLE 4.8 (CONT.) TOT. OPT. DEPTH = 0.5 ALBEDO = 0.6 G = 0.8

[SOLAR ZENITH ANGLE INCREASING -----]

RATIO OF INTENSITIES UP OBSERVER AZIMUTH = 180 TAU = 0.500

0.0	0.0	0.0	0.0	0.0	0.0	0.0
0.0	0.0	0.0	0.0	0.0	0.0	0.0
0.0	0.0	0.0	0.0	0.0	0.0	0.0
0.0	0.0	0.0	0.0	0.0	0.0	0.0
0.0	0.0	0.0	0.0	0.0	0.0	0.0
0.0	0.0	0.0	0.0	0.0	0.0	0.0
0.0	0.0	0.0	0.0	0.0	0.0	0.0

RATIO OF INTENSITIES DOWN OBSERVER AZIMUTH = 180 TAU = 0.500

1.19958	1.32309	1.44350	1.60653	1.85279	2.16440	2.28998
1.32308	1.41586	1.52730	1.69439	1.94808	2.26701	2.38409
1.44350	1.52729	1.64125	1.82365	2.09950	2.44932	2.58452
1.60653	1.69440	1.82362	2.01289	2.34122	2.77509	2.98338
1.85280	1.94808	2.09955	2.34119	2.68323	3.34742	3.88719
2.16440	2.26701	2.44933	2.77522	3.34709	5.00819	10.08241
2.28998	2.38409	2.58451	2.98336	3.88709	10.08148	1000 ++++

TABLE 4.9 RATIO OF LOWTRANSX TO PLANE PARALLEL INTENSITIES FOR THE CASE OF ISOTROPIC SCATTERING USING 1962 STANDARD ATMOSPHERE AT 11 μm (Single Scattering)

[OBSERVER AND SOLAR ZENITH ANGLES..... 12.95, 82.57, 88.54]

OBSERVER AT 100 KM G= 0 ISOTROPIC

INTENSITY UP → Solar angles

Observer angles ↓			
	1.00215626	1.05774879	2.29551697
	0.000714218	0.001250958	0.007708263
	0.000000213	0.000000290	0.000000940

INTENSITY DOWN

0.0	0.0	0.0
0.0	0.0	0.0
0.0	0.0	0.0

OBSERVER AT 2 KM G= 0 ISOTROPIC

INTENSITY UP

1.00154781	1.06007195	2.58837509
1.01964569	1.09133911	2.50554466
1.17455769	1.28038597	2.69621849

INTENSITY DOWN

1.00000000	1.00567627	1.34543324
0.995656371	0.999867260	1 33298016
0.971774220	0.969370544	1.27793026

OBSERVER AT GROUND G= 0 ISOTROPIC

INTENSITY UP

0.0	0.0	0.0
0.0	0.0	0.0
0.0	0.0	0.0

INTENSITY DOWN

1.00028706	1.05090427	2.34002876
1.00060463	1.02801609	2.51013947
1.14060497	1.08375645	4.40731525

TABLE 4.10 RATIO OF LOWTRANSX TO PLANE PARALLEL INTENSITIES FOR THE CASE OF ANISOTROPIC SCATTERING USING 1962 STANDARD ATMOSPHERE AT 11 μm (Single Scattering)

[OBSERVER AND SOLAR ZENITH ANGLES..... 12.95, 82.57, 88.54]

OBSERVER AT 100 KM G=.8 PHI= 0

INTENSITY UP ⟶ Solar angles

Observer angles ↓			
	1.00231266	1.06745529	2.53980637
	0.000712828	0.001238167	0.007610794
	0.000000213	0.000000287	0.000000955

INTENSITY DOWN

0.0	0.0	0.0
0.0	0.0	0.0
0.0	0.0	0.0

OBSERVER AT 2 KM G=.8 PHI= 0

INTENSITY UP

1.00139332	1.05543613	2.56243706
1.01643562	1.07541847	2.46145344
1.17257404	1.26863194	2.79622650

INTENSITY DOWN

1.00000000	1.00354385	1.35827351
0.992864728	1.00059032	1.37985706
0.971548676	0.975686073	1.30217552

OBSERVER AT GROUND G=.8 PHI= 0

INTENSITY UP

0.0	0.0	0.0
0.0	0.0	0.0
0.0	0.0	0.0

INTENSITY DOWN

1.00000000	1.05172062	2.36723137
0.997923195	1.03127670	2.72884464
1.14086819	1.08088493	3.25586605

TABLE 4.10 (CONT.)

[OBSERVER AND SOLAR ZENITH ANGLES..... 12.95, 82.57, 88.54]

OBSERVER AT 100 KM G=.8 PHI= 90

INTENSITY UP

1.00240326	1.05603218	2.27564812
0.000714208	0.001249183	0.007702570
0.000000213	0.000000276	0.000000940

INTENSITY DOWN

0.0	0.0	0.0
0.0	0.0	0.0
0.0	0.0	0.0

OBSERVER AT 2 KM G=.8 PHI= 90

INTENSITY UP

1.00144863	1.05768394	2.56569958
1.01863575	1.08981609	2.50270844
1.17263222	1.27964306	2.69502258

INTENSITY DOWN

0.996233463	1.00589180	1.35294056
0.995618880	0.999244690	1.33369064
0.969927371	0.969134331	1.27762222

OBSERVER AT GROUND G=.8 PHI= 90

INTENSITY UP

0.0	0.0	0.0
0.0	0.0	0.0
0.0	0.0	0.0

INTENSITY DOWN

0.995685399	1.05365753	2.35451031
1.00057888	1.02740669	2.51358e04
1.13899517	1.0828647e	4.40842915

TABLE 4.10 (CONT.)

[OBSERVER AND SOLAR ZENITH ANGLES..... 12.95, 82.57, 88.54]

OBSERVER AT 100 KM G=.8 PHI=180

INTENSITY UP

1.00199699	1.03780556	2.01509380
0.000713983	0.001250720	0.004630759
0.000000213	0.000000290	0.000000940

INTENSITY DOWN

0.0	0.0	0.0
0.0	0.0	0.0
0.0	0.0	0.0

OBSERVER AT 2 KM G=.8 PHI=180

INTENSITY UP

1.00150490	1.05701733	2.57046986
1.01775074	1.08541203	2.43811417
1.17387867	1.27116680	2.60291195

INTENSITY DOWN

0.990720093	1.00441265	1.35198593
0.994664669	0.999370277	1.32555103
0.970852494	0.967585027	1.31540680

OBSERVER AT GROUND G=.8 PHI=180

INTENSITY UP

0.0	0.0	0.0
0.0	0.0	0.0
0.0	0.0	0.0

INTENSITY DOWN

0.990753770	1.051e3956	2.35011196
0.999193847	1.02470112	2.3790e837
1.14007759	1.07867050	3.57632828

4.4 Spectral Redundancy

For high resolution, plane-parallel, multiple scattering radiative transfer in inhomogeneous media, the gaseous absorption causes the radiative properties to be highly dependent on frequency. Such complex spectral structure requires the monochromatic calculations to be done on a fine frequency grid over the entire spectrum. Computational times are consequently large and procedures to decrease them are sought. Two rather distinct approaches have evolved to deal with this spectral problem. The first, and more highly developed method, is to spectrally model or average the extinction coefficient in some manner and then attempt to use such averaged properties in an appropriately modified radiative transfer equation or its solution. The literature on this approach is too extensive to discuss in detail and shows successful applications for many specific problems [Refs. 22 and 23]. The major limitations of this method are 1) the modeling or averaging is not general, 2) the radiative transfer using averaged properties is almost always an approximation, and 3) that only spectrally averaged quantities can be predicted. In other words this approach lacks generality and has unknown and uncontrolled errors.

The second method of dealing with the spectral problem, and the one pursued in this section, exploits the idea that monochromatic radiative transfer calculations can be highly redundant over a spectral region containing many gaseous absorption/emission lines. Therefore, only a relative few monochromatic multiple scattering calculations are required to represent radiative transfer at all points in the spectral region. Prior research on this approach has taken several forms using the nomenclature of the K or opacity distribution function [Refs. 24 through 27], and is well developed

only for homogeneous atmospheres or when scattering is neglected. The work on exponential-sum fitting of the direct transmission function [Ref. 28 and 29] can also be related to this method. The research proposed here builds on this previous work and presents the method in a more general manner using the properties of the diffuse transmission functions associated with the adding/doubling computational method for multiple scattering. This different viewpoint makes it easier to understand when and how spectral redundancy can be used to advantage.

To study the spectral redundancy for multiple scattering radiative transfer in the generality being proposed, a general and fast radiative transfer computational code is required. The method of Adding/Doubling has been developed over a period of time by several research groups and is now able to solve any monochromatic, multiple scattering problem in plane-parallel media [Refs. 5, 6, 7, 30, 31 and 32]. Although the particular adding/doubling algorithm to be used here, and developed by one of the authors, is general (internal and external radiative sources, inhomogeneous and non-isothermal media, arbitrary scattering properties of medium and surfaces) and computationally rather fast (5 to 10 CPU seconds on an IBM 370/158 per monochromatic run), it is not fast enough to allow high resolution, point-by-point calculations to be done over the entire spectrum in a realistic gaseous medium for all of the various conditions encountered in modeling engineering and atmospheric environments. Therefore, the following scheme is one possible approach to decrease computational times for obtaining both the total energy flux and the spectral intensity emerging from, or found within, a multiple scattering medium. The concept is rather simple. The approximation is made that all spectral points having the same total optical

depth also have the same, or very similar, direct and diffuse transfer or transmission functions. This is not true in the general case, and the research discussed here is to find out through analysis and numerical experiments the accuracy of this approach in simulating radiative transfer in realistic atmospheres and what further parameters may be required.

As a simple example, consider the problem of radiative transfer through an inhomogeneous medium illuminated by solar radiation. The monochromatic intensity I_ν (ν denotes frequency) exiting the top and bottom of the medium of total optical depth t_{ν_o} can be written as [Ref. 5]

$$I_\nu^+ (0, \mu, \phi) = \frac{I_{\nu_o}}{4\pi} \frac{S_s^{R-}(t_{\nu_o}, \mu \quad \phi)}{\mu} \tag{4.19}$$

and

$$I_\nu^- (t_{\nu_o}, \mu, \phi) = I_{\nu_o} \left\{ \exp(-t_{\nu_o}/\mu)\ \delta\ (\mu-\mu_o, \phi-\phi_o) + \frac{T_s^{R-}(t_{\nu_o}, \mu, \phi)}{4\pi\ \mu} \right\}. \tag{4.20}$$

Here the diffuse transmission functions S_s^{R-} and T_s^{R-} are calculated by the Adding/Doubling method and have been modified (superscript R) for any reflecting surface located at t_{ν_o}. I_{ν_o} is the solar intensity at the top of the atmosphere in the direction of μ_o ($\cos\theta_o$), ϕ_o, where θ and ϕ are the zenith and azimuthal angles, respectively. The direct solar beam is angularly turned on by the Dirac delta function δ. The optical depth t_ν is based on the extinction coefficient K_{E_ν} by

$$t_\nu = \int_0^x K_{E_\nu}(\tilde{x})d\tilde{x} ,$$

where x is the perpendicular distance measured down from the top of the medium, while upward (downward) hemispheric intensities are labeled with a +(-) superscript. Also note that the full functional arguments for S_s and T_s are not given, and they are calculated for a solar flux of 4π.

If one is concerned with only the direct radiative transfer, the spectral variation of the incident solar flux is usually considered to be smooth and the spectrally summed intensity can be written as

$$I^- (x_o, \mu_o, \phi_o) = I_o \int_{\Delta\nu} \exp(-t_{\nu_o}/\mu_o)d\nu . \qquad (4.21)$$

The spectrally averaged direct transmission function is the integral in the equation, and it is often approximated by a sum of exponentials as discussed at length in several references [see Refs. 28 and 29]. The exponential - sum fitting method is also directly related to the K-distribution method where the spectrally averaged, direct transmission function is written as (for an homogeneous medium)

$$T(U) = \frac{1}{\Delta\nu} \int_{\Delta\nu} \exp(-K_{E_\nu} U)d\nu = \int_0^\infty f(K_E) \exp(-K_E U)d K_E , \qquad (4.22)$$

where U is the gas amount and $f(K_E)$ is the K distribution function. This function weights the spectrum according to how often the extinction coefficient has values between K_E and $K_E + d K_E$. Such a function can then be used in several different ways [Ref. 26]. The common factor in these constructs

is that all spectral points with the same K_E or t_o should be grouped and would then constitute a single monochromatic radiative transfer calculation.

The more general approach is to include the diffuse transmission (scattering) or transfer functions S_s^{R-} and T_s^{R-}. An intensity spectral sum would then appear as

$$I^+ = \frac{I_o}{4\pi\mu} \int_{\Delta\nu} S_s^{R-}(t_{\nu_o}, \mu \quad \phi)d\nu \ . \tag{4.23}$$

Now one must ask for what parametric values does one obtain the same S_s^{R-}. For this, the complete functional dependence of S_s^{R-} is required and can be expressed as

$$S_s^{R-} = S_s^{R-}(t_{\nu_o}, \mu, \phi; \omega_{\nu_o}(t_\nu), P_\nu(t_\nu), \mu_o, \phi_o). \tag{4.24}$$

Here ω_{ν_o} and P_ν are the single scattering albedo and phase function, respectively. To make this more explicit, it can be rewritten as

$$S_s^{R-} = S_s^{R-}\left(\int_o^{x_o} K_{E_\nu}\, dx, \mu, \phi; \frac{K_{s_\nu}(x)}{K_{E_\nu}(x)}, P_\nu(x), \mu_o, \phi_o\right), \tag{4.25}$$

where K_{s_ν} is the scattering coefficient. When the medium is <u>homogeneous</u> and one assumes K_{s_ν} and P_ν are spectrally smooth, the only remaining spectral parameter is t_{ν_o}, or

$$S_s^{R-} = S_s^{R-}(t_{\nu_o}) \tag{4.26}$$

and S_s^{R-} calculations can be grouped into t_o bins in the same way as discussed above for direction transmission.

For a given homogeneous medium, the procedure is conceptually straightforward and without physical approximations. A line-by-line algorithm like HIRACC [Ref. 33] which is contained in FASCOD1B [Ref. 4] would be used to produce the required t_o over the spectral region of interest. Using these results, one would then performed a mapping of all frequencies with common t_o values. This mapping is retained. The monochromatic multiple scattering code (Adding/Doubling) is then run for a small number of t_o's each of which represent many different values of frequency. The results of these calculations are then used to perform the spectral sums as expressed in Eq. (5), which now takes the form

$$I^+ = \frac{I_o}{4\pi\mu} \int_o^\infty S_s^{R-}(t_o) f(t_o) d\, t_o \ . \qquad (4.27)$$

The function $S_s^{R-}(t_o)$ and the extinction or opacity distribution function $f(t_o)$ are smooth functions so the integral can be evaluated accurately using only a few carefully selected values of t_o. In addition the high resolution spectral intensity given by Eq. (4.19) can be constructed by an inverse mapping of t_o results back to their associated frequency values.

For the realistic situation of an inhomogeneous atmosphere under discussion here, the redundancy for radiative transfer with scattering is more complex. Referring back to the general functional form given by Eq. (4.25) and making the reasonable assumption that $K_{S_\nu}(x)$ and $P_\nu(x)$ are known in x and spectrally smooth over the spectral region of interest, then

progress can be made with the redundancy concept for inhomogeneous media. The remaining spectral parameter besides t_{ν_o} is $K_{E_\nu}(x)$ that with $K_s(x)$ makes up the single scattering albedo. If $K_E(\nu, x)$ could be written as $K_E(t_o, x)$ when $t_o = t_o(\nu)$, then redundancy would be valid and such a situation is called the correlated opacity approximation. For certain simple line models such as equally spaced overlapping lines of equal strength the above parameterization of K_{E_ν} is valid and redundancy is an exact approach. For realistic inhomogeneous atmospheres it will be shown that the line absorption is not exactly correlated but progress can be made by working with an average (over the ν's associated with a given t_o) K_{E_ν} or equivalently an appropriately averaged single scattering albedo.

The above theoretical arguments and functional relations can be made clear by an example calculation. This will also give some initial results that will show how successful the redundancy approximation can be for inhomogeneous atmospheres. This initial calculation is not sufficient, however, to say that redundancy will work for all model atmospheres over their entire spectral region.

Although a theoretical argument can and has been made for spectral redundancy, its accuracy and usefulness can only be demonstrated by numerical experiments with realistic model atmospheres. For an initial experiment, a small spectral region was chosen from a standard atmosphere (Model six) of FASCODE (Ref. 4). The total transmittance for this atmosphere, which did not include aerosols, is shown in Fig. 4.2 over the narrow spectral region from 4950 to 4954 cm^{-1} that contains a mixture of CO_2 (uniformly mixed gas) and H_2O (nonuniformly mixed gas) lines. A part of this atmosphere was chosen to work with and was made up of 12 layers that extended from ground to 30 Km. The upper part of the atmosphere from 30 to 100 Km was

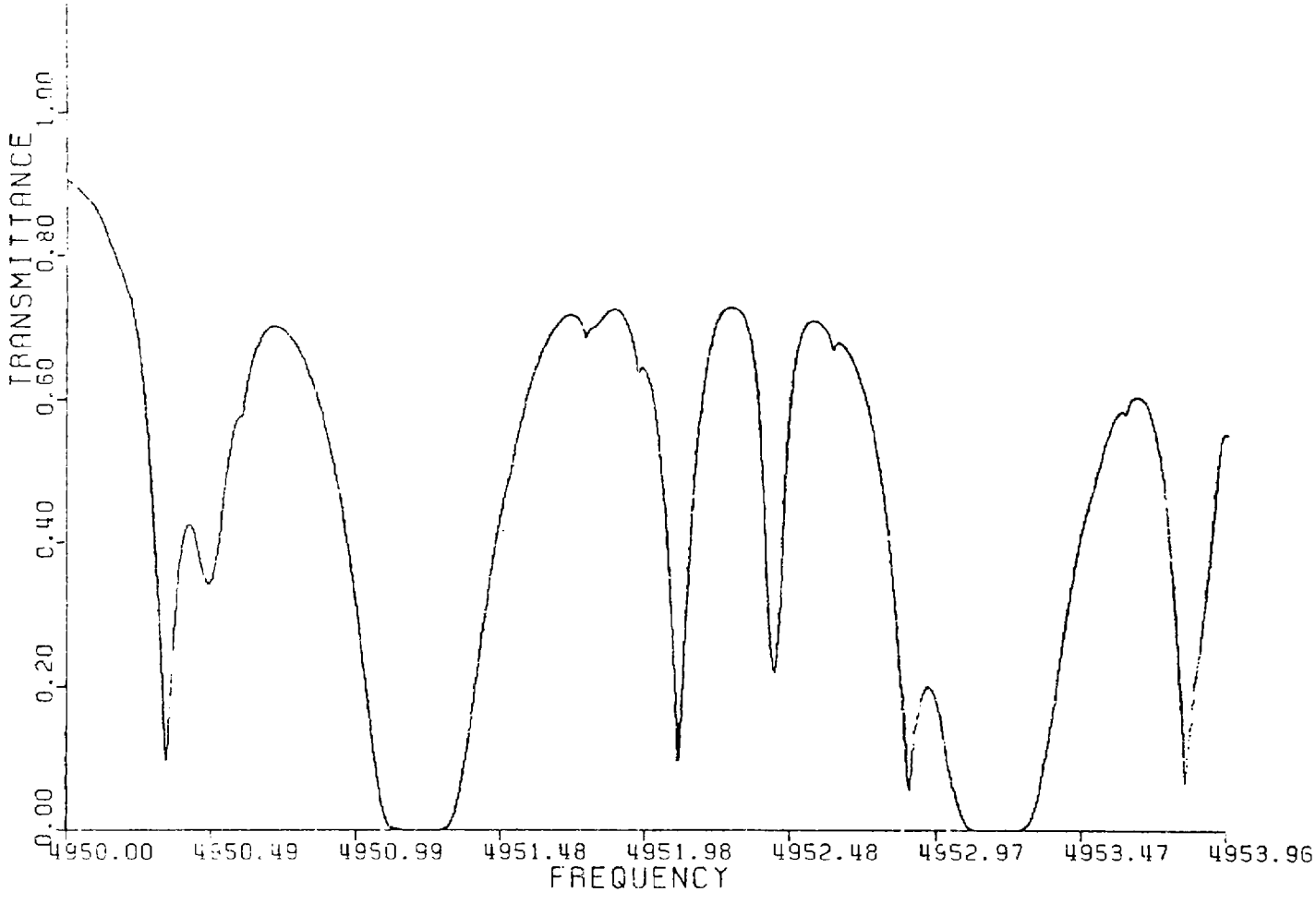

Figure 4.2 Spectral total transmittance for FASCOD standard atmospheric model six.

not used since it contributed little to the optical depths. For a total transmittance of 0.40 (optical depth t_o of 0.9163), there are fourteen corresponding frequencies in this spectral region. For each of these frequencies the optical depths of each of the 12 layers were found along with the average (over frequency) optical depth for each layer. In this initial sample calculation, aerosols were added to each layer by assuming the scattering optical depth was 1/9 of the average absorption optical depth. This gave an average single scattering albedo in each layer of 0.1. A single scattering albedo distribution over the 12 layers was then computed for each of the 14 frequencies by using the actual molecular optical depth in each layer, again for each frequency under study. Note that $1/\omega$ averaged over the frequencies gives the value of 10 for each layer.

To use this data in the multiple scattering Adding/Doubling code, it is convenient to reduce the 12 layers to six layers, five of which have optical depths of 0.127 and the bottom layer has an optical depth of 0.3825.* The new single scattering albedoes were formed from the originals by optical depth weighted averages.+ The data from this optical depth and albedo modeling are given in Table 4.11 (note that Ref. doesn't mean average of the albedoes given).

Each of the 14 different frequencies along with their unique single scattering albedo distributions were used in Adding/Doubling multiple scattering calculations for the flux exiting the top and bottom of the atmosphere. The results of these runs were averaged and compared with the one Adding/Doubling run using averaged layer properties. The results are presented in Figs. 4.3 and 4.4 for three sun angles.

*The physical layers therefore become frequency dependent, but this doesn't effect the present calculations.

+Because layers have been merged, the albedoes listed in Table 4.11 no longer give an average (as $1/\omega$) over frequency of 10.

Table 4.11 Layer optical depth, and albedoes for the fourteen spectral points corresponding to the total transmittance of 0.4.

FREQ. POINT	OPTICAL DEPTH BY LAYER FROM BOTTOM ⟶											
1	0.3468	0.2211	0.1405	0.0903	0.0527	0.0289	0.0164	0.0093	0.0052	0.0028	0.0026	0.0006
2	0.4127	0.2356	0.1290	0.0689	0.0355	0.0183	0.0096	0.0053	0.0029	0.0015	0.0014	0.0003
3	0.4623	0.2494	0.1165	0.0518	0.0209	0.0092	0.0042	0.0022	0.0012	0.0006	0.0006	0.0001
4	0.4453	0.2389	0.1123	0.0506	0.0220	0.0120	0.0078	0.0059	0.0050	0.0040	0.0072	0.0042
5	0.3638	0.2293	0.1397	0.0827	0.0467	0.0258	0.0138	0.0075	0.0039	0.0021	0.0019	0.0004
6	0.3561	0.2365	0.1375	0.0841	0.0478	0.0265	0.0147	0.0077	0.0041	0.0022	0.0019	0.0004
7	0.3114	0.2208	0.1532	0.0985	0.0597	0.0316	0.0181	0.0106	0.0055	0.0031	0.0029	0.0007
8	0.3112	0.2224	0.1508	0.1001	0.0590	0.0334	0.0192	0.0106	0.0061	0.0032	0.0031	0.0007
9	0.5550	0.2124	0.0737	0.0284	0.0134	0.0076	0.0052	0.0038	0.0027	0.0021	0.0028	0.0011
10	0.5786	0.2207	0.0742	0.0273	0.0114	0.0052	0.0026	0.0013	0.0009	0.0003	0.0003	0.0001
11	0.3549	0.2292	0.1439	0.0950	0.0491	0.0258	0.0137	0.0076	0.0040	0.0022	0.0020	0.0005
12	0.3693	0.2254	0.1374	0.0827	0.0481	0.0272	0.0144	0.0077	0.0042	0.0021	0.0020	0.0004
13	0.3804	0.2290	0.1345	0.0788	0.0442	0.0229	0.0122	0.0068	0.0034	0.0018	0.0017	0.0004
14	0.4532	0.2424	0.1201	0.0685	0.0263	0.0130	0.0064	0.0032	0.0018	0.0009	0.0008	0.0002
AVE.	0.4072	0.2295	0.1259	0.0705	0.0383	0.0205	0.0113	0.0064	0.0036	0.0021	0.0022	0.0007

FREQ.	ALBEDO BY LAYER FROM TOP ⟶					
1	0.07389	0.08222	0.09071	0.10341	0.10433	0.11541
2	0.10877	0.09893	0.09773	0.09766	0.09832	0.09880
3	0.15167	0.10532	0.09276	0.09276	0.08925	0.08914
4	0.12665	0.11239	0.09734	0.09644	0.09283	0.09223
5	0.08498	0.08839	0.09291	0.10008	0.10228	0.11061
6	0.08268	0.08793	0.09351	0.09733	0.09953	0.11273
7	0.06677	0.07338	0.08367	0.09832	0.10353	0.12532
8	0.06506	0.07214	0.08489	0.09804	0.10286	0.12525
9	0.18983	0.12617	0.10719	0.08322	0.07538	0.07538
10	0.21100	0.11507	0.10357	0.07658	0.07253	0.07253
11	0.08286	0.08596	0.09017	0.10012	0.10191	0.11307
12	0.08228	0.08881	0.09429	0.10163	0.10345	0.10914
13	0.09164	0.09236	0.09627	0.10020	0.10230	0.10630
14	0.13461	0.10433	0.09556	0.09518	0.09132	0.09077
REF.	0.10000	0.10000	0.10000	0.10000	0.10000	0.10000

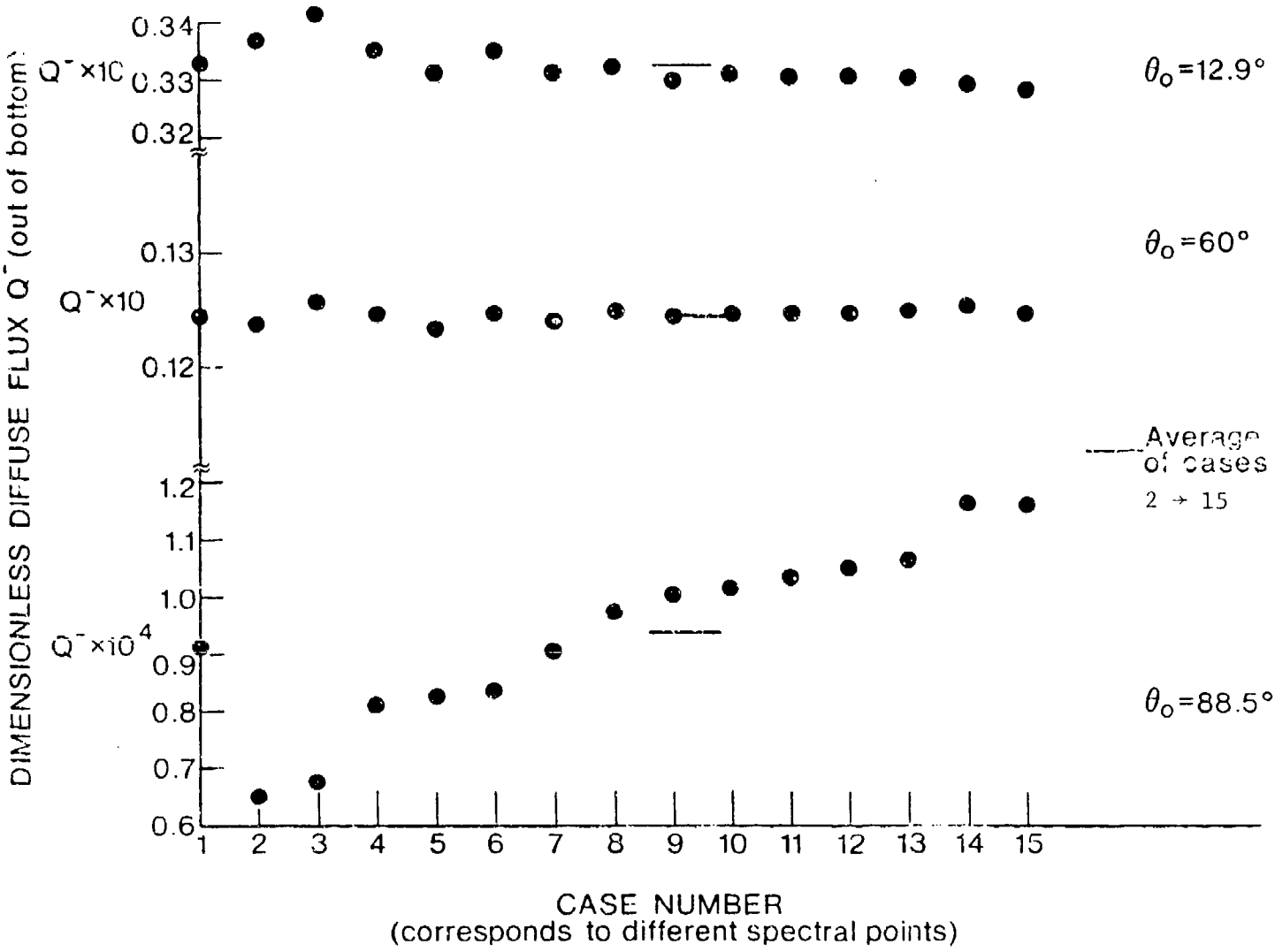

Figure 4.3 Transmittance diffuse flux for a total molecular transmittance of 0.4 at each of the fourteen corresponding frequencies (case #'s 2 thru 15) and for average layer properties (case #1).

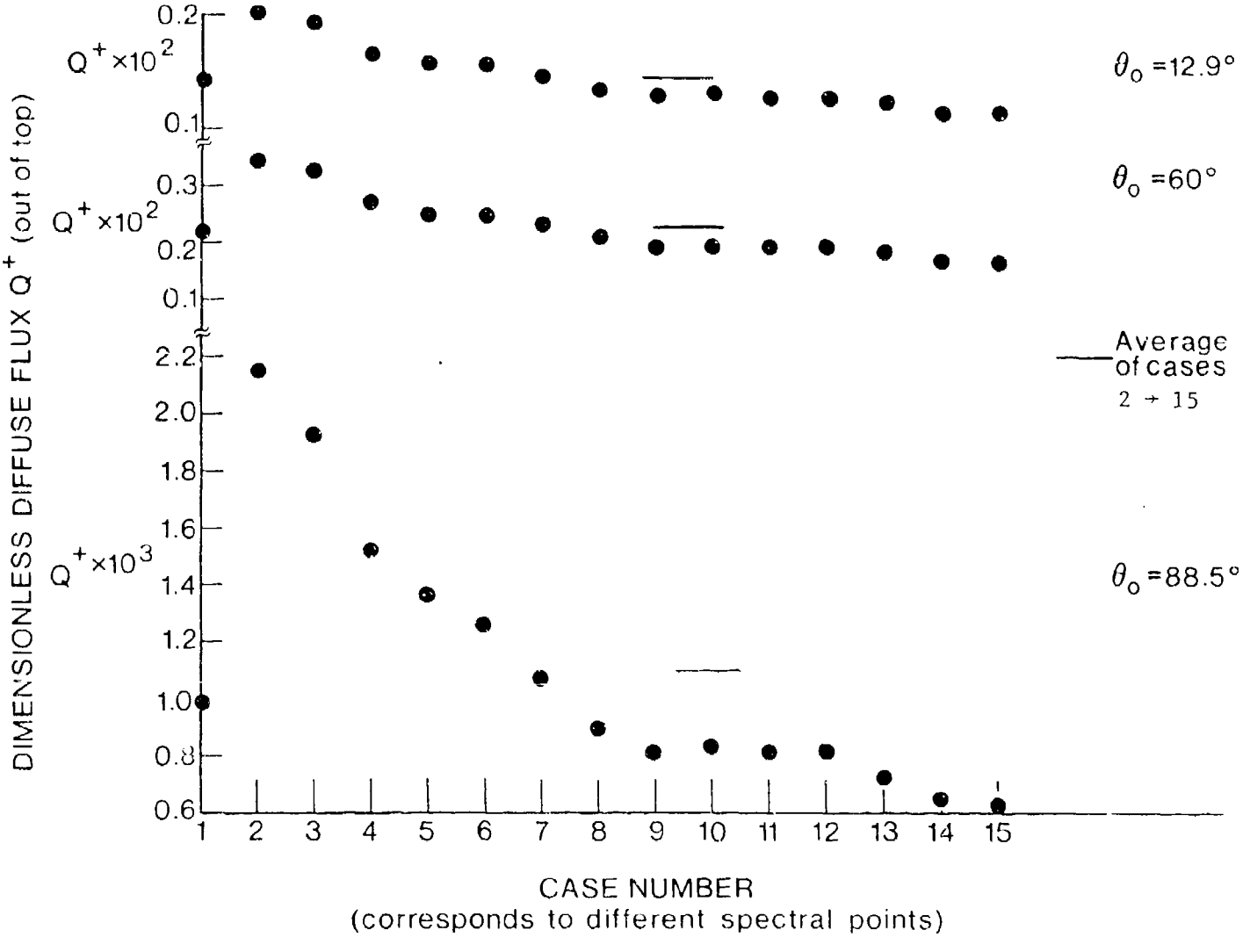

Figure 4.4 Reflected diffuse flux for a total molecular transmittance of 0.4 at each of the fourteen corresponding frequencies (case #'s 2 thru 15) and for averaged layer properties (case #1).

The diffusely transmitted flux out of the bottom with sun angles of 12.9°, 60° and 88.5° for each frequency (case number) is shown in Fig. 4.3. Case number one is the run using averaged layer properties and the bar denotes the averages of all the other cases (2 through 15). For the more overhead (lower angles) sun angles the cases show small amounts of variance, while grazing sun angles produce more variance. This variance says that the total optical depth does not control the multiple scattering radiative transfer problem. On the other hand, the averaged property run agrees quite well with the average over frequencies or case number. For example, when the sun is at 88.5° the run using averaged properties gives $Q^- \times 10^4 = 0.914$ while the average of all runs gives $Q^- \times 10^4 = 0.940$. This results in a 2.8% error and the smaller sun angles produce even less error. The result of this experiment is that the total optical depth and layer properties averaged over all corresponding frequencies for this optical depth can be used in a single multiple scattering run to predict the radiative flux with good accuracy.

The diffusely scattered flux out of the top of the atmosphere for the same conditions discussed above is presented in Fig. 4.4. Here the case by case variance is larger since the reflected flux is more sensitive to the albedo distribution than the diffusely transmitted flux. Again the greatest variance is observed at the more grazing sun angle of 88.5°. For this sun angle, the calculation using the averaged layer properties gives $Q^+ \times 10^3 = 0.991$ while the average of all calculated cases results in $Q^+ \times 10^3 = 1.108$. Here the error is 10%, but do note that when the sun angle is 12.9° this error reduces to 2%. Although the error introduced by the redundancy argument is greater for diffusely scattered radiation than for diffusely transmitted radiation and the grazing sun angles produce the

maximum errors, there does appear to be a great deal of spectral redundancy in multiple scattering radiative transfer.

4.5 Recommendations For Further Research

The need to reduce the number of spectral-like, multiple-scattering calculations was discussed at the beginning of this section. The spectral redundancy concept subsequently developed along with an initial numerical experiment is one logical approach that does reduce the number of multiple scattering calculations required to obtain radiative fluxes. However, more theoretical and numerical work is required before spectral redundancy is reduced to a practical and useful method. More (different line features) and larger spectral regions have to be analyzed to find out if redundancy arguments remain valid. This will require a fair number of numerical experiments.

The final goal of spectral redundancy studies is to produce a set of spectrally averaged (over a specified spectral resolution) atmospheric properties that can be used in any monochromatic multiple scattering calculation (Adding/Doubling, Monte Carlo, two-stream Delta Approximation, etc.) to produce accurate radiative transfer predictions. This will not be an easy or simple task, but it is basic to all other so called alternative approaches that have been proposed.

REFERENCES

1. Kneizys, F.X., Shettle, E.P., Gallery, W.O., Chetwynd, J.H., Abreu, L.W., Selby, J.E.A., Fenn, R.W., and McClatchy, R.A., "Atmospheric Transmittance/Radiance: Computer Code LOWTRAN 5", AFGL-TR-80-0067 (1980).

2. Ridgway, W.L., Moose, R.A., and Cogley, A.C., "Atmospheric Transmittance/Radiance Computer Code FASCOD2", AFGL-TR-80-0250 (1980).

3. Smith, H.J.P., Dube, D.J., Gardiner, M.E., Clough, S.A., Kneizys, F.X., and Rothman, L.S., "FASCOD - Fast Atmospheric Signature Code (Spectral Transmittance and Radiance)", AFGL-TR-78-0081 (1978).

4. Clough, S.A., Kneizys, F.X., Rothman, L.S., Gallery, W.O., "Atmospheric Spectral Transmittance and Radiance: FASCOD1B", SPIE Vol 277 - Atmospheric Transmission. pp. 152-166.

5. Cogley, A.C., "Adding and Invariant Imbedding Equations in Matrix Notation for All the Scattering Functions," J. Quant. Spectrosc. Radiat. Transfer, 19, 113-125 (1978).

6. Cogley, A.C., and Bergstrom, R.W., "Numerical Results for the Thermal Scattering Functions," J. Quant. Spectrosc. Radiat. Transfer, 21, 263-278 (1979).

7. Bergstrom, R.W. and Cogley, A.C., "Scattering of Emitted Radiation from Inhomogeneous and Nonisothermal Layers," J. Quant. Spectrosc. Radiat. Transfer, 21, 279-292 (1979).

8. Lampley, C.M. and Blattner, C.M., "E-O Sensor Signal Recognition Simulation: Computer Code Spot 1", RRA-T7809, Radiation Research Associates, Fort Worth, Texas (1978).

9. Selby, J.E.A., Shettle, E.P., and McClatchey, R.A., "Atmospheric Transmittance from 0.25 to 28.5 μm: Supplement LOWTRAN 3B", AFGL-TR-76-0258, AD A040 701 (1976).

10. Selby, J.E.A., Kneizys, F.X., Chetwynd Jr., J.H., and McClatchey, R.A., "Atmospheric Transmittance/Radiance: Computer Code LOWTRAN 4", AFGL-TR-78-0053, AD A058 643 (1978).

11. Shettle, E.P., and Fenn, R.W., "Models of the Aerosols of the Lower Atmosphere and the Effects of Humidity Variations on their Optical Properties", AFGL-TR-79-0214, 17 September (1979).

12. Shettle, E.P., and Fenn, R.W., "Models of the Atmospheric Aerosols and their Optical Properties", in AGARD Conference Proceedings No. 183 Optical Propagation in the Atmosphere. Presented at the Electromagnetic Wave Propagation Panel Symposium , Lyngby, Denmark, 27-31 October 1975, AGARD-CP-183, available from U.S. National Technical Information Service (No. AD-A028-615)(1976).

13. Collins, D.G. and Marshall, J.D., "Utilization Instructions for the MIE-2 Program", Radiation Research Associates, Inc. Report RRA-N918 (1969).

14. Blättner, W., "Utilization Instructions for Operation of the MIE Programs on the CDC-6600 Computer at AFCRL", Radiation Research Associates, Inc. Research Note RRA-N7240 (1972).

15. Shettle, E.P., Private Communication (1982).

16. Collins, D.G. and Wells, M.B., "Flash, a Monte Carlo Procedure for Use in Calculating Light Scattering in a Spherical Shell Atmosphere", AFCRL-70-0206 (1970).

17. Blättner, W.G., Collins, D.G., and Wells, M.B., "Monte Carlo Calculations in Spherical-Shell Atmospheres", AFCRL-71-0382 (1971).

18. Blättner, W.G. and Wells, M.B., "Monte Carlo Studies of Light Transport Through Natural Atmospheres," AFCRL-73-0109 (1973).

19. Lenoble, J. (Editor), "Standard Procedures to Compute Atmospheric Radiative Transfer in a Scattering Atmosphere", International Association of Meteorology and Atmospheric Physics (I.U.G.G.), Radiation Commission (1974).

20. Sharma, S., "An Accurate and Computationally Fast Formulation for Radiative Fields and Heat Transfer in General, Plane-Parallel, Non-Grey Media with Anisotropic Scattering", Ph.D. Thesis, University of Illinois at Chicago (1980).

21. Cogley, A.C., "Derivation and Application of the Reciprocity Relations for Radiative Transfer with Internal Illumination", J. Quant. Spectrosc. Radiat. Transfer, 15, 749-760 (1975).

22. Goody, R.M., Atmospheric Radiation. Oxford University Press (1964).

23. Sparrow, E.M. and Cess R.D., Radiation Heat Transfer. McGraw-Hill, New York (1978).

24. Arking, A. and Grossman, K., "The Influence of Line Shape and Band Structure on Temperatures in Planetary Atmospheres," Journal of the Atmospheric Sciences, 29, 936-949 (1972).

25. Lacis, A.A. and J.E. Hansen, "A Parameterization for the Absorption of Solar Radiation in the Earth's Atmosphere" Journal of the Atmospheric Sciences, 31, 118-133 (1974).

26. Lacis, A.A., Wang, W.C., and Hansen, J.E., "Correlated K-Distribution Method for Radiative Transfer in Climate Models: Application to Effect of Cirrus Clouds on Climate," Paper No. 51, Fourth NASA Weather and Climate Program Science Review (1979).

27. Ackerman, T.P., private communication.

28. Wiscombe, W.J. and Evans, J.W., "Exponential-Sum Fitting of Radiative Transmission Functions," Journal of Computational Physics, 24, 416-444 (1977).

29. Fouquart, Y., Irvine, W.M., and Lenoble, J., Editors, "Standard Procedures to Compute Atmospheric Radiative Transfer in a Scattering Atmosphere," Volume II, International Association of Meteorology and Atmospheric Physics, Radiation Commision, National Center for Atmospheric Research, Boulder, Colorado 80307 (1980).

30. Cogley, A.C., Pandey, D.K. and Bergstrom, R.W., "A Fast, Exact Code for Scattered Thermal Radiation Compared with a Two-Stream Approximation," Icarus, 43, 96-101 (1980).

31. Sharma, A., Cogley, A.C. and Tonon, S.S., "Error Analysis of the Adding/Doubling Method for Radiative Scattering in Inhomogeneous Media", Journal of Quantitative Spectroscopy and Radiative Transfer, 26 39-48 (1981).

32. Sharma, A. and Cogley, A.C., "Radiative Heat Transfer in a Completely General Plane-Parallel Environment," International Journal of Heat and Mass Transfer, vol. 25, pp. 523-534 (1982).

33. Clough, S.A., Kneizys, F.X. and Chetwynd, J.H., "Algorithm for the Calculation of Absorption Coefficient - Pressure Broadened Molecular Transitions," AFCRL-TR-77-0164 (1977).

34. Thekaekara, M.P., "Extraterrestrial Solar Spectrum, 3000-6100 A at 1-A Intervals," Applied Optics, Vol. 13, No. 3 (1974).

35. Turner, R.E., et.al.,"Natural and Artifical Illumination in Optically Thick Atmospheres", Environmental Research Institute of Michigan, Report No. 108300-4-F (1975).

36. Condron, T.P., J.J. Lovett, W.H. Barnes, L. Marcotte and R. Nadile, "Gemini 7 Lunar Measurements", AFCRL-68-0438 (1968).

37. Lane, A.P. and Irvine, W.M., Astron. J. 78, No. 3 (1973).

38. Bullrich, K., Ber. Deutsch. Wettered., U.S. Zone No. 4 (1948).

39. Kreith, F. and Kreider, J.F., Principles of Solar Engineering. McGraw-Hill Book Company, New York (1978).

APPENDIX A: MIE DATA ACCESS CODE

As mentioned in Chapter 2, the complete output of the MIE calculations was much too large for continuous online storage. Therefore, the data was stored in binary format on a magnetic tape at the AFGL computer center. The volume serial number of the tape is CC-0366, and the file name is MIEOUTPUT10. This file is actually composed of 39 records each containing the results for a particular model at many (up to 27) wavelengths. A summary of the records follows:

RECORD #	AEROSOL MODEL	WAVELENGTHS (μm)
1	RURAL 0% RH*	.2 - 1.06
2	" *	1.536 - 5.0
3	"	6.0 - 40.0
4	RURAL 70% RH*	.2 - 1.536
5	" * ✓	2.0 - 3.392
6	RURAL 80% RH* ✓	.2 - 3.392
7	RURAL 99% RH	.2 - 40.0
8	URBAN 0% RH*	.2 - 5.0
9	"	6.0 - 40.0
10	URBAN 70% RH*	.2 - 5.0
11	"	6.0 - 40.0
12	URBAN 80% RH	.2 - 5.0
13	"	6.0 - 40.0
14	URBAN 99% RH	.2 - 40.0
15	OCEANIC 0% RH*	.2 - 5.0
16	"	6.0 - 40.0
17	OCEANIC 70% RH*	.2 - 5.0
18	"	6.0 - 40.0

19	OCEANIC 80% RH*	.2	-	3.392
20	"	5.0	-	40.0
21	OCEANIC 99% RH*	.2	-	40.0
22	TROPOSPHERIC 0% RH*	.2	-	2.5
23	"	2.7	-	18.5
24	"	21.3	-	40.0
25	TROPOSPHERIC 70% RH*	.2	-	2.5
26	"	2.7	-	40.0
27	TROPOSPHERIC 80% RH*	.2	-	2.5
28	"	2.7	-	40.0
29	"	21.3	-	40.0
30	TROPOSPHERIC 99% RH	.2	-	40.0
31	BACKGROUND	.2	-	40.0
32	AGED VOLCANIC	.2	-	40.0
33	FRESH VOLCANIC	.2	-	40.0
34	RADIATION FOG	.2	-	2.0
35	RADIATION FOG	2.5	-	40.0
36	ADVECTION FOG	.2	-	40.0
37	METEORIC+	.2	-	6.0
38	METEORIC +	7.2	-	10.0
39	METEORIC +	12.5	-	40.0

*This data was generated by a version of the code that had under-dimensioned arrays. Data other than the normalized phase Matrix may be incorrect and should be used with caution.

The data for these two models at wavelengths from 5.0 to 40.0 μ were not saved.

+It has recently been discovered that these records were generated using incorrect refractive index data. The reader is referred to Eric Shettle of AFGL, who has recalculated these phase functions using the correct data.

The data can only be accessed with the FORTRAN program (called RDTP10B) listed below:

```
      PROGRAM RDTP10B(INPUT,OUTPUT,TAPE5,TAPE6)
C
C     THIS PROGRAM IS USED TO READ THE BINARY OUTPUT
C     OF THE MIE CALCULATIONS STORED ON "TAPE5" AND
C     WRITE THE OUTPUT TO "TAPE6".
C
C     PLEASE CONSULT APPENDIX A OF THE LOWTRAN SINGLE
C     SCATTERING REPORT REGARDING THE VALIDITY OF
C     SOME OF THE DATA.
C
C     NTHETA IS THE NUMBER OF SCATTERING ANGLES, =34
C
C     NFANG IS THE NUMBER OF COSINES FOR EQUAL PROBABILITY
C     INTERVALS, EQUALS 26 OR 36.
C
C     THE CONTENTS OF THE ENTIRE FILE ARE COPIED, I.E. THE
C     PHASE FUNCTION DATA FOR A GIVEN AEROSOL MODEL AT
C     UP TO 27 WAVELENGTHS.  REFER TO THE CHAPTER 2 OF
C     THE SINGLE SCATTERING REPORT FOR A SUMMARY OF THE
C     FILE CONTENTS
C
      COMPLEX PM
      DIMENSION THET(34),PHAS1(34),PHAS2(34),PHAS3(34),
     1 PHAS4(34),COEQP(36)
C
900   FORMAT(///"        INDEX OF REFRACTION     WAVELENGTH    K EXT
     1    K SCT")
      DO 100 IWAVE=1,27
      WRITE(6,900)
      READ(5) PM,IPROB,WAVEL,CEXT,SCOE,NTHETA,NFANG
      IF(EOF(5)) 200,5
5     READ(5) (THET(I),I=1,NTHETA),
     1 (PHAS1(I),I=1,NTHETA),(PHAS2(I),I=1,NTHETA),(PHAS3(I)
     2 ,I=1,NTHETA),(PHAS4(I),I=1,NTHETA),(COEQP(I),I=1,NFANG)
      WRITE(6,910) PM,WAVEL,CEXT,SCOE
910   FORMAT(2X,5E13.6,2X,2I4)
      WRITE(6,920)
920   FORMAT(/"  SCT ANG     I1          I2          I3          I4
     A    IAVE")
      DO 10 I=1,NTHETA
      PHS=(PHAS1(I)+PHAS2(I))/2.0
10    WRITE(6,930) THET(I),PHAS1(I),PHAS2(I),PHAS3(I),PHAS4(I),PHS
930   FORMAT(1X,F7.2,5E12.6)
      WRITE(6,940)
940   FORMAT(/"  COSINES FOR EQUAL PROBABILITY INTERVALS")
      DO 20 I=1,NFANG
20    WRITE(6,950) COEQP(I)
950   FORMAT(1X,E13.6)
100   CONTINUE
200   CONTINUE
      STOP
      END
```

The program reads one record from "TAPE5" (the binary data file) and writes the information to "TAPE6" for examination, cataloging, etc. While this program is capable of operating directly on the magnetic tape, it is not recommended. The binary data file should be copied (in binary) from the tape to a mass storage disk file. This allows interactive execution of the program and avoids the possibility of repeated tape mounts in the event that problems arise.

The following example should clarify the use of the program. Assuming that a compiled version of RDTP10B is local file LGO and the binary data file is local file DATATP, the following commands could be used to retrieve the aged volcanic data in record number 32.

```
COPYBR, DATATP, DUMMY, 31
COPYBR, DATATP, TAPE5
REWIND, TAPE5
LGO
```

The first three commands copy the data in record number 32 to TAPE5 and then rewind it. The last command executes the problem. A copy of the contents of file number 32 would appear in coded format in local file TAPE6. A portion of the output that would result from the above sequence fill is shown below: The headings above the output are self-explanatory. The first line of output consists of the complex index of refraction, wavelength, extinction coefficient, and scattering coefficient. This is followed by six columns of data. Each column has 34 entires, one for each scattering angle. The first column lists the scattering angles. The next four columns are the four Stokes parameters, and the last column the phase function for unpolarized light (i.e. the numerical average of the first two Stokes parameters). The final portion of output is

a single column containing the cosines for equal probability intervals. Similar sets of output would be repeated for each of the remaining 26 wavelengths.

INDEX OF REFRACTION		WAVELENGTH	K EXT	K SCT
.150000E+01	-.700000E-01	.200000E+00	.113554E-08	.631550E-09

SCT ANG	I1	I2	I3	I4	I4VF
0.00	.850921E+01	.850921E+01	.850921E+01	-.161701E-14	.850921E+01
2.00	.743046E+01	.743097E+01	.743055E+01	-.360986E-01	.743069E+01
4.00	.543572E+01	.543706E+01	.543524E+01	-.955765E-01	.543639E+01
6.00	.375511E+01	.375609E+01	.375259E+01	-.118468E+00	.375560E+01
8.00	.259069E+01	.259021E+01	.259549E+01	-.122213E+00	.259045E+01
10.00	.182269E+01	.182031E+01	.181497E+01	-.113356E+00	.182150E+01
12.00	.131650E+01	.131235E+01	.130671E+01	-.997515E-01	.131443E+01
16.00	.744205E+00	.738155E+00	.732327E+00	-.722250E-01	.741132E+00
20.00	.462108E+00	.455607E+00	.449953E+00	-.510151E-01	.458858E+00
24.00	.309028E+00	.302701E+00	.297247E+00	-.362093E-01	.305864E+00
28.00	.218503E+00	.212640E+00	.207385E+00	-.258727E-01	.215572E+00
32.00	.158875E+00	.155868E+00	.150697E+00	-.196714E-01	.156371E+00
36.00	.122088E+00	.117953E+00	.112922E+00	-.137230E-01	.120020E+00
40.00	.949039E-01	.913609E-01	.862785E-01	-.102151E-01	.931323E-01
50.00	.542440E-01	.519437E-01	.459947E-01	-.483100E-02	.530933E-01
60.00	.335111E-01	.317772E-01	.269509E-01	-.226760E-02	.326441E-01
70.00	.218657E-01	.206071E-01	.159316E-01	-.914617E-03	.212364E-01
80.00	.150860E-01	.141554E-01	.943246E-02	-.181235E-03	.146259E-01
90.00	.109406E-01	.102233E-01	.561110E-02	.290215E-03	.106319E-01
100.00	.829381E-02	.809308E-02	.324049E-02	.547980E-03	.819645E-02
110.00	.672739E-02	.684422E-02	.175736E-02	.603566E-03	.678508E-02
120.00	.567277E-02	.625939E-02	.913226E-03	.131814E-02	.596625E-02
125.00	.531965E-02	.619245E-02	.627293E-03	.115462E-02	.575055E-02
130.00	.508772E-02	.629013E-02	.413275E-03	.131752E-02	.568893E-02
135.00	.495330E-02	.656410E-02	.274527E-03	.151615E-02	.576370E-02
140.00	.492873E-02	.701579E-02	.197813E-03	.176063E-02	.597376E-02
145.00	.494478E-02	.769640E-02	.178341E-03	.202054E-02	.632059E-02
150.00	.493336E-02	.858587E-02	.157605E-03	.221621E-02	.675962E-02
155.00	.476146E-02	.940157E-02	-.912087E-05	.211843E-02	.708152E-02
160.00	.429741E-02	.943451E-02	-.593294E-03	.132409E-02	.686596E-02
165.00	.381212E-02	.813359E-02	-.191352E-02	-.227264E-03	.597286E-02
170.00	.436401E-02	.669532E-02	-.438819E-02	-.134200E-02	.552997E-02
175.00	.642957E-02	.701856E-02	-.659894E-02	-.772183E-03	.672412E-02
180.00	.779181E-02	.779181E-02	-.779181E-02	-.330468E-17	.779181E-02

COSINES FOR EQUAL PROBABILITY INTERVALS

.999177E+00
.998204E+00
.997097E+00
.995730E+00
.994293E+00
.992313E+00
.990334E+00
.987819E+00
.984622E+00
.980627E+00
.975794E+00
.969359E+00
.963391E+00
.954341E+00
.943303E+00
.929560E+00
.913058E+00
.889020E+00
.857952E+00
.816480E+00
.757466E+00
.671010E+00
.544295E+00
.337975E+00
-.775706E-01
-.100000E+01

APPENDIX B: LOWTRANSX STRUCTURE

This section of the report describes the structure of the single scattering portions of the LOWTRANSX code. A complete description of the original LOWTRAN code can be found in Reference [1]. Changes made in the original LOWTRAN routines are described first. Next a discussion and flow chart is presented for each of the newly introduced subroutines. Finally, a list of new variables and their definitions is provided.

B.1 Changes in Original LOWTRAN Routines

1. In the main routine LOWEM, the control parameter ISCTTR and control card 2A were added to the input data file to provide for specification of the single scattering control parameters. The definitions of the new control parameters can be found in the comments at the beginning of the code and also in Appendix C of this report. Additional blank common areas have been added to provide space for the new single scattering quantities. The only major change in program flow was the addition of a CALL SSGEO statement. Subroutine SSGEO is a new driving routine which will be discussed along with all other new routines in Section B.2.

2. Subroutine TRANS has been modified to perform two, rather than one transmittance calculations at each scattering point along the line-of-sight. The first calculation is for the L-shaped path from the extraterrestrial source to the scattering point on the optical path, then along the optical path to the observer. The second transmittance calculation is for the path from the scattering point to the observer. After each transmittance calculation subroutine SSRAD (a new routine) is called to either save the transmittances (during the first call) or perform the single scattering intensity calculation (during the second call).

3. Subroutine RFPATH has been modified to save the earth centered angle increment DBETA, and the path zenith angle THETA, in arrays ADBETA and ATHETA, respectively. These quantities are necessary for specifying the scattering point-to-sun paths and the scattering angles.

No other significant changes have been made to the original LOWTRAN routines.

B.2 New Subroutines

1. Subroutine SSGEO drives the single-scattering geometry calculations. If ISCTTR = 1, (i.e. the single scattering calculation is desired) SSGEO is called immediately after GEO is called for the optical path geometry calculations. SSGEO first saves all path quantities such as H1, H2, ANGLE, etc., along with the arrays WLAY, WPATH and TBBY. This is done to avoid losing the information during subsequent GEO calls for the scattering point to sun amounts. Next, SSGEO calls subroutine PSIDEL to determine the values of PSIO (the relative azimuth between the optical path and the sun's rays at the observer) and DELO (the angle subtended at the earth's center by the observer and the subsolar point). This is followed by the loop over the scattering points, during which SSGEO calls function PSI, DEL and SCTANG along with subroutine GEO (the LOWTRAN geometry routine) to determine the cumulative point to sun absorber amounts. These absorber amounts are then stored in the array WPATHS, which is analogous to the optical path absorber amount array WPATH. Upon completion of all geometry calculations, the optical path parameters and arrays are restored, and control is returned to LOWEM.

2. Subroutine PSIDEL computes and returns the values of PSIO and DELO.

3. Function PSI returns the value of the relative azimuth angle between the line-of-sight and the direct solar path.

4. Function DEL returns the value of the angle subtended at the earth's center by the subsolar point and a scattering point. This is also the straight path approximation for the sun's zenith angle at the scattering point. An iteration of the geomtry calculation is performed by SSGEO if the bending along the sun path is greater than one-tenth degree.

5. Function SCTANG determines the value of the included angle for single scattering, i.e., the angle between the sun's rays and the line-of-sight optical path.

6. Subroutine SSRAD is called by TRANS after each transmittance calculation. TRANS has been modified to perform two transmittance calculations at each scattering point along the optical path. When called following the first transmittance calculation, SSRAD saves the total transmittance for the L path. After the second call SSRAD uses the current optical path transmittance along with the previously saved L path transmittance to calculate the single scattering intensity contribution from the current layer.

7. Subroutine SOURCE contains the extraterrestrial source intensity data as a function of wavelength [34]. A correction factor accounts for the earth's elliptic orbit. Lunar intensities (when required) are based on the solar intensity and stored values of the wavelength dependent albedo [36, 37] and angle dependent phase function [38] of the lunar surface.

8. Subroutine SUBSOL determines the sub-solar point angles, that is the longitude and latitude where the sun is directly overhead.

9. Subroutine PHASEF returns the value of the aerosol phase function when the MIE data base is used. First the aerosol model number and the bounding angle, wavelength and humidity (if within the 0-2 Km boundary layer) indices are determined. Function PF is then called to obtain the appropriate data from the PFnn subroutines which contain the results of the MIE calcualtions described in Chapter 2. Subroutine INTERP is called to perform any necessary interpolutions.

10. Function PF calls the appropriate PFnn data subroutine.

11. Subroutines PFnn(where nn = 01 to 22) contain the phase function data for aerosol model nn.

12. Subroutine INTERP performs linear and logarithmic interpolation.

B.3 Flow Charts of New Subroutines

Figure B1 through B12 are flow charts of the subroutines described above.

B.4 New Variables and Their Definitions

Variables introduced in the development of LOWTRANSX are listed and defined below.

VARIABLE	FIRST REFERENCE	DEFINITION
ADBETA	MAIN	Optical path, earth-centered-angle increment array
AH1	MAIN	Scattering point altitude array
ALAM	PHASEF	Wavelength
ALB	SOURCE	Lunar albedo array
ALT	PHASEF	Altitude
ANGD	SSGEO	Optical path zenith
ANGF	MAIN	User supplied phase function scattering angle array
ANGLO	SSGEO	Straight line approximation of solar zenith

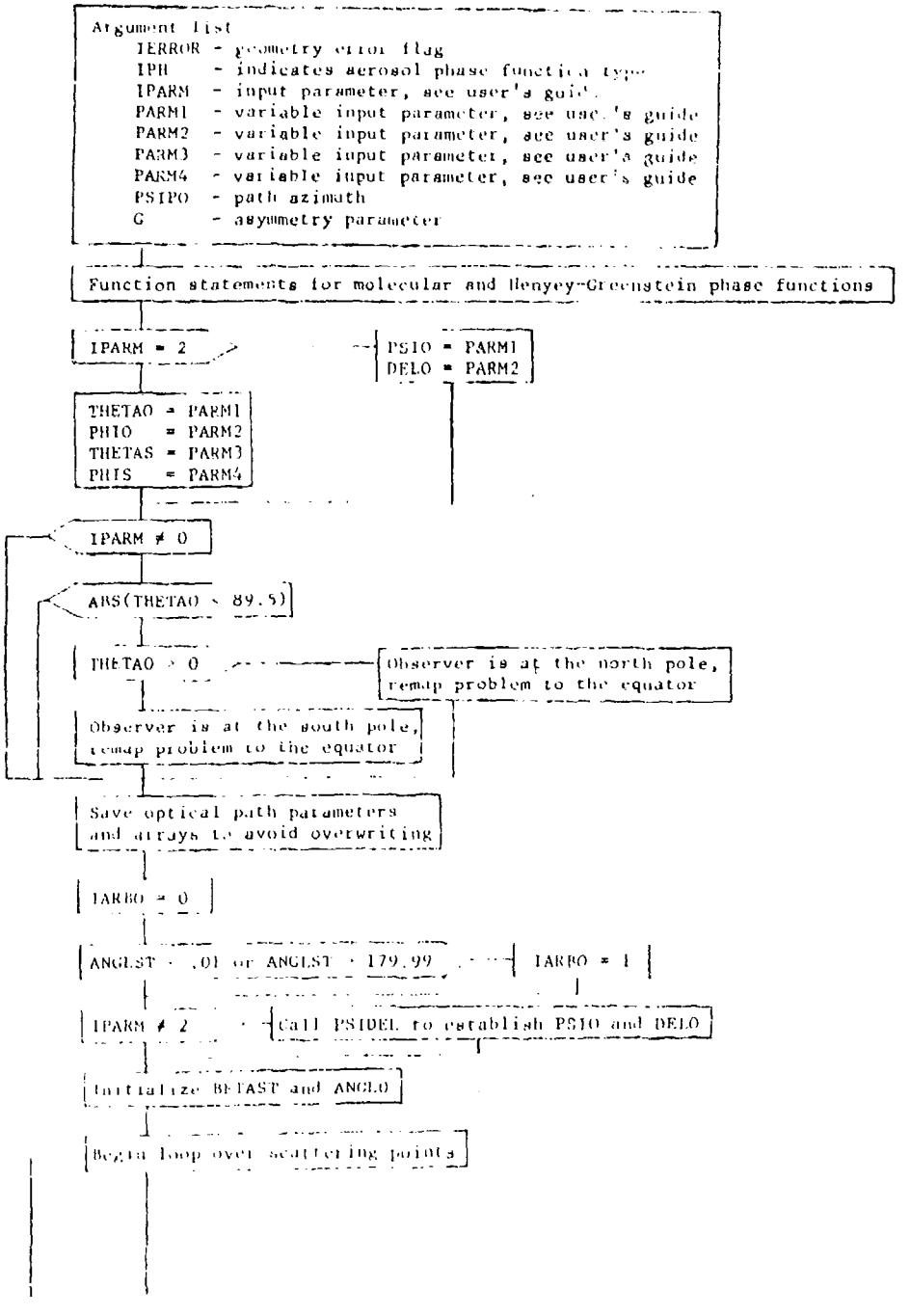

Figure B1 Flow chart of subroutine SSGEO.

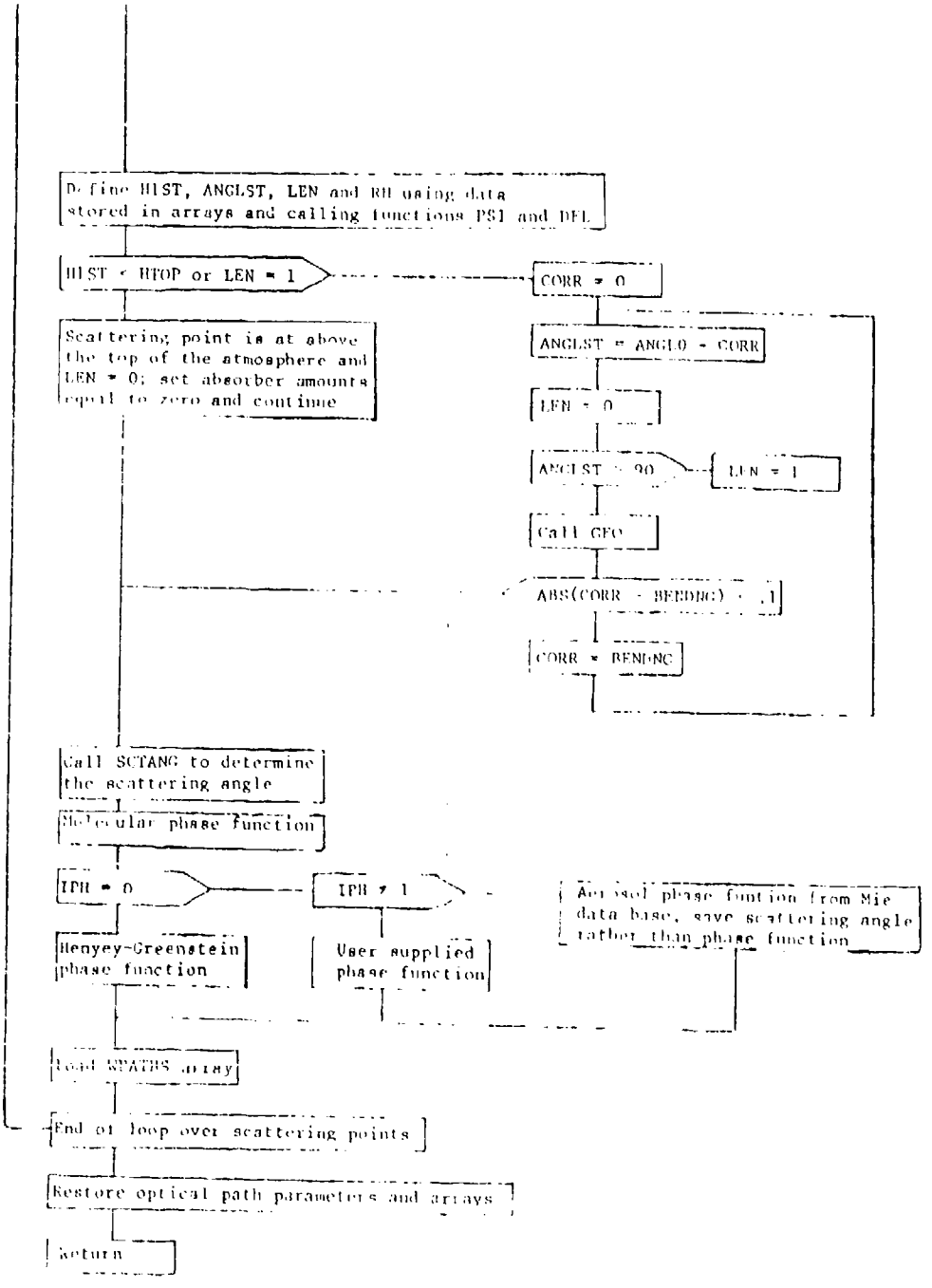

Figure B1 (cont'd)

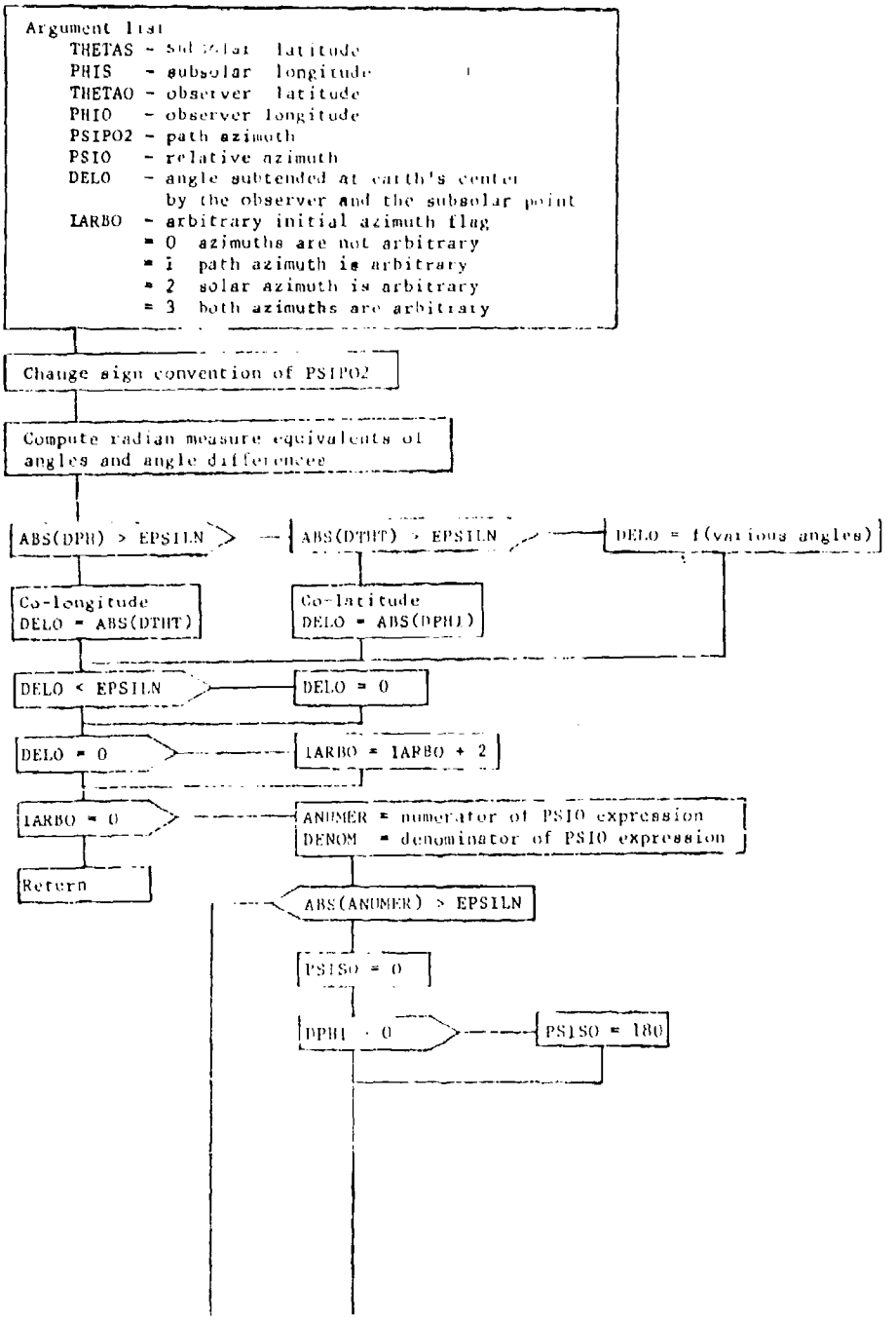

Figure B2 Flow Chart of subroutine PSIDEL

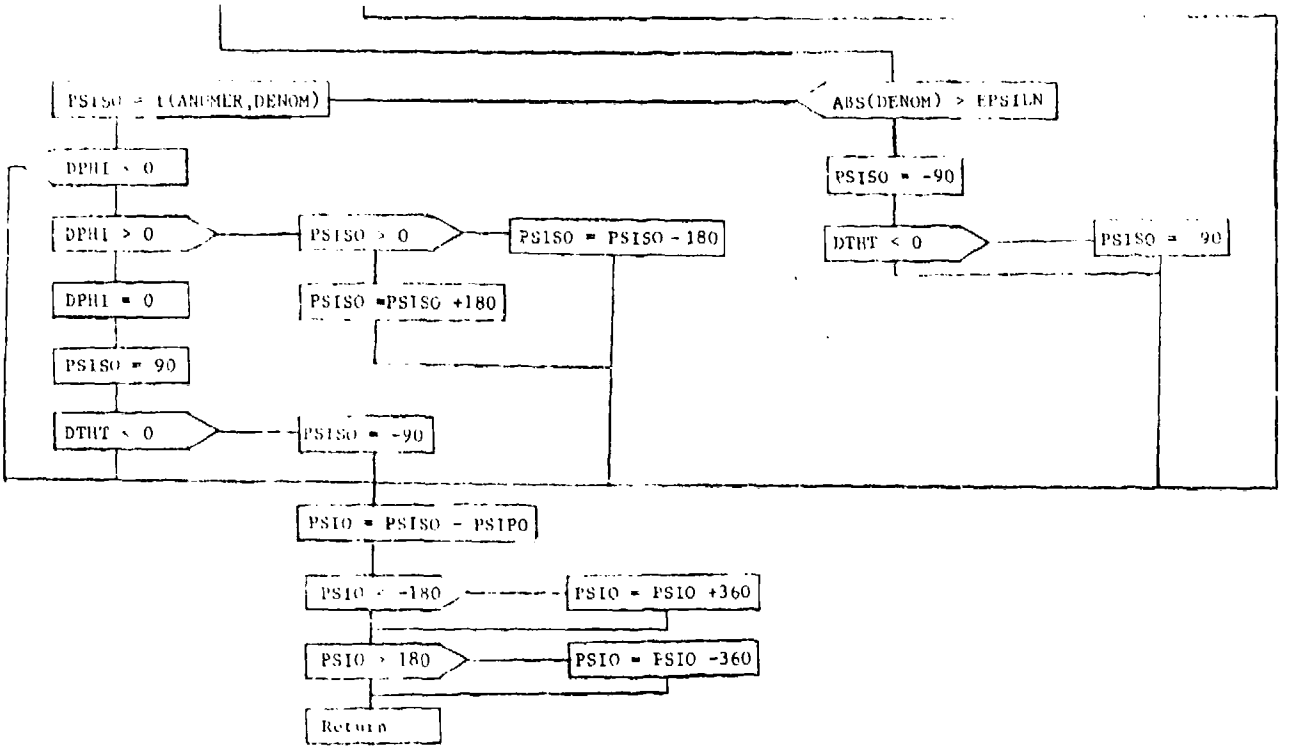

Figure B2 (cont'd)

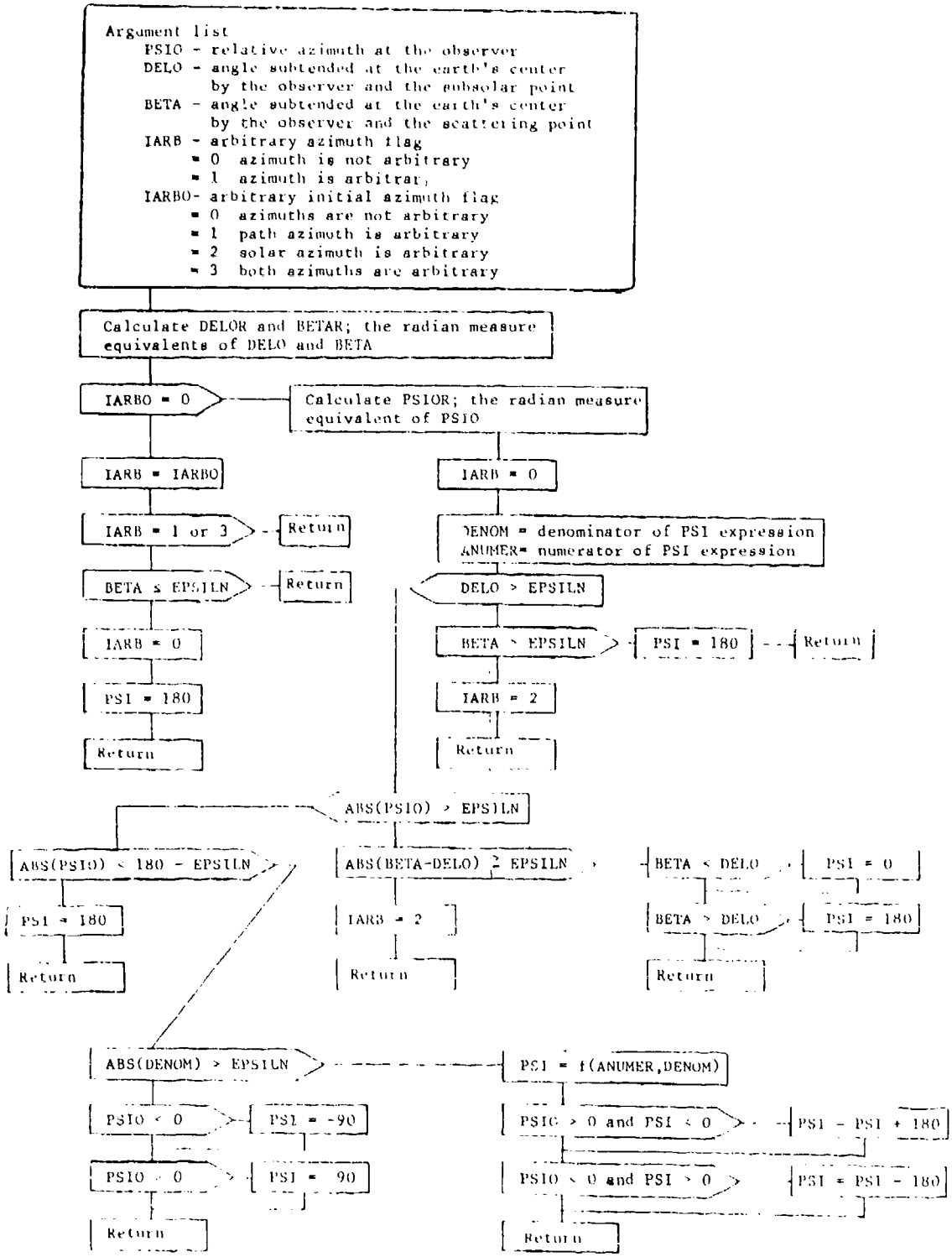

Figure B3 Flow chart of function PSI

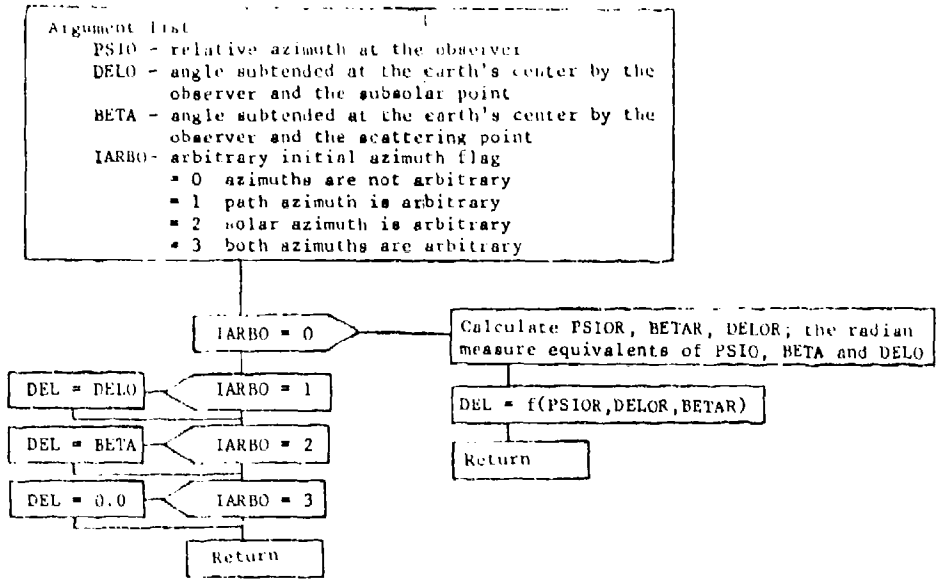

Figure B4 Flow chart of function DEL

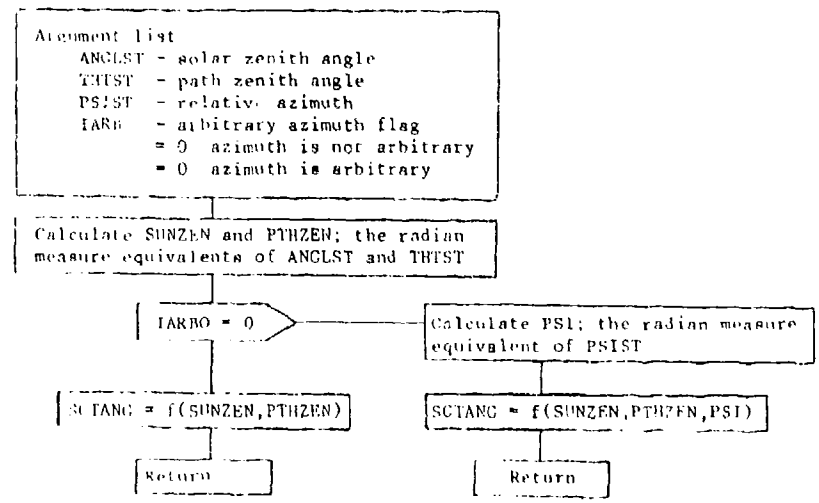

Figure B5 Flow chart of function SCTANG

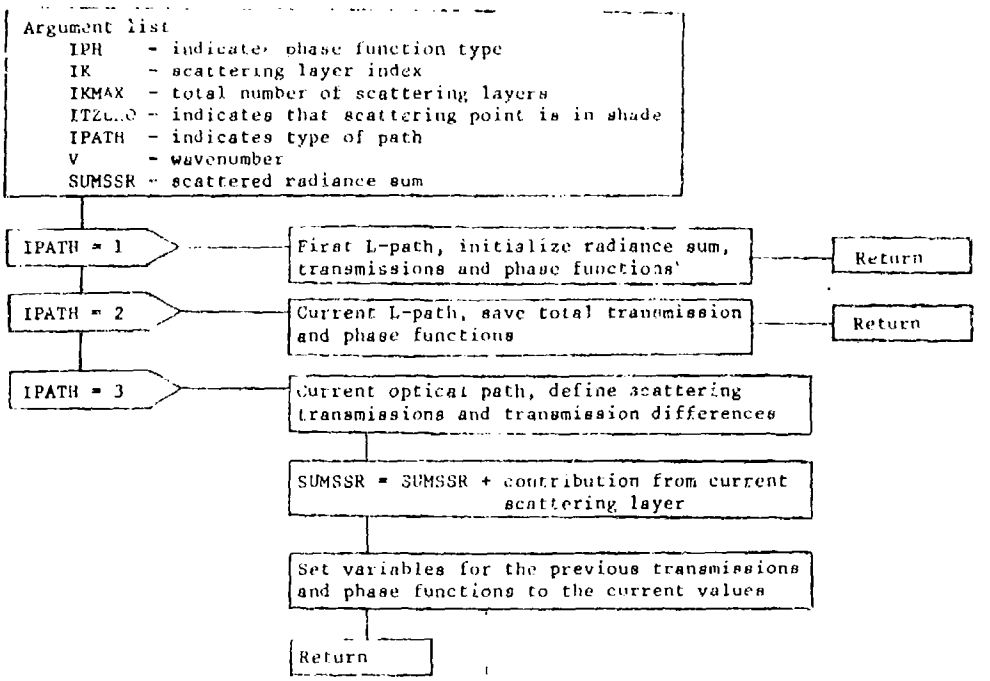

Figure B6 Flow chart of subroutine SSRAD

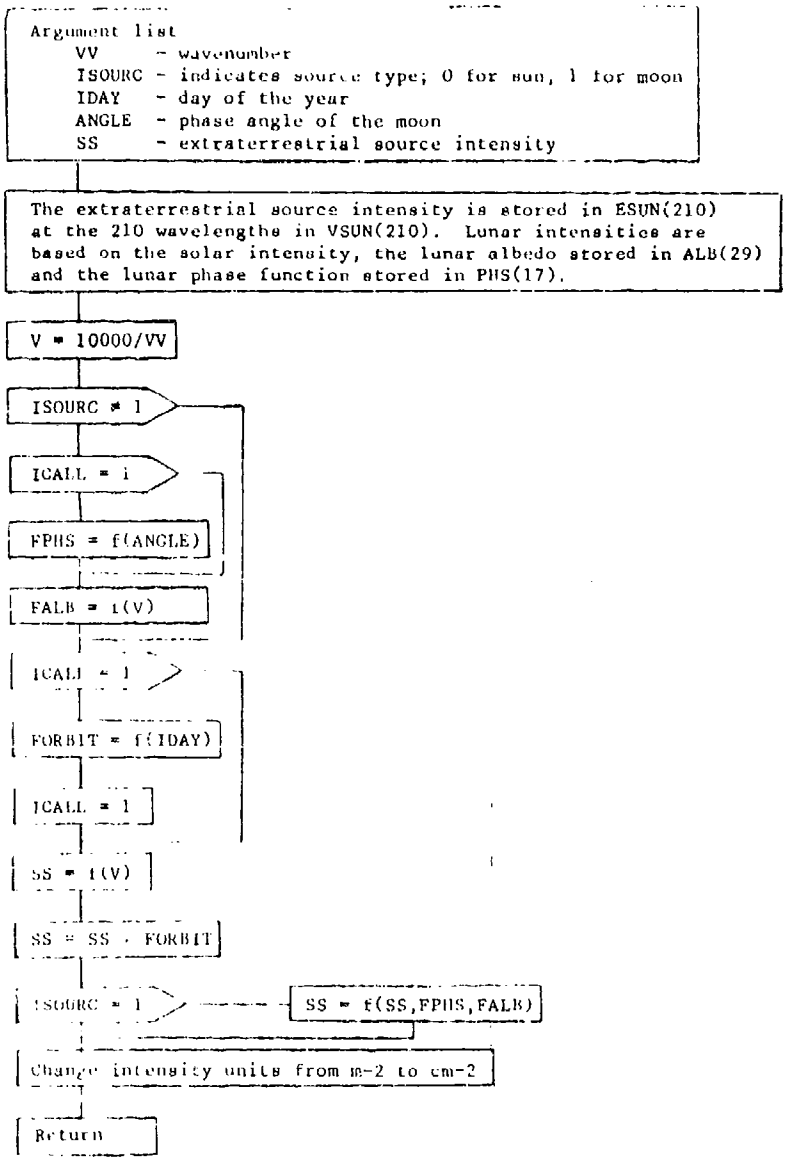

Figure B7 Flow chart of subroutine SOURCE

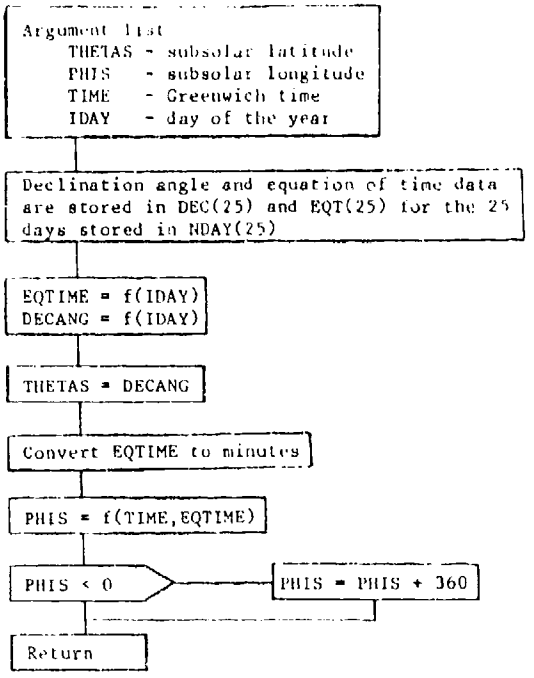

Figure B8 Flow chart of subroutine SUBSOL

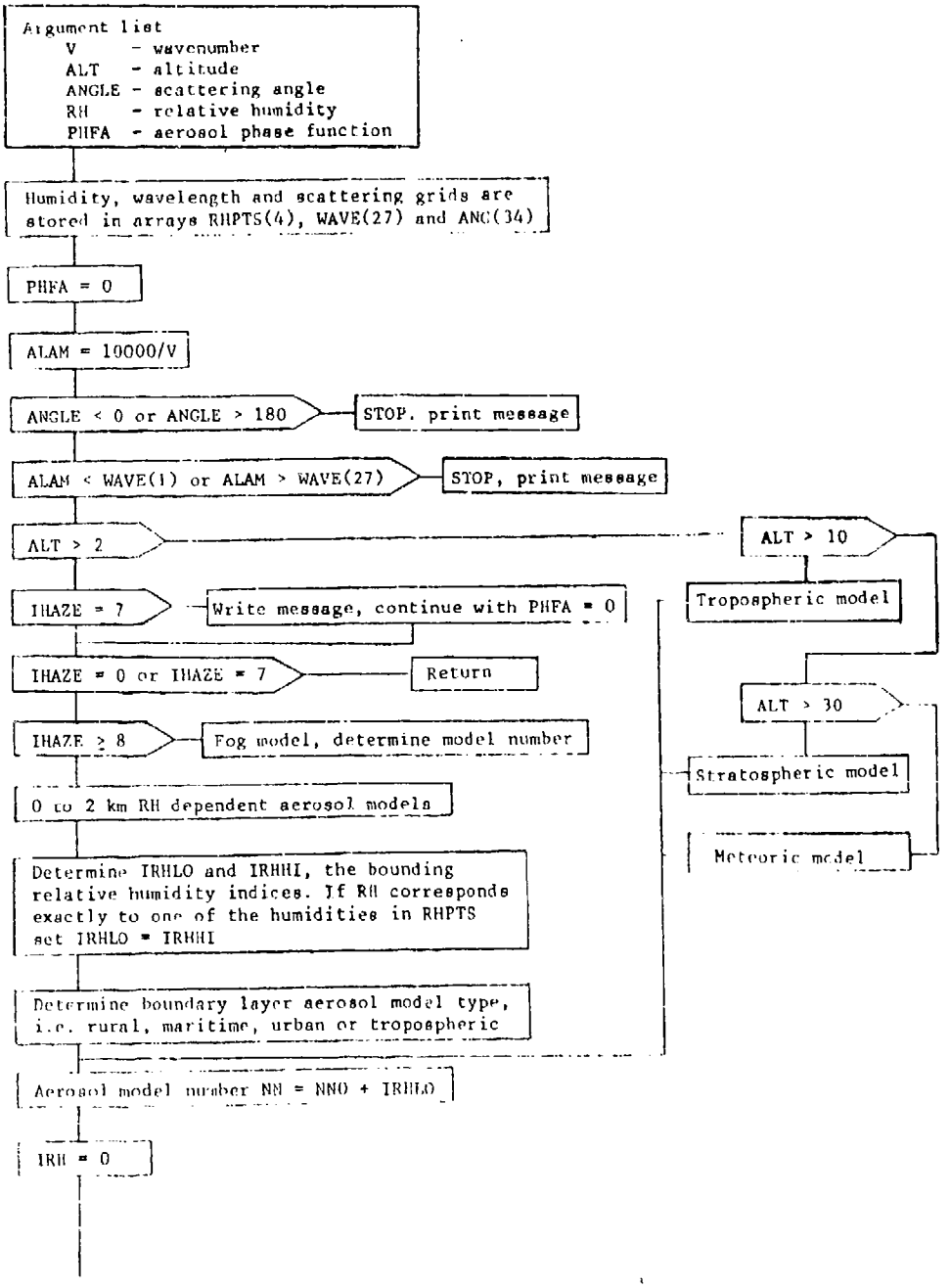

Figure B9 Flow chart of subroutine PHASEF

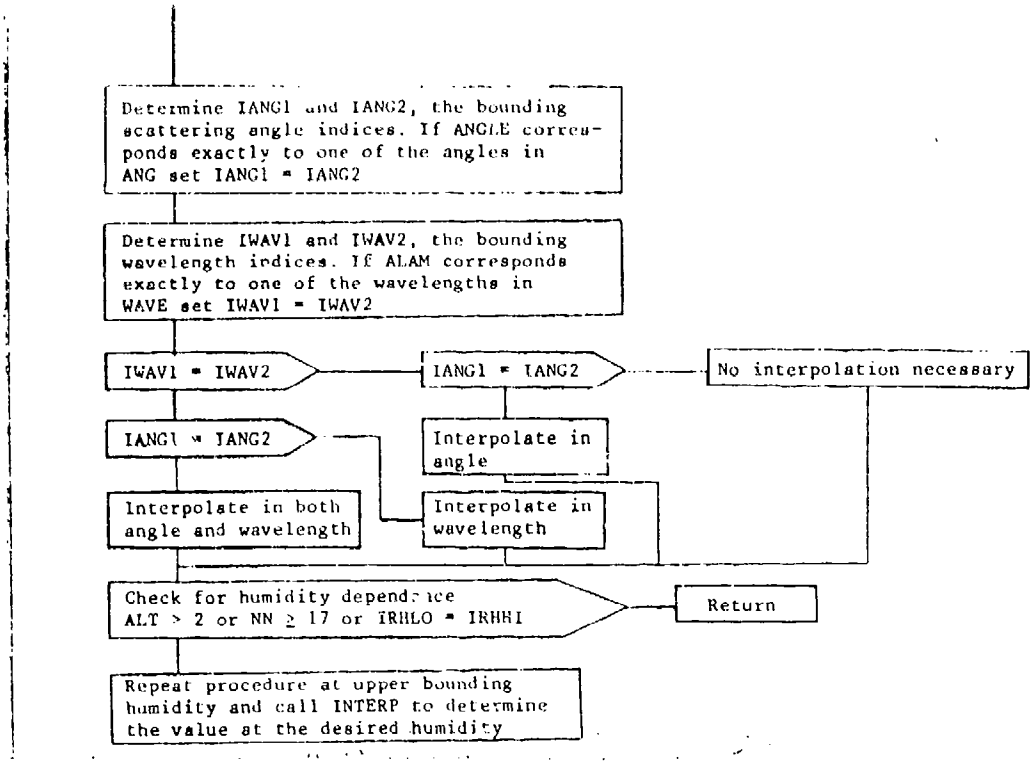

Figure B9 (cont'd)

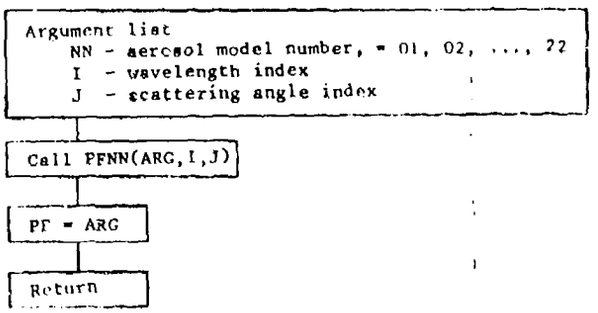

Figure B10 Flow chart of function PF

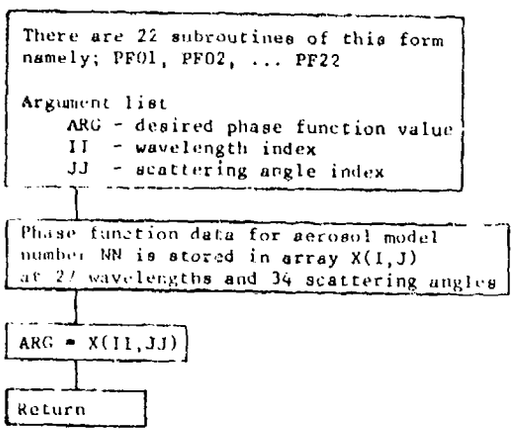

Figure B11 Flow chart of subroutine PFnn

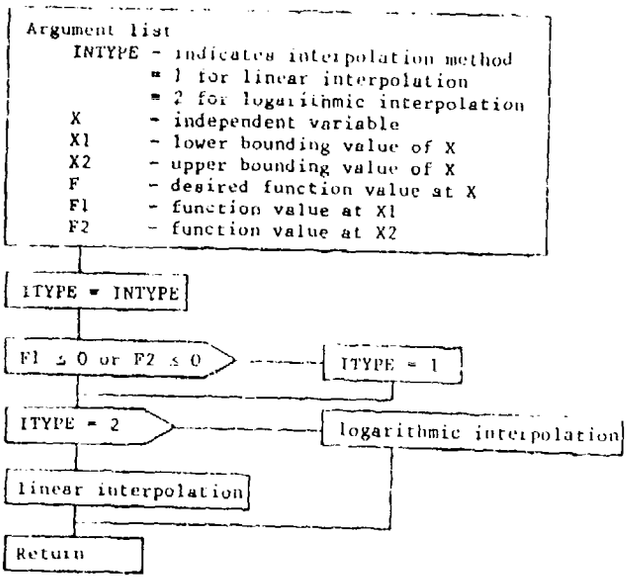

Figure B12 Flow chart of subroutine INTERP

VARIABLE	FIRST REFERENCE	DEFINITION
ANGLE	SOURCE	Lunar phase angle
ANGLEM	MAIN	Same as "ANGLE" above
ANGLST	SSGEO	Solar zenith
ARH	MAIN	Relative humidity array
ATHETA	MAIN	Optical path zenith angle array
AZ	SEGEO	Layer boundary altitude array
BENDNG	SSGEO	Solar path bending
CORR	SSGEO	Solar path bending correction
DEC	SUBSOL	Solar declination angle
DELO	SSGEO	Angle subtended at the earth's center by the observer and the subsolar point
EQT	SUBSOL	Equation of time
ESUN	SOURCE	Extraterrestrial solar intensity array
F	MAIN	User supplied phase function array
FALB	SOURCE	Lunar albedo
FORBIT	SOURCE	Solar elliptic orbit factor
FPHS	SOURCE	Lunar phase function
G	MAIN	Asymmetry parameter, see user's guide
IANG1	PHASEF	Lower bounding angle index
IANG2	PHASEF	Upper bounding angle index
IARB	SSGEO	Flag indicating arbitrary azimuth
IARBO	SSGEO	Flag indicating arbitrary inital azimuth
IDAY	MAIN	Day of the year, see user's guide
IPARM	MAIN	Control parameter, see user's guide
IPATH	SSGEO	Flag indicating straight or L-path
IPH	MAIN	Control parameter, see user's guide
IRHHI	PHASEF	Lower bounding relative humidity index
IRHLO	PHASEF	Upper bounding relative humidity index
ISCTTR	MAIN	Control parameter, see user's guide
ISOURC	MAIN	Control parameter, see user's guide
ITZERO	TRANS	Flag indicating that scattering point is in the shade
IWAV1	PHASEF	Lower bounding wavelength index
IWAV2	PHASEF	Upper bounding wavelength index
NANGLS	MAIN	Control parameter, see user's guide

VARIABLE	FIRST REFERENCE	DEFINITION
NN	PHASEF	Aerosol model number
P/	MAIN	Aerosol phase function array
PAL	SSRAD	Aerosol phase function at previous scattering point
PAER2	SSRAD	Aerosol phase function at current scattering point
PARM1	MAIN	Variable input parameter, see user's guide
PARM2	MAIN	Variable input parameter, see user's guide
PARM3	MAIN	Variable input parameter, see user's guide
PARM4	MAIN	Variable input parameter, see user's guide
PHFA1	PHASEF	Phase function at lower bounding relative humidity
PHFA2	PHASEF	Phase function at upper bounding relative humidity
PHIO	SSGEO	Observer longitude
PHIS	SSGEO	Subsolar longitude
PHS	SOURCE	Lunar phase function array
PMOL1	SSRAD	Molecular phase function at previous scattering point
PMOL2	SSRAD	Molecular phase function at current scattering point
PR	MAIN	Molecular phase function array
PSIO	SSGEO	Relative azimuth at the observer
PSIPO	MAIN	Line of sight azimuth at the observer
PSISO	SSGEO	Solar azimuth at the observer
PSIST	SSGEO	Relative azimuth
RAT	SOURCE	Solar ellipic orbit factor array
RHD		Relative humidity array
RHPTS	PHASEF	Bounding relative humidities array
SANGLE	SSGEO	Scattering angle
SS	SOURCE	Extraterrestrial source intensity
SUMSSR	TRANS	Total scattering single-radiance at the observer
TASP1	SSRAD	Aerosol scatter transmittance at previous scattering point

VARIABLE	FIRST REFERENCE	DEFINITION
TASP2	SSRAD	Aerosol scatter transmittance at current scattering point
TEB1	SSRAD	Total extinction trasmittance at previous scattering point
TEB2	SSRAD	Total extinction transmittance at current scattering point
THETAO	SSGEO	Observer latitude
THETAS	SSGEO	Subsolar latitude
TIME	MAIN	Greenwich time
TMSPI	SSRAD	Molecular scattering transmittance at at previous scattering point
TMSP2	SSRAD	Molecular scattering transmittance at at current scattering point
VSUN	SOURCE	Wavelength array corresponding to to the solar intensity array ESUN
WPATHS	MAIN	Cummulative absorber amount array for the solar paths

APPENDIX C: LOWTRANSX USER'S GUIDE

The instructions for using LOWTRAN with single scattering are very similar to those for using LOWTRAN 5. The parameter ISCTTR has been added to the LOWTRAN input card 1. Control card 2A which contains all of the single scattering parameters (with the exception of ISCTTR) has also been added. The format of the new card sequence, definitions of new input parameters and a sample run are presented in this appendix.

C.1 Input Data and Format

The parameters required to specify a particular problem are contained on the four or five (if single scattering is included) input cards as follows:

CARD 1 MODEL, IHAZE, ITYPE, LEN, JP, IM, M1, M2, M3, ML, IEMISS, RO, TBOUND, ISEASN, IVULCN, ISCTTR, VIS
FORMAT (1113, 2F10.3, 313, F10.3)

CARD 2 H1, H2, ANGLE, RANGE, BETA
FORMAT (7F10.3)

The following card must be included if ISCTTR = 1

CARD 2A PARM1, PARM2, PARM3, PARM4, TIME, PSIPO, ANGLEM, G, IPH, IDAY, ISOURC, IPARM
FORMAT (8F7.2, 4I3)

CARD 3 V1, V2, DV FORMAT (3F10.3)

CARD 4 IXY FORMAT (I3)

If MODEL = 0 or 7 (user supplied meteorological data) the above card sequence and format for CARD 2 is changed. The user is referred to Reference 1 for a complete description of these cases.

C.2 Basic Instructions

It is assumed that the user is familar with all of the earlier LOWTRAN control parameters as described in Reference 1. The following discussion deals only with the new parameters and their effect, if any, on the original ones.

CARD 1 Remains unchanged except for the addition of the parameter ISCTTR defined as follows:

ISCTTR = 0 The program runs in the usual transmission or emission mode. Single scattering effects are not included, and CARD 2A must be omitted.

ISCTTR = 1 The program must be run in the emission mode (IEMISS = 1). If the user has specified ISCTTR = 1 and IEMISS = 0 the program automatically sets IEMISS = 1 and continues. CARD 2A must be included in the input card sequence. Single scattering intensity calculations are performed, and the results are written on TAPE6 and TAPE7.

CARD 2 All parameters as defined in Reference 1.

CARD 2A PARM1, PARM2, PARM3, PARM4, TIME, PSIPO, ANGLEM, G, IPH, ISOURC, IDAY, IPARM

Definitions of PARM1, PARM2, PARM3, PARM4 determined by value of IPARM.

For IPARM = 0

PARM1 = observer latitude (-90 to +90)
Note if ABS(PARM1) is greater than 89.5 the observer is assumed to be at either the north or the south pole. In this case the path azimuth is undefined. The direction of the line-of-sight must be specified as the longitude that the path lies along. This quantity rather than the usual azimuth is read in.

PARM2 = observer longitude (0 to 360)

PARM3 = source (sun or moon) latitude, see note regarding sun angle

PARM4 = source (sun or moon) longitude

For IPARM = 1

(TIME must be specified, cannot be used with ISOURC = 1)

PARM1 = observer latitude (-90 to +90)

PARM2 = observer longitude (0 to 360)

PARM3, PARM4 are not required

For IPARM = 2

PARM1 = azimuthal angle between the observer's line of sight and the observer-to-sun path, measured from the line of sight, positive east of north, between -180 and 180

PARM2 = the sun's zenith angle

PARM3, PARM4 are not required

TIME = Greenwich time in decimal hours, i.e. 8:45 am is 8.75, 5:20 pm is 17.33 etc).

PSIPO = path azimuth (degrees east of north, i.e due north is 0.0 due east is 90.0 etc.

ANGLEM = phase angle of the moon, i.e. the angle formed by the sun, moon and earth (required if ISOURC = 1)

G = asymmetry factor for use with H.G. phase function

IPH = 0 Henyey-Greenstein aerosol phase function

IPH = 1 user supplied aerosol phase function

The user supplied phase function data follows input card 2A and must have the following format:

CARD 2B	NPTF	/ FORMAT (15)
CARD 2C	ANG(1), F(1, I), F(2, I), F(3, 1), F(4, I)	/ FORMAT (5E10.3)

CARD 2C is repeated NPTF times

The variables are defined as follows:

NPTF - the number of scattering angles at which the phase function is to be specified. NPTF < 50

ANG(I) - the I'th scattering angle at which the phase function is specified. 0 < ANG(1) < 180 (in ascending order)

F(n, I) - the value of the phase function at the l'th scattering angle in altitude region n.

n = 1 0 to 2 km region
n = 2 2 to 10 km region
n = 3 10 to 30 km region
n = 4 30 to 100 km region

I - scattering angle index, I varies from 1 to NPTF

IPH = 2 MIE data base used for aerosol phase function

ISOURC = 0 extraterrestrial source is the sun

ISOURC = 1 extraterrestrial source is the moon

IDAY - day of the year; value from 1 to 365

IPARM indicates method of specifying the observer to source orientation

= 0 specify obeerver and subsolar longitude and latitude

= 1 specify observer longitude and latitude along with date and time

= 2 specify solar zenith and azimuth relative to observer

Note the following sign conventions:

Latitude is positive north of the equator.

Longitude is positive west of Greenwich, Eng.

Azimuth is positive east of north.

CARD 3 all parameters as defined in Ref. 1.

CARD 4 IXY

If ISCTTR = 0 the definition of IXY remains as in Ref. 1.

IF ISCTTR = 1 cards 2 and 2A are treated as a unit as far as the IXY parameter is concerned.

IXY = 0 to end the program
IXY = 1 to select new cards 3 and 4
IXY = 2 to select an entirely new data sequence
IXY = 3 to select new cards 2, 2A and 4
IXY = 4 to select new cards 1 and 4

If the user specifies IXY = 4 and ISCTTR = 0 on the original input card sequence, ISCTTR must remain unchanged since no CARD 2A has been or would be read in. Therefore, the only way to change from ISCTTR = 0 to ISCTTR = 1 is by specifying IXY = 2 and supplying the entire data sequence. As an example, if the user desired to specify various geometrical configurations (optical paths and sun positions) the following card sequence could be used:

```
CARD 1
CARD 2
CARD 2A
CARD 3
CARD 4   IXY = 3
CARD 2
CARD 2A
CARD 4   IXY = 3
.
.
.
CARD 4   IXY = 0
```

The final IXY card must be zero (or blank) to ensure proper termination of the program. There are no default conditions built into the single scattering routines of the LOWTRAN code.

C.3 Solar and Lunar Sources

The extraterrestrial solar intensity is obtained from the data compiled by Thekaekara [Ref. 34]. The lunar extraterrestrial intensity is obtained by reflecting the solar intensity off of the moon's surface as [Ref. 35].

$$I_{moon}(\lambda) = 2.04472 \times 10^{-7} \; I_{SUN}(\lambda) \;\; \alpha(\lambda) \; P(\gamma).$$

Here $\alpha(\lambda)$ is the wavelength - dependent geometric albedo of the moon [Ref. 36 and 37], while $P(\gamma)$ is the moon's phase function giving the relative intensity as a function of the phase angle [Ref. 38]. Note that $P(\gamma = 0) = 1$ for a full moon.

C.4 LOWTRANSX Example Run

An example run of LOWTRANSX will serve to illustrate the structure and format of the input and output files. The input "file" consists of three records. The first record contains the job control language necessary to access, load, and execute the program. LOWTRANSX is structured to allow segmentation during loading to reduce central memory requirements. The structure of the segmented program is defined by the directives in the second record. The third record contains the input cards that describe the example run. The particular input file shown defines a line of sight from 2 Km to 5 Km altitude, at a zenith angle of 45 degrees and azimuth of 30 degrees. The observer is located at 40 north latitude and 160 degrees longitude, which the subsolar point is at 40 degrees north latitude and 240 degrees longitude. Details of the atmospheric composition and wavenumber region of interest are relatively unimportant and will not be described here. The output file is similar to the one produced by the original LOWTRAN code. Additional output pertaining specifically to the single scattering radiance calculation is clearly labelled and includes:

1. A summary of the single scattering control parameters following the standard LOWTRAN summary,
2. A summary of the geometric aspects of the scattering point to sun paths and,
3. Both scattered and total radiance as additional entries in the radiance table normally produced by LOWTRAN.

A listing of the example run output file is shown on the following pages.

C.5 Concluding Comments

Before executing the program in the single scattering mode, the user should be made aware of the following characteristics of the code:

1. Execution time can be expected to increase when operating in the single scattering mode. This is largely a result of the following:

   a) The code must be run in the emission mode.

   b) The geometry routines are called once for each scattering point to sun path (i.e. at each layer boundary contained in the optical path) in addition to the single call normally made for the optical path.

   c) The transmittance calculations are done twice (rather than once) for each scattering point along the optical path.

   For most applications one can expect the run time to be about twice as long in the scattering-emission mode as in the emission mode alone.

2. To avoid unnecessary and misleading calculations the user should review Chapter 4 of this report regarding the validity of the single scattering assumption.

3. Depending upon his specific interests the user may or may not want intermediate results printed. For this reason modification of the printed output is left to the user.

```
SCRAF,CM110000,T60.                                    2710    MOOSE
ATTACH(LOWB,LOWXSSB,ID=MOOSE,MR=1)
ATTACH(GEOB,LOWXSSGEOB,ID=MOOSE,MR=1)
ATTACH(PF6,LOWXSSPF8,ID=MOOSE,MR=1)
ATTACH(PFNNSB,LOWXSSPFNNSB,ID=MOOSE,MR=1)
REQUEST,LOWOUT,*PF.
REQUEST,TAPE7,*PF.
MAP,PART.
LDSET,PRESET=INDEF.
LOAD,PFNNSB,PFSB,GEOB,LOWB.
SEGLOAD.
EXECUTE,LOWEM.
EXIT(U)
CATALOG(TAPE7,LOWXSSTAPE7,ID=MOOSE)
REWIND,OUTPUT.
COPYCF,OUTPUT,LOWOUT.
CATALOG(LOWOUT,LOWXSSTAPE6,ID=MOOSE)
EOR  EXITIUT
     LOWTRAN TREE LOWEM=(NSMOL,HPROF,SSGEO,EXABIN,XTRANS)
     LOWEM GLOBAL CARD1,CARD2,CARD3,CNTRL,MDATA,SOLS,USRDTA,IFIL-SAVE
     NSMOL INCLUDE NSMOL,AEPROF,PRFDTA
     HPROF INCLUDE HPROF,AEPROF,PRFDTA
     SSGEO INCLUDE SSGEO,GEO,EXPINT,PSIDEL,PSI,DEL,STANG,PHIS,F
     SSGEO GLOBAL MODEL,PARMTR,PERPTH-SAVE
     EXABIN INCLUDE EXABIN,EXTDTA
     XTRANS TREE TRANS-(SSRAD-(PHASES-(PF-(PF01,PF02,PF03,PF04,PF05,
     ,PF06,PF07,PF08,PF09,PF10,PF11,PF12,PF13,PF14,PF15,PF16,PF17,PF18,
     ,PF19,PF20,PF21,PF22)))))
     TRANS INCLUDE TRANS,AEROXT,C40TA,SOURCE
     TRANS GLOBAL SRAD=SAVE
EOR  END LOWEM
   6  1  2  0                    1                                  1
      2.000       5.000      45.000
    40.00  160.00   40.00  240.00          30.00          2  0  65
 15500.000 15520.000    20.000
```

LOWTRANSX Example Output File

```
S
1 PROGRAM WILL BE EXECUTED IN THE EMISSION MODE
  6  1  2  0  5  0  0  0  0  0  1        0.000      0.000  0  0  1        0.000
     2.000      5.000     45.000      0.000     0.000
  40.00 160.00  40.00 240.00   0.00  30.00  30.00    .90  2  0 65  0
 15500.000 15520.000    20.000

                    HAZE MODEL  =  23.0 KM VISUAL RANGE AT SEA LEVEL

                    MODEL ATMOSPHERE 6 = 1962 US STANDARD

                    HAZE MODEL  1 =  RURAL      VIS= 23.0KM

                    SEASON =  SPRING SUMM

                    VERTICAL PROFILE AEROSOL MODEL =  STRAT BKGD

          FREQUENCY RANGE V1= 15500.0 CM-1 TO V2= 15520.0 CM-1 FOR DV =  20.0 CM-1  (  .64 =  .65 MICRONS )

 SINGLE SCATTERING CONTROL PARAMETER SUMMARY

      OBSERVER LATITUDE  =     40.000  DEGREES, +N OF THE    EQUATOR
      OBSERVER LONGITUDE =    160.000  DEGREES WEST OF GREENWICH
      SUBSOLAR LATITUDE  =     40.000  DEGREES, +N OF THE EQUATOR
      SUBSOLAR LONGITUDE =    240.000  DEGREES WEST OF GREENWICH
      TIME (<0 IS UNDEF) =      0.000  GREENICH TIME
      PATH AZIMUTH =           30.000  DEGREES EAST OF NORTH
      DAY OF THE YEAR =           65
      EXTRATERRESTRIAL SOURCE IS THE SUN
      PHASE FUNCTIONS FROM MIE DATA BASE
1

            HORIZONTAL PROFILES

  ID      ALT        P          T          H2O        CO2         O3          N2        CNTMSLP      HOLS       (N-1)      ST(UV)
   1     0.00  1013.000    296.100  2.760E-02  9.229E-01  2.493E-03  7.838E-01  1.566E+20  9.481E-01  2.759E-04  2.523E-03
   2     1.00   898.600    281.300  3.719E-01  7.776E-01  2.367E-03  6.814E-01  7.935E+19  8.604E-01  2.505E-04  2.329E-03
   3     2.10   795.000    275.100  2.724E-01  5.447E-01  2.281E-03  4.677E-01  3.793E+19  7.732E-01  2.269E-04  2.162E-03
   4     3.00   701.200    268.700  1.702E-01  5.377E-01  2.021E-03  3.929E-01  1.457E+19  7.027E-01  2.049E-04  2.337E-03
   5     4.00   616.600    262.200  7.197E-02  4.427E-01  1.775E-03  2.152E-01  5.443E+18  6.424E-01  1.847E-04  2.147E-03
   6     5.00   540.500    255.700  3.746E-02  3.648E-01  1.692E-03  2.515E-01  1.842E+18  5.900E-01  1.668E-04  2.147E-03
   7     6.00   472.200    249.200  1.692E-02  2.987E-01  1.575E-03  1.955E-01  6.435E+17  5.410E-01  1.488E-04  2.118E-03
   8     7.00   411.100    242.700  9.846E-03  2.428E-01  1.633E-03  1.577E-01  1.984E+17  4.567E-01  1.331E-04  2.287E-03
   9     8.00   356.500    236.200  5.041E-03  1.984E-01  1.545E-03  1.272E-01  6.467E+16  4.076E-01  1.196E-04  2.442E-03
  10     9.00   308.000    229.700  1.723E-03  1.598E-01  2.131E-03  9.991E-02  2.520E+15  3.616E-01  1.053E-04  3.313E-03
  11    10.00   265.600    223.200  5.997E-04  1.267E-01  2.597E-03  7.412E-02  1.457E+15  3.201E-01  9.378E-05  4.268E-03
  12    11.00   227.000    216.800  2.056E-04  1.007E-01  3.493E-03  5.531E-02  3.225E+14  2.823E-01  8.226E-05  6.067E-03
  13    12.00   194.000    216.600  9.279E-05  7.627E-02  4.838E-03  4.156E-02  6.759E+13  2.414E-01  7.037E-05  7.467E-03
  14    13.00   165.800    216.600  5.910E-05  5.794E-02  6.029E-03  3.035E-02  1.457E+13  2.064E-01  6.014E-05  7.923E-03
```

CASE 2A: GIVEN H1, H2, ANGLE

SLANT PATH PARAMETERS IN STANDARD FORM

H1	=	2.000 KM
H2	=	5.000 KM
ANGLE	=	45.000 DEG
PHI	=	135.023 DEG
HMIN	=	2.000 KM
LEN	=	0

1CALCULATION OF THE REFRACTED PATH THROUGH THE ATMOSPHERE

I	ALTITUDE FROM (KM)	ALTITUDE TO (KM)	THETA (DEG)	PRESS (KM)	RANGE (KM)	DTHETA (DEG)	BETA (DEG)	SUM (DEG)	TBEND (DEG)	BENDING (DEG)	PBAR (MB)	TBAR (K)	PHOBAR (CM-3)
					H1 TO H2								
1	2.000	3.000	45.000	1.414	1.414	.009	.009	135.009	.001	.001	787.916	271.942	9.57E-04
2	3.000	4.000	44.992	1.414	2.827	.009	.018	135.018	.001	.002	650.727	265.493	8.63E-04
3	4.000	5.000	44.984	1.414	4.242	.009	.027	135.027	.001	.003	537.191	258.994	7.77E-04

CUMULATIVE ABSORBER AMOUNTS FOR THE PATH FROM H1 TO 2

J	Z (KM)	TAVE (K)	H2O (G-CM-2)	CO2 (KM)	O3 (ATM-CM)	HNO3 (G-CM-2)	O3 MW (ATM-CM)	CNTMSLE1 (MOL CM-2)	CNTMSLE2 (MOL CM-2)	CNTMSLE3 (MOL CM-2)
1	3.000	271.942	2.439E-01	5.355E-01	3.040E-03	0.	3.430E-03	3.448E+19	2.384E+19	8.746E+21
2	4.000	265.493	3.881E-01	1.427E+00	5.713E-03	0.	6.595E-03	4.759E+19	3.415E+19	1.361E+22
3	5.000	258.994	4.827E-01	2.197E+00	8.169E-03	0.	9.670E-03	5.882E+19	3.385E+19	1.624E+22

J	Z (KM)	H2 CONT (KM)	MOL SCAT (KM)	AER 1	AER 2	AER 3	AER 4
1	3.000	6.201E-01	1.048E+00	4.391E-02	2.446E-02	0.	0.
2	4.000	1.119E+00	1.992E+00	4.391E-02	6.382E-02	0.	0.
3	5.000	1.517E+00	2.843E+00	4.391E-02	7.974E-02	0.	0.

0SUMMARY OF THE GEOMETRY CALCULATION

H1	=	2.000 KM
H2	=	5.000 KM
ANGLE	=	45.000 DEG
RANGE	=	4.242 KM
BETA	=	.027 DEG
PHI	=	135.023 DEG
HMIN	=	2.000 KM
BENDING	=	.003 DEG
LEN	=	1

15	14.00	141.700	216.600	1.588E-05	4.482E-02	4.229E-03	2.217E-02	3.174E+12	1.784E-01	3.140E-05	8.867E-03	
16	15.00	121.100	216.600	1.182E-05	3.344E-02	4.389E-03	1.661E-02	2.382E+12	1.508E-01	4.392E-05	9.902E-03	
17	16.00	103.500	216.600	8.691E-06	2.454E-02	4.711E-03	1.183E-02	1.674E+12	1.288E-01	3.754E-05	1.120E-02	
18	17.00	88.500	216.600	6.435E-06	1.931E-02	5.162E-03	8.647E-03	1.216E+12	1.102E-01	3.210E-05	1.307E-02	
19	18.00	75.650	216.600	4.728E-06	1.466E-02	5.541E-03	6.318E-03	8.798E+11	9.417E-02	2.744E-05	1.493E-02	
20	19.00	64.670	216.600	4.106E-06	1.118E-02	5.692E-03	4.617E-03	6.428E+11	9.051E-02	2.746E-05	1.633E-02	
21	20.00	55.290	216.600	3.455E-06	8.479E-03	5.805E-03	3.375E-03	4.719E+11	8.283E-02	2.004E-05	1.773E-02	
22	21.00	47.290	217.600	3.372E-06	6.432E-03	5.444E-03	2.465E-03	1.038E+12	9.865E-02	1.707E-05	1.773E-02	
23	22.00	40.470	218.600	3.159E-06	4.880E-03	5.248E-03	1.753E-03	1.816E+12	4.992E-02	1.454E-05	1.820E-02	
24	23.00	34.670	219.600	3.016E-06	3.676E-03	4.907E-03	1.300E-03	1.481E+12	4.257E-02	1.240E-05	1.773E-02	
25	24.00	29.720	220.600	2.814E-06	2.773E-03	4.274E-03	9.468E-04	1.574E+12	3.623E-02	1.058E-05	1.680E-02	
26	25.00	25.490	221.600	2.687E-06	2.119E-03	3.703E-03	6.932E-04	1.959E+12	3.102E-02	9.027E-06	1.587E-02	
27	30.00	11.970	226.500	7.614E-07	5.479E-04	1.641E-03	1.479E-04	5.445E+11	1.425E-02	4.152E-06	9.333E-03	
28	35.00	5.746	236.500	1.624E-07	1.429E-04	6.674E-04	3.189E-05	1.152E+11	6.551E-03	1.909E-06	5.173E-03	
29	40.00	2.871	253.400	3.531E-08	3.857E-05	2.222E-04	7.592E-06	2.213E+10	3.055E-03	3.931E-07	2.257E-03	
30	45.00	1.491	264.200	9.176E-09	1.164E-05	5.892E-05	1.822E-06	4.630E+09	1.522E-03	4.434E-07	7.933E-04	
31	50.00	.796	270.600	1.933E-09	3.751E-06	1.072E-05	5.533E-07	6.477E+08	7.950E-04	2.316E-07	1.857E-04	
32	70.00	.055	219.700	2.406E-12	4.662E-09	9.259E-08	3.293E-09	1.012E+06	6.775E-06	1.974E-06	4.011E-06	
33	100.00	.010	210.000	1.572E-16	3.421E-12	8.151E-12	1.046E-13	4.495E+01	3.562E-07	1.125E-10	2.307E-04	
34	99999.00	0.000	210.000	0.	0.	0.	0.	0.	0.	0.	0.	

1

HORIZONTAL PROFILES

ID	H1	B	T	[illegible]	[illegible]	[illegible]	[illegible]	[illegible]	[illegible]	(AE+1*SH)	SP
1	0.00	1013.000	288.100	2.009E+22	0.	1.680E-01	0.	0.	0.	7.228E+00	4.578E+01
2	1.00	898.600	281.600	1.700E+22	0.	9.081E-02	0.	0.	0.	4.962E+00	4.908E+01
3	2.00	795.000	275.100	6.141E+21	0.	6.210E-02	0.	0.	0.	3.238E+00	5.214E+01
4	3.00	701.200	268.700	4.573E+21	0.	0.	3.485E-02	0.	0.	0.	0.
5	4.00	616.600	262.200	2.519E+21	0.	0.	1.850E-02	0.	0.	0.	0.
6	5.00	540.500	255.700	1.316E+21	0.	0.	9.310E-03	0.	0.	0.	0.
7	6.00	472.200	249.200	7.021E+20	0.	0.	7.710E-03	0.	0.	0.	0.
8	7.00	411.100	242.700	3.478E+20	0.	0.	6.270E-03	0.	0.	0.	0.
9	8.00	356.500	236.200	1.767E+20	4.073E-55	0.	3.370E-03	0.	0.	0.	0.
10	9.00	308.000	229.700	6.019E+19	3.616E-06	0.	1.820E-03	0.	0.	0.	0.
11	10.00	265.000	223.200	2.086E+19	1.056E-05	0.	0.	1.140E-03	0.	0.	0.
12	11.00	227.000	216.800	8.379E+18	2.259E-05	0.	0.	7.990E-04	0.	0.	0.
13	12.00	194.000	216.600	3.234E+18	2.898E-05	0.	0.	5.410E-04	0.	0.	0.
14	13.00	165.800	216.600	1.345E+18	2.893E-05	0.	0.	5.171E-04	0.	0.	0.
15	14.00	141.700	216.600	5.587E+17	2.822E-05	0.	0.	4.420E-04	0.	0.	0.
16	15.00	121.100	216.600	3.929E+17	2.714E-05	0.	0.	3.950E-04	0.	0.	0.
17	16.00	103.500	216.600	2.845E+17	2.448E-05	0.	0.	3.920E-04	0.	0.	0.
18	17.00	88.500	216.600	2.074E+17	2.203E-05	0.	0.	4.250E-04	0.	0.	0.
19	18.00	75.650	216.600	1.500E+17	1.978E-05	0.	0.	5.290E-04	0.	0.	0.
20	19.00	64.670	216.600	1.282E+17	1.352E-05	0.	0.	5.310E-04	0.	0.	0.
21	20.00	55.290	216.600	1.096E+17	2.056E-05	0.	0.	5.930E-04	0.	0.	0.
22	21.00	47.290	217.600	1.019E+17	2.154E-05	0.	0.	5.320E-04	0.	0.	0.
23	22.00	40.470	218.600	9.395E+16	2.097E-05	0.	0.	4.200E-04	0.	0.	0.
24	23.00	34.670	219.600	8.782E+16	2.214E-05	0.	0.	3.330E-04	0.	0.	0.
25	24.00	29.720	220.600	8.020E+16	2.280E-05	0.	0.	1.980E-04	0.	0.	0.
26	25.00	25.490	221.600	7.409E+16	1.179E-05	0.	0.	1.310E-04	0.	0.	0.
27	30.00	11.970	226.500	1.960E+16	3.705E-06	0.	0.	3.320E-05	0.	0.	0.
28	35.00	5.746	236.500	3.794E+15	1.441E-07	0.	0.	0.	1.540E-05	0.	0.
29	40.00	2.871	253.400	7.405E+14	3.055E-07	0.	0.	0.	7.990E-06	0.	0.
30	45.00	1.491	264.200	1.752E+14	0.	0.	0.	0.	4.311E-06	0.	0.
31	50.00	.796	270.600	3.465E+13	0.	0.	0.	0.	2.100E-06	0.	0.
32	70.00	.055	219.700	3.578E+11	0.	0.	0.	0.	1.600E-07	0.	0.
33	100.00	.010	210.000	1.398E+06	0.	0.	0.	0.	9.310E-11	0.	0.
34	99999.00	0.000	210.000	0.	0.	0.	0.	0.	0.	0.	0.

EQUIVALENT SEA LEVEL TOTAL ABSORBER AMOUNTS

H2O (GM-CM-2)	CO2* (KM)	O3 (ATM-CM)	HNO3 (GM-CM-2)	O3 UV (ATM-CM)	CNTMSLF1 (MOL-CM-2)	CNTMSLF2 (MOL-CM-2)	CNTMFRN (MOL-CM-2)
4.682[illegible]E-01	2.197E+00	8.169E-03	0.	9.[illegible]0E-04	5.228E+19	3.385E+19	1.624E+22

N2 CONT	MOL SCAT (KM)	AER 1	AER 2	AER 3	AER 4	MEAN RH (PERCENT)
1.517E+00	2.343E+00	4.791E-02	7.374E-02	0.	0.	52.1%

SINGLE SCATTERING POINT TO SOURCE PATHS

ALL POINT-TO-SOURCE PATHS ARE GEO TYPE 3A
SPECIFYING H1 ,ANGLE AND SPACE. ANGLE IS THE STRAIGHT
LINE APPROXIMATION, THE ACTUAL ANGLE IS DETERMINED
BY ITERATION

SCTR POINT	SCTR ALT	SUBTENDED ANGLE	SOLAR ZENITH	PATH ZENITH	RELATIVE AZIMUTH	SCTR ANGLE	MOLECULAR PHASE F	AE-DSOL PHASE F
1	2.00	0.00	80.00	45.00	-91.65	94.11	.612E-01	.941E+02
2	3.00	.01	80.00	44.99	-91.65	94.11	.612E-01	.941E+02
3	4.00	.02	80.00	44.98	-91.65	94.11	.612E-01	.941E+02
4	5.00	.03	80.00	44.98	-91.65	94.11	.612E-01	.941E+02

1 RADIANCE(WATTS/CM2-STER-XXX)

CM-1	WVL(MICRON)	PATH PER CM-1	PATH PER MICRON	SCATTERED PER CM-1	SCATTERED PER MICRON	TOTAL PER CM-1	TOTAL PER MICRON	INTEGRAL	TRANS
15503.0	.6457	.4453[illegible]E-37	.2[illegible]63E-33	.11916E-07	.2862[illegible]E-03	.11916E-07	.2862[illegible]E-03	.4453[illegible]E-36	.8[illegible]5082
15520.0	.6443	.4[illegible]147E-37	.9[illegible]7[illegible]3E-33	.11894E-07	.2865[illegible]E-03	.11894E-07	.2865[illegible]E-03	.4[illegible]677E-36	.884[illegible]41

INTEGRATED ABSORPTION FROM 15503.0[illegible] TO 15[illegible]2 CM-1 = 2.[illegible]CAV PATH TRANSMITTANCE = .8[illegible]5[illegible]

INTEGRATED RADIANCE = .4[illegible]677E-36WATTS CM-2 SR

RADMIN 15520.000 .4[illegible]147E-37

RADMAX 15503.000 .4[illegible]53E-37

APPENDIX D: INPUT ANGLES FOR THE SUBSOLAR POINT

The user has the option of specifying the orientation of the sun by direct input of the subsolar longitude and latitude, i e. that point on the earth where the sun is directly overhead. To find the subsolar point angles, the sun's declination angle and the equation of time are required. The declination angle is defined as the longitude at which the sun is directly overhead at solar noon. The equation of time represents the difference between local (standard) time and true solar time. The American Ephemeris and Nautical Almanac published annually by the U.S. Goverment Printing Office contains precise values of the declination angle and equation of time for each day of each year. For illustrative purposes consider the sample data for a single year, taken directly from Reference 39 and shown in Table D1 and graphically in Figure D1. With this data, it is a simple task to determine the subsolar point angles. An example follows:

THETAS = subsolar latitude = the sun's declination angle

PHIS = subsolar longitude = STM + 15* (ST+ET-12.0)

where,

STM = the standard time zone meridian in degrees. The standard time zones for the continental U.S. are Pacific - 120, Mountain - 105, Central - 90, and Eastern - 75.

ST = local (or standard) time in hours, expressed as a decimal number between 0.0 and 24.0 (i.e. 2:40 PM would be 14.66). Note, if a region is on daylight savings time the correct time is one hour earlier.

ET = equation of time in hours.

As an example:

Determine the subsolar point angles on October 13 and 1:45 PM Central Standard Time.

Solution:

From Table D1 -

declination angle = -7 deg 29 min = -7.48 deg

equation of time = +13 min 30 sec = .225 hours

Therefore -

THETAS = -7.48

PHIS = 90 + 15*(13.75 + 0.225 - 12.0) = 119.63 degrees

Date		Declination		Equation of time		Date		Declination		Equation of time	
		Deg	Min	Min	Sec			Deg	Min	Min	Sec
Jan.	1	−23	4	− 3	14	Feb.	1	−17	19	−13	34
	5	22	42	5	6		5	16	10	14	2
	9	22	13	6	50		9	14	55	14	17
	13	21	37	8	27		13	13	37	14	20
	17	20	54	9	54		17	12	15	14	10
	21	20	5	11	10		21	10	50	13	50
	25	19	9	12	14		25	9	23	13	19
	29	18	8	13	5						
Mar.	1	− 7	53	−12	38	Apr.	1	+ 4	14	− 4	12
	5	6	21	11	48		5	5	46	3	1
	9	4	48	10	51		9	7	17	1	52
	13	3	14	9	49		13	8	46	− 0	47
	17	1	39	8	42		17	10	12	+ 0	13
	21	− 0	5	7	32		21	11	35	1	6
	25	+ 1	30	6	20		25	12	56	1	53
	29	3	4	5	7		29	14	13	2	33
May	1	+14	50	+ 2	50	June	1	+21	57	+ 2	27
	5	16	2	3	17		5	22	28	1	49
	9	17	9	3	35		9	22	52	1	6
	13	18	11	3	44		13	23	10	+ 0	18
	17	19	9	3	44		17	23	22	− 0	33
	21	20	2	3	34		21	23	27	1	25
	25	20	49	3	16		25	23	25	2	17
	29	21	30	2	51		29	23	17	3	7
July	1	+23	10	− 3	31	Aug.	1	+18	14	− 6	17
	5	22	52	4	16		5	17	12	5	55
	9	22	28	4	56		9	16	6	5	33
	13	21	57	5	30		13	14	55	4	57
	17	21	21	5	57		17	13	41	4	12
	21	20	38	6	15		21	12	23	3	19
	25	19	50	6	24		25	11	2	2	18
	29	18	57	6	23		29	9	39	1	10
Sep.	1	+ 8	35	− 0	15	Oct.	1	− 2	53	+10	1
	5	7	7	+ 1	2		5	4	26	11	17
	9	5	37	2	22		9	5	58	12	27
	13	4	6	3	45		13	7	29	13	30
	17	2	34	5	10		17	8	58	14	25
	21	+ 1	1	6	35		21	10	25	15	10
	25	− 0	32	8	0		25	11	50	15	46
	29	2	6	9	22		29	13	12	16	10
Nov.	1	−14	11	+16	21	Dec.	1	−21	41	+11	16
	5	15	27	16	23		5	22	16	9	43
	9	16	38	16	12		9	22	45	8	1
	13	17	45	15	47		13	23	6	6	12
	17	18	48	15	10		17	23	20	4	17
	21	19	45	14	18		21	23	26	2	19
	25	20	36	13	15		25	23	25	+ 0	20
	29	21	21	11	59		29	23	17	− 1	39

Table D1 Tabular example of the equation of time.

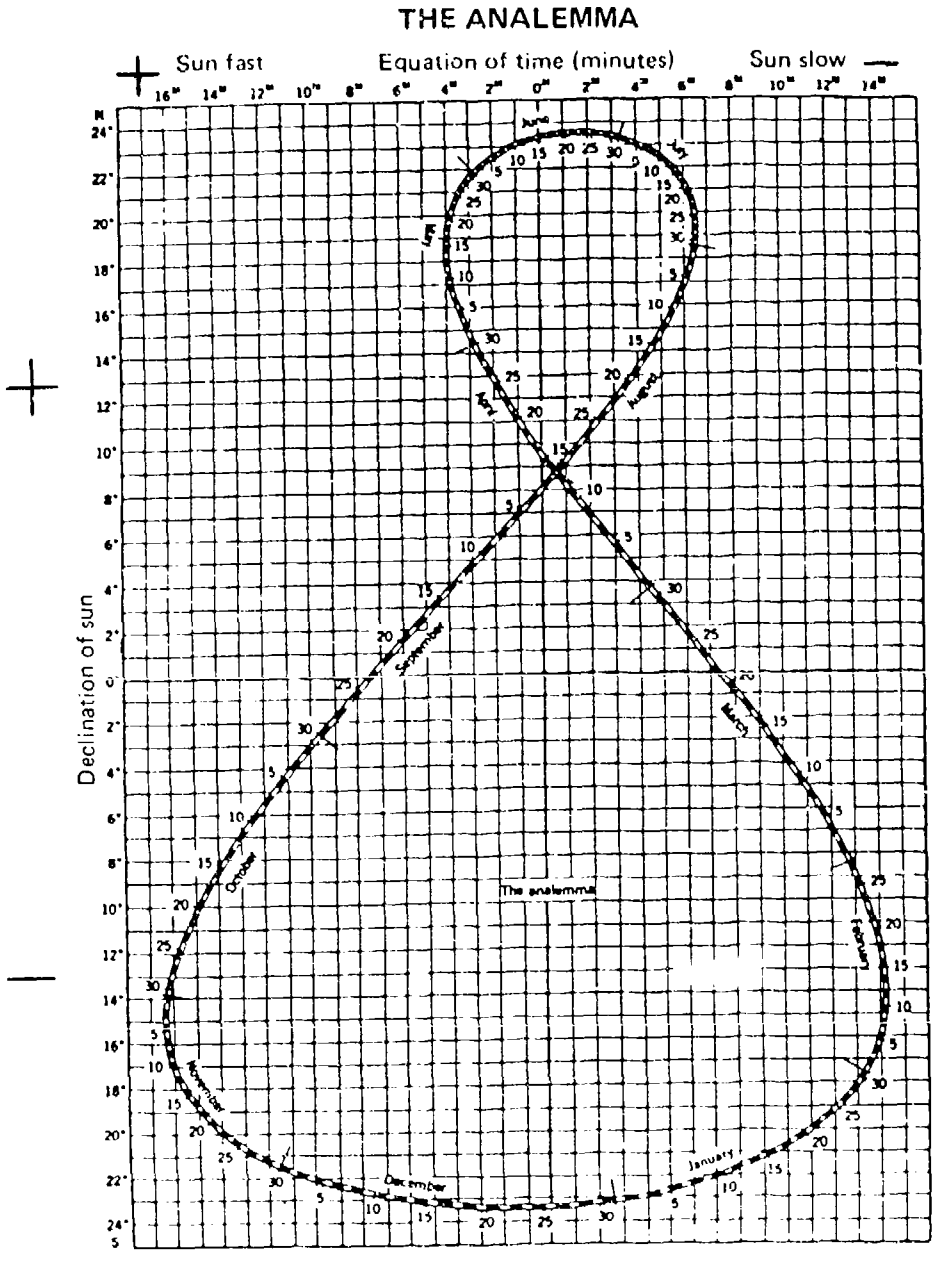

Figure D1 Graphical equation of time.

```
**********************************************************************
*                                                                    *
*   USER'S MANUAL FOR ADDING CODE VERSION 8.2 OF 02/02/80            *
*                                                                    *
*   MANUAL LAST UPDATED - 02/17/80 by Ajay Sharma.                   *
*                                                                    *
**********************************************************************
```

1. INTRODUCTION

The ADDING code VERSION 8.2 computes the following scattering functions :

$S_S^{\pm}$, $T_S^{\pm}$, $S_F^{\pm}$, $T_F^{\pm}$,

$c^{\pm}$, $(a^- \pm a^+)$ and f^+.

These functions are calculated from Equations (2.42)-(2.66) and (2.30) as described in Chapters II and III and Appendix 2 of Ajay Sharma's thesis. In addition, this program calculates the emerging intensities and one-sided heat fluxes for problems with given temperature profiles (see Chapter IV of the thesis). The program is capable of calculating any Fourier component of the above quantities for plane-parallel, anisotropic scattering, inhomogeneous media bound by top and bottom surfaces with arbitrary specified bidirectional reflectivity or directional emissivity, at a given wavelength.

2. USER DEFINABLE FUNCTIONS

This version of ADDING code has FIVE subroutines and function subprograms that specify various media and surface conditions. The five are FUNCTION PHASFN (XMU1, XMU2), FUNCTION OMEGFUN (T), FUNCTION ASYFUN (T), FUNCTION TMPFUN(T) and SUBROUTINE SURINP. All these functions and subroutines must ALWAYS be included at run time although some of them may not be called or used. All of these can be replaced by the users to suit their needs. The function of these routines is as follows :

A. FUNCTION OMGFUN (T)

This user defined function subprogram supplies the ADDING code with the single scattering albedo ω as a function of the optical depth T. Any arbitrary ω profile can be specified. The function must set OMGFUN = value of ω at optical depth T. This function is called ONLY if omega is specified as being inhomogeneous by INHOMO parameter discussed in Section 5.

B. FUNCTION ASYFUN (T)

Should specify the value of asymmetry factor for the scattering phase function. The use of this function is linked to the use of Henyey-Greenstein phase function. The function is called only if inhomogeneous asymmetry factor is specified by INHOMO.

C. FUNCTION TMPFUN (T)

For a nonisothermal case, this function should return the medium temperature (degrees Kelvin) at optical depth T, to be used in intensity and heat flux calculations in direct problems.

D. FUNCTION PHASFN (XMU1, XMU2)

Can be replaced by the user to specify any scattering phase function other than H.-G., but associated parameters will have to be carefully checked.

E. SUBROUTINE SURINP

This routine can be replaced to specify any arbitrary reflecting, emitting or scattering bottom surface. The replacement routine must set function values as described in the comment cards at the beginning of the example SURINP routine supplied with the deck. NOTE that Black surfaces, surfaces with known emissivity and a "reflection peakyness parameter", or surfaces with known bidirectional reflectivity can be handled by existing routines by specifying ISURF as 1, 2 and 3 respectively. See Section 6 of this manual for details.

3. EXTERNAL ROUTINES USED BY ADDING CODE.

The ADDING code uses five library routines - QA05AD, FR01AD, TIMDAT, CPUTIM and ERRSET. Their functions and need are described in the comment cards in the beginning of the MAIN program.

4. INPUT/OUTPUT FILES.

ADDING VERSION 8.2 uses many input/output files as described in the comment cards. The following is a description of the physical organization of these files :

NOTE : DSRN means the FORTRAN 'Data Set Reference Number' or Unit number in READ and WRITE statements.

DSRN 01 : Is used through a READ(1,*) statement to enter a run label of upto 80 characters. The program also writes interactive messages on this file. It is strongly recommended that this file be the user TERMINAL.

DSRN 02 : Is an INPUT file from which the program can read one card long equations defining OMGFUN, ASYFUN and TMPFUN, respectively, on three consequitive cards. These equation are used for INFORMATIVE OUTPUT ONLY and have no effect on computations.

DSRN 05 : PRIMARY INPUT file for the program, used through a READ (5,CASE) input statement (using NAMELIST CASE) and for input of surface properties by SURINP/SURIN2 routines as necessary. The inputs on this file are described in detail in Sections 5 and 6 of this document.

DSRN 06 : PRIMARY OUTPUT file, used through many WRITE (6, ...) statements. This file should usually be attached to the line printer. The printing on DSRN 06 is controlled by the parameter IOCTL1.

DSRN 11 : Is an OUTPUT file controlled by parameter IOCTL2 and would contain unformatted output records of the exiting intensities (see line numbers 21070-21100 in program). This should be a disk or a tape file to work right. Typically this output might be read by another program for plotting purposes.

DSRN 12 : Is an input/output file controlled by IOCTL3 which should preferably be a disk file. The ADDING code uses this file to store and retrieve RESTART information, i.e., ADDING can write sufficient inforamtion on this file at the end of a run so that it can add DIFFERENT surfaces at the top and bottom of a particular medium, without computing medium properties all over again. This process is called RESTARTING in this document. The file is written in subroutines HEADER and OUTPR (lines 17650, 21130-21220) and is read in subroutine INPUT (lines 4770-4890). The use of this file is purely internal to ADDING.

DSRN 13 : ADDING writes all the functions computed on this file under control of IOCTL4. The output is unformatted and should be disk or tape resident. Typically this output can be read by another program for the purpose of comparing the adding technique with the results of another theory. Lines 21240-21300 in subroutine OUTIR contain the WRITE statements for this file.

DSRN 14 : This file is used by ADDING to write the generated f and a functions using unformatted writes. These functions can later be read by another program for printing or computing purpose. The output on this file is controlled by the IOCTL5 parameter. NOTE that this is the ONLY file on which these functions are written, ADDING does not write them on DSRN 06.

5. PRIMARY INPUT PARAMETERS

The following is a list of parameters together with their functions which are read in by ADDING using NAMELIST CASE from DSRN 5. If any of the parameters are omitted from the input data, they take the default values shown :

NAME	RANGE	DEFAULT VALUE	FUNCTION
ASY	-1.0 to 1.0	0.0	ASY is the asymmetmy factor "g" for the H.-G. phase function and is used only if ASY is specified to be HOMOGENEOUS by INHOMO as described below.
C	--	GAUSS	The C array contains the quadrature weights for the angle integrations. The default values result in a Gaussian quadrature. There should be N values for this array if the default is to be overriden.
DTMAX	--	--	Variable not for user modification.
DTRLR	0.0 to TO1	1.0	Where TO1 is the optical thickness (TNOTLR) for the first layer. This variable specifies the c function spacing desired. The program will pick DTR such that DTR .LE. DTRLR and DTR = TO1 / (2 ** I) where I is an integer.
IOCTL1	1,2,3,4,5	1	Control parameter for primary output on DSRN 06. The effect of IOCTL1 is : =1 : All functions generated are printed after adding each layer. =2 : Only Intensities and Heat Fluxes are printed after adding each layer. =3 : All functions are printed after adding upto the final optical thickness.

			=4 : Only Intensities and Heat fluxes are printed after adding upto final optical thickness. =5 : NO OUTPUT on DSRN 06 except the header page.
IOCTL2	0,1,2	0	This parameter controls output on DSRN 11 as follows : =0 : NO output is written on this file. =1 : output on this file after adding upto the final optical thickness. =2 AND IOCTL1>3 : output on this file after adding each layer.
IOCTL3	0,1,2	0	Controls output on DSRN 12 as follows : =0: NO restart file is written or read. =1 : Restart file is written for later use by ADDING. =2 : ADDING runs to only add a surface to medium whose properties were last written on this restart file.
IOCTL4	0 or 1	0	Causes output to be written on DSRN 13 if IOCTL4 = 1.
IOCTL5	0,1,2,3	0	Controls a function writing on DSRN 14 as follows: =0 : NO output on DSRN 14. =1 : Only the c and f functions written after adding all the layers. =2 : The c, f and a functions written after adding ALL the layers. =3 : The c, f, and a functions are all written after adding each layer.
INHOMO	0,1,2,3	0	Specifies the medium as follows : =0 : HOMOGENEOUS medium, values of ASY and OMEGA are both used. =1 : Omega is inhomogeneous and values obtained from OMGFUN (T) are used, OMEGA value is ignored. =2 : Asymmetry factor is assumed to be inhomogeneous, values from ASYFUN(T) are used, ASY value is ignored. =3 : BOTH Asymmetry factor and Omega are assumed to be inhomogeneous.
ISURF	0,1,2,3	0	Specifies bottom surface to be added, SEE discussion in section 6. If ISURF =0 : No bottom surface. =1 : BLACK bottom surface to be added.

			=2 : A reflecting surface with GIVEN directional spectral emissivity and peakyness parameter is to be added. =3 : A reflecting surface with given bidirectional reflectivity is added.
ISURFT	0,1,2,3	0	Specifies top surface to be added, SEE discussion in section 6. If ISURFT =0 : No top surface. =1 : BLACK top surface to be added. =2 : A reflecting surface with GIVEN directional spectral emissivity and peakyness parameter is to be added. =3 : A reflecting surface with given bidirectional reflectivity is added.
M	--	1	Fourier component number.
N	1,2,..,10	7	Number of Quadrature points to be used.
NONISO	0,1	0	If medium is nonisothermal : NONISO=1. Also then TMPFUN (T) would be called to specify the temperature profile.
NLAYER	1,2,..,40	1	Number of medium layers to be added.
OMEGA	0.0 to 1.0	0.8	Albedo (ω) for the homogeneous case.
REFIDX	0.0 to --	1.0	Medium refractive index.
TMPRM	0.0 to --	325.0	Medium temperature (deg. K) for isothermal media with surfaces.
TMPSUR	0.0 to --	325.0	BOTTOM Surface temperature (deg. K).
TMPSUT	0.0 to --	325.0	TOP Surface temperature (deg. K).
TNOTLR	--	1.0	A vector of NLAYER numbers giving the optical thicknesses of all the NLAYER layers to be added. The final optical thickness is the sum of these numbers. Note that each layer can be of any optical thickness as long as it is such that TNOLR(J)=(2**I)*DTRLR for all J and any integer I.
WAVELN	0.0 to --	5.0	Wavelength at which all calculations are to be done in MICRONS.
SURFACE PROPERTIES			See Section 6.

---------- X ----------

C. REFLECTING SURFACE CASES.

When the input data specifies ISURF as 2 or 3 then that implies that a REFLECTING surface is present at the bottom of the medium. In that case NOTE THAT THE ADDING PACKAGE MUST USE c-function integrations for intensity calculations. This means that the user must be careful about specifying c function spacing (DTRLR) and also in writing subprogram TMPFUN. Even if the medium is specified as isothermal (NONISO = 0), in the case of adding a reflecting surface, TMPFUN would be called during the surface adding step. Therefore TMPFUN must be DEFINED to be equal to the medium temperature.

The second important point to note in this case is that the primary input file on DSRN 05 must contain ADDITIONAL DATA, after the NAMELIST CASE data cards, as follows :

IF ISURF = 2, the ADDING package reads a 'peakyness parameter' (CP) and the Emissivity vector. The read statement for this is in SUBROUTINE SURIN2 and it uses the List Directed Input facility of IBM FORTRAN. The input should contain CP value followed by emissivities at all quadrature angles. An ISOTROPIC (diffuse) reflector is given by CP=0.0 and a perfect SPECULAR reflector by CP=1.0. Values of CP between 0.0 and 1.0 specify a surface with specular+diffuse nature.

IF ISURF = 3, the program reads the bidirectional reflectivity (ρ) in SUBROUTINE SURINP. The input should contain only the UPPER TRIANGULAR matrix as RHO satisfies reciprocity relation. Each I-th row of the matrix input should begin on a NEW LINE and should contain values of RHO(I,I), RHO(I,I+1), ... , RHO(I,N); although one row can occupy more than one input line if neccessary. The input again uses the IBM FORTRAN's list directed input facility.

TOP SURFACE : When the input has ISURFT.GT.0, then ADDING assumes the presence of a top surface. This surface is specified exactly like the bottom surface is, with the temperature given by TMPSUT. The comments about surface properties input apply to the top surface also.

NOTE that if BOTH TOP AND BOTTOM SURFACES ARE PRESENT, the input on DSRN 05 must contain TOP surface emissivity/reflectivity FIRST, followed by properties of the bottom surface. Of course, if ISURFT is less than 2, no data is needed for the top surface.

APPENDIX F: USER'S GUIDE FOR ADDING/DOUBLING PACKAGE FOR EXTERNAL ILLUMINATION.

This appendix describes the package of three computer codes which uses the ADDING/DOUBLING method to compute multiple scattering diffuse intensities. The three codes are designated ADNGFFT, ADNGV90, and ADINTEN. They have been designed to run in sequence using temporary intermediate storage files which are not normally saved once the run is completed. The codes perform the following functions:

ADNGFFT: Transforms the user-supplied or Henyey-Greenstein phase functions into sets of phase matrices for each layer and each azimuth Fourier component based on a set of zenith quadrature angles.

ADNGV90: Computes the exterior and interior scattering matrices for an inhomogeneous multilayer atmosphere. Each matrix represents the response to a single Fourier component of the external radiative source.

ADINTEN: Recombines the Fourier components of the diffuse scattering intensity to produce the azimuth and zenith angle dependent intensities for each source zenith angle.

The codes use monochromatic scattering and absorption data appropriate to a particular model atmosphere. The required data would generally be provided from line-by-line molecular absorption calculations and aerosol scattering and absorption data. Specifically, the algorithm requires (1) the optical thickness of each scattering layer, (2) the layer single scattering albedo, and (3) the phase function for single scattering in each layer. The multiple scattering geometry is plane-parallel and the codes simultaneously compute intensities at up to 10 upward and 10 downward observer zenith angles for up to 10 different solar zenith angles. The number of azimuthal orientations or angles can be set by the user, but must be 65 or less. The number of Fourier components generated by the COSINE FFT (Fast Fourier Transform) will be the same as the number of azimuth angles between 0 and 180 degrees

which are used. The accuracy of the computed intensity at any angle will tend to be uncertain if fewer than about ten Fourier components (angles) are used.

F.1 PROGRAM 1, ADNGFFT

The ADNGFFT code augments the main Adding/Doubling calculation by preparing layer-by-layer phase function data for use by ADNGV90. The program allows a different phase function to be used with each atmospheric layer, if desired. Each phase function is first prepared as a numerical function of the included scattering angle γ. This function can be directly read from File 5 or calculated from the Henyey-Greenstein form with any chosen asymmetry parameter g, that is

$$P(g, \gamma) = \frac{1 - g^2}{[1 + g^2 - 2g \cos \gamma]^{3/2}} \quad . \tag{F.1}$$

The phase function is next evaluated in terms of the incident and scattered zenith angles θ_j and θ_i, and azimuth angle ϕ separating the two vertical planes (reference and sun planes) by the relation

$$\cos \gamma = \mu_i \mu_j + \sqrt{1 - \mu_i^2} \sqrt{1 - \mu_j^2} \cos \phi \ , \tag{F.2}$$

where $\mu_i = \cos \theta_i$ and $\mu_j = \cos \theta_j$. This gives $P_{ij}(g, \phi)$ (or more precisely $P_{ij}^{++} = P_{ij}^{--}$ and $P_{ij}^{+-} = P_{ij}^{-+}$, for forward and backward scattering, respectively)* for a set of quadrature zenith angles defined on the hemisphere. For each pair of quadrature points (i, j), P_{ij}^{++} and P_{ij}^{+-} are functions of the azimuth angle ϕ, and Fast Fourier Transforms (FFT's) can be carried out successively so that the ϕ dependence is replaced by the Fourier component

*For seven quadrature angles the phase function is a 14 X 14 array. Since scattering depends only on the included angle, the four corner submatrices (like P^{++}, etc) are related. The superscripts stand for probe-response directions.

index n. The actual FFT is performed by the subroutine TFC which is described below.

Subroutine TFC

Purpose

Given a finite Fourier cosine series

$$X_j = \frac{1}{2} c_o + \sum_{k=1}^{2n-1} c_k \cos \frac{\pi}{2n} jk + \frac{(-1)^j}{2} c_{2n}$$

$(j = 0, 1, \ldots, 2n)$

the subroutine performs the following computations:

IOPT < 0 : Fourier analysis (computation of the coefficients c_k for given values X_j).

IOPT > 0 : Fourier synthesis (evaluation of the series for given c_k).

Usage

CALL (D)TFC(X,N,IOPT,IER,AUX,NMAX)

X . GIVEN vector of dimension 2*N + 1 containing the values X_j if IOPT<0, or coefficients c_k if IOPT>0.

RESULTANT vector containing the coefficients c_k if IOPT<0, or values X_j of the series if IOPT>0.

IOPT . GIVEN option parameter. The sign of IOPT specifies the selected operation (refer to the section Purpose), the magnitude of IOPT (normally 1) specifies the indexing increment for given and resultant data within vector X.

IER . RESULTANT error indicator.

AUX . AUXILIARY vector of dimension NMAS used as working storage in subroutine (D) TFG which is called in TFC.

NMAS . GIVEN number of elements within vector AUX which may be used as working storage.

RESULTANT auxiliary storage size which is actually needed by subroutine (D) TFG.

Error Table

Code	Explanation	Program action	Comments
0	No error was detected.		
1000	N < 2	Operation is bypassed	
2000	IOPT = 0	Operation is bypassed	
3000	NMAX is too small.	Actual storage requirement of (D) TFG is returned in NMAX, vector X is destroyed, further operation is bypassed.	

Remarks

. If (D) TFC is used to approximate an even function with period T, the given function values X_j (refer to the section Purpose) must correspond to the (equidistant) argument values

$$\frac{T}{4n} j \quad (j = 0, 1, \ldots, 2n).$$

Method

The algorithm is based on the Fast Fourier Transform algorithm. The Fourier cosine series of order 2n is evaluated by relating it to a real Fourier series of order n.

The Fourier cosine series

$$X_j = \frac{1}{2} c_o + \sum_{k=1}^{2n-1} c_k \cos \frac{\pi}{2n} jk + \frac{(-1)^j}{2} c_{2n} \quad (j = 0, 1, \ldots, 2n)$$

can be evaluated by means of the real Fourier series

$$Y_j = \frac{1}{2} a_o + \sum_{m=1}^{n-1} (a_m \cos \frac{\pi}{n} jm + b_m \sin \frac{\pi}{n} jm) + \frac{(-1)^j}{2} a_n$$

$(j=0, 1, \ldots, 2n-1)$ with $a_m = c_{2m}$ $(m=0, 1, \ldots, n)$

and $b_m = c_{2m+1} - c_{2m-1}$ $(m=1, 2, \ldots, n-1)$.

The values Y_j can be computed using subroutines (D)TFT and (D)TFG and the values X_j are then obtained from

$$X_o = Y_o + \sum_{k=0}^{n-1} c_{2k+1}$$

$$2X_j = (Y_j + Y_{2n-j}) - (Y_j - Y_{2n-j})/(2 \sin \frac{\pi}{2n} j) \quad (j = 1, 2, \ldots, 2n-1)$$

$$X_{2n} = Yo - \sum_{k=0}^{n-1} c_{2k+1}$$

For the Fourier analysis, i.e., the computation of the coefficients c_k for given X_j, the relation

$$c_k = \frac{1}{n} (\frac{1}{2} X_o + \sum_{j=1}^{2n-1} X_j \cos \frac{\pi}{2n} kj + \frac{(-1)^k}{2} X_{2n})$$

$(k=0, 1, \ldots, 2n)$ allows the same algorithm to be used.

ADNGFFT: MAIN PROGRAM LISTING

```
CCC
C     PROGRAM ADNGFFT: Fourier Decomposition of The Phase Function.
CCC
      COMMON /INTCOM/ XMU(10), DWT(10), N
      COMMON /INTERC/ NI, DTHETA, P(101)
      DATA PI/3.141592d/, NEMAX/32/
      DIMENSION PP(65), PM(65), PNP(65,10,10), PNM(65,10,10), AUX(513),
     ;          PHI(65), POUTP(10,10), POUTM(10,10)
      DIMENSION LABEL(20)
C
CCC
C     Read in the GIVEN Phase Function and other control variables.
C
C     Phase Function given must be for equispaced values of Theta,
C     for NI values of theta, where NI is an ODD integer, so that
C     the Phase function values are given for THETA=H*(I-1), for
C     I=1,2,...,NI, where H=2*Pi/(NI-1).
C     NI is the number of Phase Function values (< or = 101) per layer,
C     NL is the number of layers, N the number of quadrature (Mu)
C     angles to be used in the ADDING program, and NF the number of
C     Fourier terms to be used in the Fourier Series decomposition.
CCC
C
      READ(5,*) NI, NL, N, NF, IPHRPT, IFLUX, IHENGR, INOFT
      WRITE(6,905)  NI, NL, N, NF, IPHRPT, IFLUX, IHENGR, INOFT
905   FORMAT('1PARAMETERS USED FOR THE PHASE FUNCTION CALCULATION',
     1   ////,30X,'NI       =  ',I3,
     2      /,30X,'NL       =  ',I3,
     3      /,30X,'N        =  ',I3,
     4      /,30X,'NF       =  ',I3,
     5      /,30X,'IPHRPT   =  ',I3,
     6      /,30X,'IFLUX    =  ',I3,
     7      /,30X,'IHENGR   =  ',I3,
     8      /,30X,'INOFT    =  ',I3,//////)
C
C
C   NI       ---  NUMBER OF VALUES OF THETA FROM 0-PI
C   NL       ---  NUMBER OF LAYERS
C   N        ---  NUMBER OF ZENITH QUADRATURE POINTS
C   NF       ---  2*NF+1 IS NUMBER OF FOURIER TERMS
C   IPHRPT   ---  0  IF NEW PHASE FUNCTION USED IN EACH LAYER
C                 1  IF SAME PHASE FUNCTION IS USED
C   IFLUX    ---  0  TO DO AN ORDINARY INTENSITY CALCULATION
C                 1  TO DO A FLUX CALCULATION ONLY
C   IHENGR   ---  0  TO READ IN NI VALUES OF A NUMERICAL PHASE FUNCT.
C                 1  TO READ IN A VALUE OF G FOR EACH LAYER
C
C   GPAR     ---  ASYMMETRY PARAMETER  G  APPEARS ON NEXT CARD(S)
C
C
```

```
      IF (NF .LE. NFMAX) GO TO 910
        WRITE(6,901)
901     FORMAT('1'//' NUMBER OF FOURIER COMPONENTS REQUESTED IS LARGER'/
     ;   ' THAN ALLOWED BY ARRAY SIZES, EXECUTION TERMINATED.'/)
        STOP
910   NF2=2*NF+1
      WRITE(7) NI, NL, N, NF2
      CALL QUADWT
      NIM=2*NI
      NI1=NI-1
      DTHETA=PI/NI1
      N2F=2*NF
      DPHI=PI/N2F
      DO 1 I=1,NF2
1     PHI(I)=COS(DPHI*(I-1))
C
C     Loop for Layers:
C
      DO 900 L=1,NL
C
C   SKIP THE PHASE FUNCTION TRANSFORM IF THE SAME ONE IS USED
C   IN EACH LAYER.
C
      IF (IPHIRPT.EQ.0) GO TO 50
      IF (L.EQ.1.) GO TO 50
      GO TO 350
C
C
C   CONSTRUCT THE HENYEY-GREENSTEIN FUNCTION IF  IHENGR=1
C
50    IF(IHENGR.EQ.0) GO TO 70
      READ(5,*) GPAR
      GPAR2=GPAR*GPAR
      DO 60 I=1,NI
      DOT=COS(DTHETA*(I-1))
      DOT=(1.0+GPAR2-2.0*GPAR*DOT)**1.5
      P(I)=(1-GPAR2)/DOT
60    CONTINUE
C
      WRITE(6,920) GPAR
920   FORMAT(//,' HENYEY-GREENSTEIN USED WITH   G =',F6.3,///)
C
      GO TO 75
C
70      READ(5,*) (P(I), I=1,NI)
75      DO 80 I=1,NI1
80        P(NIM-I)=P(I)
```

```
CC
C      For each MU(I) and MU(J), calculate the Fourier Coefficients:
CC
         DO 300 I=1,N
          A=SQRT(1.0-XMU(I)*XMU(I))
          Do 200 J=1,N
              B=SQRT(1.0-XMU(J)*XMU(J))*A
              C=XMU(I)*XMU(J)
              DO 100 K=1,NF2
               D=R*PHI(K)
               PP(K)=FINTER(ACOS(D+C))
100            PM(K)=FINTER(ACOS(D-C))
C
C  BYPASS FOURIER TRANSFORM IF INOFT=1
C
       IF(INOFT.EQ.1)  GO TO 125
C
              IOPT= -1
              IER=0
              CALL TFC (PP, NF, IOPT, IER, AUX, 513)
              IOPT= -1
              IER=0
              CALL TFC (PM, NF, IOPT, IER, AUX, 513)
              PP(1)=PP(1)/2.0
              PM(1)=PM(1)/2.0
       PP(NF2)=PP(NF2)/2.0
       PM(NF2)=PM(NF2)/2.0
C
125    CONTINUE
C
              DO 150 K=1,NF2
               PNP(K,I,J)=PP(K)
150            PNM(K,I,J)=PM(K)
200           CONTINUE
300       CONTINUE
350    CONTINUE
C
       NF2WRT=NF2
       IF(IFLUX.NE.0) NF2WRT=1
C
         DO 400 K=1,NF2WRT
              WRITE(7) ((PNP(K,I,J),I=1,N),J=1,N)
400           WRITE(7) ((PNM(K,I,J),I=1,N),J=1,N)
900    CONTINUE
C
C      TRANSPOSE THE PHASE FUNCTION DATASET TO WRITE LAYERS FIRST:
C
       WRITE(8) NL, NL, N, NF2WRT
```

```
      DO 30 K0=1,NF2WRT
       REWIND 7
      READ (7) NI, NL, N, NF2
       DO 30 L=1,NL
        DO 10 K=1,NF2WRT
         READ(7) ((PNP(K,I,J),I=1,N),J=1,N)
10       READ(7) ((PNM(K,I,J),I=1,N),J=1,N)
C
C
        DO 20 I=1,N
        DO 20 J=1,N
         POUTP(I,J)=PNP(K0,I,J)
20       POUTM(I,J)=PNM(K0,I,J)
        WRITE(8) ((POUTP(I,J),I=1,N),J=1,N)
        WRITE(8) ((POUTM(I,J),I=1,N),J=1,N)
30    CONTINUE
      STOP
      END
```

The results of the FFT's are written to File 7 and the entire process is repeated (if $P(\gamma)$ is different) for each successive layer. Since the A/D code performs calculations based on all layer data for a single Fourier component at a time, the phase function data must be reordered by Fourier component and then by layer rather than vice versa. The data is therefore read from File 7, reordered, and then written to File 8, which is then passed to ADNGV90.

F.2 PROGRAM 2, ADNGV90

Some key features of the adding/doubling algorithm and its application to solar scattering are outlined below. The reader is also referred to Appendix E where a description of the original A/D code can be found. The code was first developed specifically to model radiative transfer in plane-parallel media with internal infrared emission sources. The solar scattering problem requires a change in perspective, but the same equations apply. Specific changes which supercede the code description of Appendix E are given here.

The user will note that some of the options related to thermal emission which are described in Appendix E have been "turned off" in this solar scattering code. The original A/D code was also controlled interactively from a terminal and some modifications have been made to allow batch processing. Phase function data is passed from ADNGFFT through File 12 rather than from the user directly via File 5. The albedo data is specified at the end of File 5 as an array indexed by layer and not in functional form as suggested by Appendix E. Most other features which remain active are unchanged.

The A/D scattering functions $S_F^{\pm}$ and $T_F^{\pm}$ are the computed quantities which directly apply to the solar scattering problem. They represent the

the radiative response of the medium at the top or bottom surfaces to an internal unidirectional source of illumination. The solar problem having an external source which drives radiative intensities within the medium (including both surfaces) calls for interchanging the source and observer orientations, or equivalently, having the photons move backward. This switch is done after the A/D calculations for each Fourier component are completed and prior to computing the actual intensities in ADINTEN. The scattering functions themselves are denoted by

$$S_F^{\pm}(i, j, n, \tau_r, \tau_o) \text{ and } T_F^{\pm}(i, j, n, \tau_r, \tau_o)$$

with the following nomenclature:

S Indicates diffuse scattering, that is, upward intensity exiting the medium at the top surface due to illumination directed downward, or downward intensity at bottom surface due to upward illumination.

T Indicates diffuse transmittance; upward intensity if the illumination is upward, or downward intensity if the illumination is downward.

+ Indicates source illumination is directed upward.

- Indicates source illumination is directed downward

F Refers to internal illumination. Response to be found at top or bottom exterior surfaces.

i Index for the zenith angle of response intensity.

j Index for the zenith angle of the source.

n Azimuthal Fourier component index. The n'th component of the intensity field responds only to the n'th component of the driver.

τ_r Optical depth of the driver (source) location as measured from the top. "1" serves as a source location index.

τ_o Total medium optical thickness.

Implicit Functional Arguments of the Scattering Functions:

$\omega(\tau)$ albedo function of optical depth (altitude).

$P_{ij}^{\pm\pm}(\tau)$ Forward (++, --) and backward (+-, -+) phase matrices by Fourier component and optical depth (altitude).

The code actually computes weighted forms of these functions which appear as

$$SFIP(i, j, r) = \frac{1 + \delta_{o,n}}{4 \mu_i} S_F^+ d_j$$

$$SFIM(i, j, r) = \frac{1 + \delta_{o,n}}{4 \mu_i} S_F^- d_j$$

$$TFIP(i, j, r) = \frac{1 + \delta_{o,n}}{4 \mu_i} T_F^+ d_j$$

$$TFIM(i, j, r) = \frac{1 + \delta_{o,n}}{4 \mu_i} T_F^- d_j \ , \qquad (F.3)$$

where d_j is the quadrature weighting factor appropriate to the j'th source zenith angle. The quantities SFIM, SFIP, TFIM, and TFIP are computed together with other scattering functions in ADNGV90. The roles of internal source and external response are then reversed through reciprocity, and two new scattering matrices SVARP and SVARM representing upward and downward internal response caused by an external source are introduced. They are given by

$$SVARP = \frac{1}{(1 + \delta_{o,n})} \frac{\mu_j}{\mu_i} TFIP(j, i) \, d_i^{-1} \ , \qquad (F.4)$$

and

$$SVARM = \frac{1}{(1 + \delta_{o,n})\pi} \frac{\mu_j}{\mu_i} SFIM(j, i)\, d_i^{-1}, \qquad (F.5)$$

for each Fourier component n and observer level r.

ADNGV90 FILE STRUCTURE:

FILE 1: This file contains a run label of 80 characters.

FILE 5: Primary input file for control of Adding/Doubling calculations.

RECORD 1: NAMELIST CASE PARAMETERS:

NLAYER : NUMBER OF HOMOGENEOUS LAYERS (=NL)

DTRLR : OPTICAL DEPTH SPACING USED FOR COMPUTING BOTH INTERNAL SCATTERING FUNCTIONS AND FOR FINAL MULTIPLE SCATTERING INTENSITIES. CONSTRAINED TO BE DTRLR= TO/(2**I) WHERE TO IS THE TOTAL OPTICAL DEPTH AND I IS ANY NON-NEGATIVE INTEGER.

TNOTLR : A SET OF NLAYER REAL NUMBERS GIVING THE OPTICAL THICKNESS OF EACH LAYER STARTING FROM THE TOP. CONSTRAINED TO BE OF THE FORM TNOTLR(J) =.(2**I) **DTRLR FOR ALL LAYERS J AND ANY NON-NEGATIVE INTEGER I.

INHOMO : =0 OPTION NOT ACTIVE
=1 INHOMOGENEOUS ATMOSPHERE; SET NLAYER=1 IF HOMOGENEOUS ATMOSPHERE IS NEEDED.

IOCTL1 : CONTROLS AMOUNT OF OUTPUT ON FILE 6.
=1 ALL SCATTERING FUNCTIONS PRINTED AFTER EACH LAYER ADDITION.
=2 OPTION NOT ACTIVE.
=3 ALL FUNCTIONS PRINTED ONLY AFTER FINAL SCATTERING FUNCTIONS COMPUTED.
=4 OPTION NOT ACTIVE.
=5 NO OUTPUT ON FILE 6 EXCEPT HEADER.

RECORD 2: OMGFUN : SET OF NLAYER REAL NUMBERS WHICH ARE LAYER-BY-LAYER SINGLE SCATTERING ALBEDOES ARRANGED FROM THE TOP LAYER DOWN.

FILE 12: Must be the same file as ADNGFFT File 8. Contains the phase function data by Fourier component.

FILE 13: A new intermediate file which is passed to ADINTEN. Contains external to internal scattering matrices by Fourier component.

F.3 PROGRAM 3 ADINTEN

The code ADINTEN carries out the last step in the calculation of internal intensities based on an external driving source. File 7 contains the external-to-internal scattering functions ordered by Fourier component and observer level. These functions are read from File 7 and transposed so as to appear as functions of the Fourier index n at each level. They are inverse Fourier transformed by the same subroutine TFC (see section F.1) as was used for the FFT of the phase function data. The intensities are given by

$$I^{+}(\tau, 0, \theta_o, \phi) = \text{IFT} \quad (\text{SVARP}) \ , \tag{F.6}$$

and

$$I^{-}(\tau, 0, \theta_o, \phi) = \text{IFT} \quad (\text{SVARM}) \ , \tag{F.7}$$

for a unidirectional external source of unit strength where IFT means inverse Fourier transform. These upward and downward intensities are written to the standard output file (File 6). In addition, the zeroth Fourier components of the scattering functions are used by themselves to calculate the upward and downward ratiative fluxes as

$$Q_j^{+}(\tau) = \sum_i \mu_i \, d_i \, [\text{SVARP}\ (i, j)]_{\tau, \, n=0} \ , \tag{F.8}$$

and

$$Q^{-}(r) = \sum_{i} \mu_i \, d_i \quad [\text{SVARM}\ (i, j)]_{r,\ n=0}, \tag{F.9}$$

at each observer level r and each solar zenith j. The flux calculation can be carried out without performing more than one Fourier component A/D calculation in ADNGV90. (See directions specifying IFLUX=1 in section F.1). For these special flux calculations, the inverse FFT is suppressed and the intensities which are printed represent the zeroth component only. These intensities are correct in the case of isotropic scattering (GPAR = 0.0). Fluxes are written directly to a separate output file [File 10].

ADINTEN : MAIN PROGRAM LISTING

```
CCC
C      THIS PROGRAM READS THE FOURIER COMPONENTS OF THE SCATTERING
C      FUNCTIONS WRITTEN BY THE ADDING PROGRAM AND INVERSE FOURIER
C      TRANSFORMS THEM TO CALCULATE THE INTERIOR INTENSITIES DUE TO
C      SOLAR INTENSITIES AT THE TOP OF THE MEDIUM.
CCC
C
C
       REAL*8 XMU, DWT, XMUDWT, DWTINV
C
C
       DIMENSION SSM(10,10,41), TSM(10,10,41), XIP(65,10,10),
      :          XIM(65,10,10), AUX(513)
       DIMENSION XMU(10), DWT(10), XMUDWT(10), DWTINV(10)
       DIMENSION FLUXP(10), FLUXM(10), FLUXQ(10)
C
C
C
       READ(7) NT, NL, N, NF2
C
C    READ THE QUADRATURE WTS. AND COSINES FROM FILE 7
C
       READ(7) (XMU(I),I=1,N)
       READ(7) (DWT(I),I=1,N)
C
C  CAN ADD XMUINV(I) NEXT TIME BOTH PROGRAMS
C  ARE COMPILED
C
C
C
       READ(7) (XMUDWT(I),I=1,N)
       READ(7) (DWTINV(I),I=1,N)
C
       NF=(NF2-1)/2
       READ(7) NRS
C
       WRITE(10,196)
C
       DO 100 IL=1,NRS
        REWIND 7
        READ(7) NT, NL, N, NF2
        READ(7) (XMU(I),I=1,N)
        READ(7) (DWT(I),I=1,N)
        READ(7) (XMUDWT(I),I=1,N)
        READ(7) (DWTINV(I),I=1,N)
        DO 5 I=1,NF2
        READ(7) NRS
```

```
      DO 10 K=1,NRS
       READ(7) ((SSM(I,J,K),I=1,N),J=1,N)
10     READ(7) ((TSM(I,J,K),I=1,N),J=1,N)
      DO 11 J=1,N
      DO 11 I=1,N
       XIP(L,I,J)=SSM(I,J,KL)
11     XIM(L,I,J)=TSM(I,J,KL)
30    CONTINUE
C
C
      DO 40 J=1,N
C
       FLUXP(J)=0.0
       FLUXM(J)=0.0
C
      DO 40 I=1,N
C
     FLUXP(J)=FLUXP(J)+XIP(1,I,J)*XMU(I)*DWT(I)
     FLUXM(J)=FLUXM(J)+XIM(1,I,J)*XMU(I)*DWT(I)
C
35   IF(NF2.EQ.1) GO TO 40
C
       IOPT=1
       IER=0
       XIP(1,I,J)=2.0*XIP(1,I,J)
     XIP(NF2,I,J)=2.0*XIP(NF2,I,J)
       CALL TFC (XIP(1,I,J), NF, IOPT, IER, AUX, 513)
       IOPT=1
       IER=0
     XIM(NF2,I,J)=2.0*XIM(NF2,I,J)
       XIM(1,I,J)=2.0*XIM(1,I,J)
       CALL TFC (XIM(1,I,J), NF, IOPT, IER, AUX, 513)
40    CONTINUE
      WRITE(6,41) KL
41     FORMAT('1'//' K-LEVEL NUMBER = ',I2/
    ;              ' --------------'//)
C
C    WRITE OUT UP AND DOWN FLUXES AT THIS LEVEL
C
     TWOPI=6.28318531
C
      DO 45 J=1,N
C
C
     FLUXP(J)=FLUXP(J)*TWOPI
     FLUXM(J)=FLUXM(J)*TWOPI
     FLUXQ(J)=FLUXP(J)-FLUXM(J)
C
45    CONTINUE
C
C
   WRITE FLUXES TO DATA STORAGE FILE NUMBER 16
```

```
      WRITE(10,197)  KL, (FLUXP(J),J=1,N)
      WRITE(10,198)  KL, (FLUXM(J),J=1,N)
      WRITE(10,199)
196   FORMAT(////,' ADDING/DOUBLING FLUXES',/////)
197   FORMAT(' R-LEV',I4,'   FLUXP  ',7E15.6,/,20X,7E15.6)
198   FORMAT(' R-LEV',I4,'   FLUXM  ',7E15.6,/,20X,7E15.6)
199   FORMAT(' ')
C
C
       DO 50 L=1,NF2
        WRITE(6,46) KL,L
46      FORMAT(//' R-LEVEL :',I2,' ;  PHI INDEX : ',I2//
     ;  ' INTENSITY-PLUS (I,J)'/
     ;  ' ---------------------'//' I',5X,'VALUES ->'//)
        DO 47 I=1,N
47       WRITE(6,48) I, (XIP(L,I,J),J=1,N)
48      FORMAT('0',I2,3(T4,10D12.4))
        WRITE(6,49)
49      FORMAT(//' INTENSITY-MINUS (I,J)'/
     ;  ' ----------------------'//' I',5X,'VALUES ->'//)
        DO 50 I=1,N
50       WRITE(6,48) I, (XIM(L,I,J),J=1,N)
100   CONTINUE
C
C  ADD A MARKER AT THE END OF DATA ON FILE 10
C
      WRITE(10,299)
299   FORMAT('    *****     *****     ',10X)
C
      STOP
      END
```

F.4 ADDING/DOUBLING SAMPLE IBM JOB CONTROL CARDS AND DATA FILES

```
/*JOBPARM R=512,T=1,L=10
//PHASEFFT EXEC PGM=MAIN
//STEPLIB DD DSN=ACCOUNT.ADNGFFT.LOAD,DISP=SHR
//FT05F001 DD *
   51     7     7     8     1     0     1     0
    0.8
//FT06F001 DD SYSOUT=A
//FT07F001 DD DSN=&TEMP1,UNIT=SCRATCH,DISP=(NEW,DELETE,DELETE),
//          SPACE=(CYL,(1,1))
//FT08F001 DD DSN=&TEMP2,UNIT=SCRATCH,DISP=(NEW,PASS),
//          SPACE=(CYL,(1,1))
//ADDING EXEC PGM=MAIN
//STEPLIB DD DSN=ACCOUNT.ADNGV90.LOAD,DISP=SHR
//FT01F001 DD DSN=ACCOUNT.LAYER.DATA,DISP=SHR
//FT05F001 DD *
 &CASE
 NLAYER=7,
 IOCTL1=3,
 TNOTLR=0.0152635,0.0152635,0.0152635,0.030527,0.0152635,0.030527,0.061054,
 DTRLR=0.0152635,
 INROMO=1,
 &END
  0.00258  0.0690  0.2777  0.2804  0.3388  0.3485  0.3485   /
//FT06F001 DD SYSOUT=A
//FT12F001 DD DSN=&TEMP2,DISP=(OLD,PASS),UNIT=SCRATCH
//FT13F001 DD DSN=&TEMP3,UNIT=SCRATCH,DISP=(NEW,PASS),
//          SPACE=(CYL,(1,1))
//ADINTEN EXEC PGM=MAIN
//STEPLIB DD DSN=ACCOUNT.ADINTEN.LOAD,DISP=SHR
//FT05F001 DD DUMMY
//FT06F001 DD SYSOUT=A
//FT07F001 DD DSN=&TEMP3,UNIT=SCRATCH,DISP=(OLD,DELETE,DELETE)
//FT10F001 DD DSN=ACCOUNT.NEWFLUX.DATA,
//       UNIT=TPUSER,
//       SPACE=(TRK,(1,1)),
//       DISP=(NEW,CATLG),
//       DCB=(DSORG=PS,LRECL=133,RECFM=FB,BLKSIZE=2660)
```

```
C
C
C
C     INPUT/OUTPUT FILES REQUIRED :
C     ----- ------ ----- --------
C
C     FT05F001 : READ(5,...) - FILE IS USED FOR PARAMETER INPUT USING
C        THE NAMELIST CASE.  FILE MUST FOLLOW NAMELIST INPUT FORMAT.
C     FT06F001 : WRITE(6,...)/PRINT - OUTPUT FILE.
C     FT10F001 : WRITE (10) - FLUX OUTPUT IS
C                              WRITTEN DIRECTLY TO DISK FILE 10.
C     FT12F001 : READ (12) - PHASE FUNCTION FOURIER COMPONENT INPUT.
C                            FOURIER COMPONENTS SHOULD NOT BE USED
C                            EXCEPT FOR N=1 FLUX CALCULATIONS.
C
C
C
C
C     The GLOBAL variables are passed to all routines through the
C     following COMMON blocks.  Any variable NOT appearing in a COMMON
C     is local to the routine and is used for temporary storage and
C     intermediate calculations.
C
C
C
      COMMON /SCALAR/  TFINAL,TLAYER,DTMAX,DTINIT,CONN,OMEGA,T1,T2,T,
     ;                 TMPSUR,TMPSUT,DTRLR,ASY2,ASYSQ,
     ;                 CONN2,TOOFT,FORPI,ASY,DTK,TMPKM, NLAYER,NAC,NCIN,
     ;                 N,M,NP1,NN,NM1,MSMALL,NDUBLE,ILAYER,NONISO,ISURF,
     ;                 NA,NDUB,NRS,NAC1,NAC2,INHOMO,IOCTL1,IOCTL2,
     ;                 IOCTL3,IOCTL4,IOCTL5,ISURFT
      COMMON /VECTOR/   XMU(10),XMUINV(10),DWT(10),DWTINV(10),
     ;                  TNOTLR(40),XMUDWT(10),
     ;                  OMGFUN(41)
      COMMON  /MATRIX/ PHASLB(10,10),PHASEF(10,10)
      DIMENSION AMNTP(7,7,41),AMNTM(7,7,41)
C
      CALL INPUT
C
      WRITE(6,990) NLAYER,(TNOTLR(IL),IL=1,NLAYER)
      WRITE(10,990) NLAYER,(TNOTLR(IL),IL=1,NLAYER)
990   FORMAT(///,' SINGLE SCATTERING CASE RUN',
     ;       //,' NUMBER OF LAYERS =',I5,
     ;       //,' WITH OPTICAL DEPTHS ---      ',5(5F12.6,/,29X),//)
C
      READ(5,*) OMGFUN
      WRITE(6,991) (OMGFUN(IL),IL=1,NLAYER)
      WRITE(10,991) (OMGFUN(IL),IL=1,NLAYER)
991   FORMAT    ,' AND WITH ALBEDOES   ---      ',5(5F12.4,/,29X),/)
      NLEVEL=NLAYER+1
```

```
C
C
C    LOOP OVER AZIMUTHAL ANGLES PHI
C
       DO 1000 NPHI=1,M
C
C
C
       DO 50 NR=1,NLEVEL
       DO 50 J=1,N
       DO 50 I=1,N
C
       AMNTP(I,J,NR)=0.0
       AMNTM(I,J,NR)=0.0
C
50     CONTINUE
C
C     LOOP OVER SOURCE LAYERS
C
C
       DO 500 ILAYER=1,NLAYER
C
C
C     READ IN THE PHASE FUNCTION FOR THIS LAYER
C     AND THIS VALUE OF PHI.
C
       READ(12) ((PHASEF(I,J),I=1,N),J=1,N)
       READ(12) ((PHASEB(I,J),I=1,N),J=1,N)
C
C       WRITE(6,919) ((PHASEF(I,J),I=1,N),J=1,N)
C       WRITE(6,919) ((PHASEB(I,J),I=1,N),J=1,N)
C919    FORMAT(///,' PHASE FUNCTION',/,
C     ;         7(7F15.6,/))
C
C     LOOP OVER BOTH QUADRATURE ANGLES
C
       DO 400 I=1,N
C
       DO 400 J=1,N
C
       SSSP=PHASEB(I,J)*OMGFUN(ILAYER)*XMUINV(I)/FORPI
C
       SSSM=PHASEF(I,J)*OMGFUN(ILAYER)*XMUINV(I)/FORPI
C
       EXPMUI=EXP(-TNOTLR(ILAYER)*XMUINV(I))
       EXPMUJ=EXP(-TNOTLR(ILAYER)*XMUINV(J))
C
       SSSP=SSSP*(1.0-EXPMUI*EXPMUJ)/(XMUINV(I)+XMUINV(J))
C
       DIFRAT=EXPMUI*TNOTLR(ILAYER)
```

```
      IF(I.EQ.J) GO TO 100
      DIFRAT=(EXPMUI-EXPMUJ)/(XMUINV(J)-XMUINV(I))
100   CONTINUE
      SSSM=SSSM*DIFRAT
C
C   MULTIPLY SCATT. SOURCES BY DIREXT SOLAR TRANS
C
      DSTRAN=1.0
C
      IF(ILAYER.EQ.1) GO TO 120
C
      MAX=ILAYER-1
      DO 110 NEXLAY=1,MAX
C
      DSTRAN=DSTRAN*EXP(-TNOTLR(NEXLAY)*XMUINV(J))
C
110   CONTINUE
120   SSSP=SSSP*DSTRAN
      SSSM=SSSM*DSTRAN
C
C   ADD CONTRIBUTION TO TOP OF SCATTERING LAYER
C
      NR=ILAYER
      AMNTP(I,J,NR)=AMNTP(I,J,NR)+SSSP
C
C   ADD PART TO BOTTOM OF SCAT. LAYER
C
      NR=ILAYER+1
      AMNTM(I,J,NR)=AMNTM(I,J,NR)+SSSM
C
      IF(ILAYER.EQ.1) GO TO 250
C
C   FILL IN ABOVE TOP OF SCAT. LAYER
C
      NRMAX=ILAYER-1
      DO 200 NRSTEP=1,NRMAX
      NR=ILAYER-NRSTEP
      SSSP=SSSP*EXP(-TNOTLR(NR)*XMUINV(I))
      AMNTP(I,J,NR)=AMNTP(I,J,NR)+SSSP
200   CONTINUE
C
C  FILL IN BELOW BOTTOM OF LAYER
C
250   IF(ILAYER.EQ.NLAYER) GO TO 350
C
      NRMIN=ILAYER+2
      DO 300 NR=NRMIN,NLEVEL
      NLAST=NR-1
      SSSM=SSSM*EXP(-TNOTLR(NLAST)*XMUINV(I))
      AMNTM(I,J,NR)=AMNTM(I,J,NR)+SSSM
```

```
300   CONTINUE
350   CONTINUE
400   CONTINUE
500   CONTINUE
C
C      WRITE OUT  ACTUAL  INTENSITIES
C
C
      DO 550 NR=1,NLEVEL
      WRITE(6,992) NR,NPHI
992   FORMAT('1',//////,' SINGLE SCATTERING INTENSITIES AT',
     ;           ' R-LEVEL :',I2,',  PHI INDEX :',I2,///)
      WRITE(6,993)  ((AMNTP(I,J,NR),J=1,N),I=1,N)
993   FORMAT(//,' INTENSITY UP                SOLAR ZENITH   ---->',
     ;      /,' ---------------',//,7(5X,7E12.4,/),//)
      WRITE(6,994)  ((AMNTM(I,J,NR),J=1,N),I=1,N)
994   FORMAT(//,' INTENSITY DOWN              SOLAR ZENITH   ---->',
     ;      /,' ---------------',//,7(5X,7E12.4,/),//)
550   CONTINUE
C
      IF(M.NE.1) GO TO 1000
C
      WRITE(10,995)
995   FORMAT(////,' INTEGRATED SINGLE SCATTERING FLUXES FOLLOW',///)
C  AT THIS POINT, ARRAYS AMNTP AND AMNTM CONTAIN
C  THE ANGLE DEPENDENT ZEROTH FOURIER INTENSITIES.
C
C   SUM OVER OBSERVER ANGLE  I  TO GET ACTUAL UP AND DOWN FLUXES
C
      DO 600 J=1,N
      DO 600 NR=1,NLEVEL
      AMNTP(1,J,NR)=AMNTP(1,J,NR)*XMU(I)*TOOPI*DWT(I)
      AMNTM(1,J,NR)=AMNTM(1,J,NR)*XMU(I)*TOOPI*DWT(I)
600   CONTINUE
C
      DO 700 J=1,N
      DO 700 NR=1,NLEVEL
      DO 650 I=2,N
      AMNTP(1,J,NR)=AMNTP(1,J,NR)+AMNTP(I,J,NR)*XMU(I)*TOOPI*DWT(I)
      AMNTM(1,J,NR)=AMNTM(1,J,NR)+AMNTM(I,J,NR)*XMU(I)*TOOPI*DWT(I)
650   CONTINUE
700   CONTINUE
C
C   WRITE OUT FLUXES LEVEL BY LEVEL
C
      DO 800 NR=1,NLEVEL
C
C   WRITE FLUXES TO EXTRA STORAGE FILE NUMBER  10
C
      WRITE(6,998)
```

```
      WRITE(10,996)  NR, (AMNTP(1,J,NR),J=1,N)
      WRITE(10,997)  NR, (AMNTM(1,J,NR),J=1,N)
      WRITE(10,998)
800   CONTINUE
1000  CONTINUE
C
      WRITE(10,999)
C
999   FORMAT(//////////,' ADDING/DOUBLING RESULTS MAY FOLLOW :',//////)
C
C
      STOP
C
996   FORMAT(' K-LEV',I4,'    FLUXP  ',7E15.6)
997   FORMAT(' K-LEV',I4,'    FLUXM  ',7E15.6)
998   FORMAT(' ')
C
      END
C
CCCCC
C
C     SUBROUTINE INPUT
C     ---------- -----
C
C
C     This subroutine determines the input and starting parameters
C
CCCCC
C
C
C
      SUBROUTINE  INPUT
C
C
      DIMENSION C(10)
      COMMON /SCALAR/  TFINAL,TLAYER,DTMAX,DTINIT,CONN,OMEGA,T1,T2,T,
     ;                 TMPSUR,TMPSUT,DTRLR,ASY2,ASYSQ,
     ;                 CONN2,TOOPI,FORPI,ASY,DTR,TMPRM, NLAYER,NAC,NCIN,
     ;                 N,M,NP1,NN,NM1,MSMALL,NDUBLE,ILAYER,NONISO,ISURF,
     ;                 NA,NDUB,NRS,NAC1,NAC2,INHOMO,IOCTL1,IOCTL2,
     ;                 IOCTL3,IOCTL4,IOCTL5,ISURFT
      COMMON /VECTOR/   XMU(10),XMUINV(10),DWT(10),DWTINV(10),
     1                  TNOTLR(40),XMUDWT(10),
     3                  GMGFUN(41)
      COMMON  /MATRIX/ PHASEP(10,10),PHASEM(10,10)
      COMMON /INTCOM/  EC1, EC2, DOMEGA, DUMY, ETA0, INHOMW
      DIMENSION XMP(5), XM+(5), XMU2(5), XMU3(5), XMU7(4), XMU8(4),
     1          XMP9(5), XMU10(5), C1(2), C4(2), C5(3), C6(3), C7(4),
     .          C8(4),C9(5), C10(5),XMU15(8),C15(8)
C
```

```
C
C     The following NAMELIST is used to input run parameters :
CCC
C
      NAMELIST /CASE/   N, M, OMEGA, XMU, C, NONISO,ISURF, ASY, DTMAX,
     ,                  NLAYER, INHOMO, TNOTLR, DTKLR, ISURFT, TMPSUT,
     ;                  TMPSUR, WAVELN, REFIDX, IOCTL1, IOCTL2,
     ;                  IOCTL3, IOCTL4, IOCTL5, TMPRM
C
      DATA NLRMAX/40/, NMUMAX/10/
C
CCC
C     DATA statements for raw data tables used to generate quadrature
C     weights for from 2 to 10 base points.  The resulting weights
C     are used for a Gaussian quadrature scheme.
CCC
C
      DATA  XMU2  /  0.5773502692 /,
     1      XMU3 /  0.7745966692 ,
     1              0.0          /,
     1       C3 /  0.5555555555,
     1             0.8888888889 /,
     1      XMU4 /  0.8611363116,
     1             0.3399810436 /,
     1        C4 /  0.3478548451,
     1             0.6521451549 /,
     1      XMU5 /  0.9061798459,
     1             0.5384693101,
     1             0.0          /,
     1       C5 /  0.2369268851,
     1             0.4786286705,
     1             0.5688888889 /
      DATA  XMU6 /  0.9324695142,
     1             0.6612093865,
     1             0.2386191861 /,
     1        C6 /  0.1713244924,
     1             0.3607615730,
     1             0.4679139346  /,
     1      XMU7 /  0.9491079123,
     1             0.7415311856,
     1             0.4058451514,
     1             0.           /
      DATA    C7 /  0.1294849662,
     1             0.2797053915,
     1             0.3818300505,
     1             0.4179591837 /,
     1      XMU8 /  0.9602898564,
     1             0.7966664774,
     1             0.5255324099,
     1             0.1834346425 /
```

```
      DATA     C8 /  0.1012285363,
     1              0.2223810345,
     1              0.3137066459,
     1              0.3626837834 /,
     1       XMU9 /  0.9681602395,
     1              0.8360311073,
     1              0.6133714327,
     1              0.3242534234,
     1              0.           /
      DATA     C9 /  0.0812743884,
     1              0.1806481607,
     1              0.2606106964,
     1              0.3123470770,
     1              0.3302393550 /,
     1      XMU10 /  0.9739065285,
     1              0.8650633667,
     1              0.6794095683,
     1              0.4333953941,
     1              0.1488743390 /
      DATA    C10 /  0.0666713443,
     1              0.1494513492,
     1              0.2190863625,
     1              0.2692667193,
     1              0.2955242247 /
      DATA XMU15 /  0.9879925180,
     1              0.9372733924,
     1              0.8482065834,
     1              0.7244177314,
     1              0.5709721726,
     1              0.3941513471,
     1              0.2011940940,
     1              0.0          /,
     1       C15 /  0.0307532420,
     1              0.0703660475,
     1              0.1071592205,
     1              0.1395706779,
     1              0.1662692058,
     1              0.1861610001,
     1              0.1984314853,
     1              0.2025782419  /
C
C
CCC
C     All run parameters are INITIALIZED to their DEFAULT values :
CCC
C
      OMEGA = 0.5
      N = 7
      M = 3
      NONISO = 0
```

```
      INHOMO = 0
      INHOMW = 0
      NLAYER = 1
      TNOT = 0.0
      TFINAL = 1.
      ASY = 0.0
      DTMAX = 3.05D-05
      TNOTLR(1) = 1.0
      DTRLR = 1.0
      FORPI = 12.56637062
      TOOPI = 6.28318531
      ISURF = 0
      TNOTSR = 5.0
      OMEGSR = 0.95
      ASYSUR = -0.8
      ISURFT = 0
      TMPSUR = 325.0
      TMPSUT = 325.0
      TMPRM  = 325.0
      WAVELN = 5.0
      REFIDX = 1.0
      IOCTL1 = 1
      IOCTL2 = 0
      IOCTL3 = 0
      IOCTL4 = 0
      IOCTL5 = 0
C
CCC
C     Parameter input overriding the defaults is done using IBM FORTRAN
C     NAMELIST input technique.  The data is read using NAMELIST /CASE/.
CCC
C
      READ(5,CASE)
      READ(12) NDUM, NLAY2, N, M
C
CCC
C     Check for possibilities of Storage overflow :
CCC
C
      IF (N .LE. NMUMAX)  GO TO 8
         WRITE(6,7) N, NMUMAX
         WRITE(1,7) N, NMUMAX
7        FORMAT(//' *****  ERROR  *****  IN ADING PACKAGE :'//
     ;    ' TOO MANY QUADRATURE POINT ' SPECIFIED.'//
     ;    ' N = ',I2,' . MAXIMUM ALLOWED = ',I2//
     ;    ' *****  EXECUTION TERMINATED  *****'/)
         CALL EXIT
8     IF (NLAYER .LE. NLRMAX)  GO TO 9
         WRITE(6,5) NLAYER, NLRMAX
         WRITE(1,5) NLAYER, NLRMAX
```

```
          CALL EXIT
5         FORMAT(////' *****  ERROR  *****  IN ADDING PACKAGE :'//
     ;    ' LAYER THICKNESS STORAGE WILL BE EXCEEDED, EXECUTION STOPPED.'
     ;    //   ' NLAYER = ',I3,';  MAXIMUM ALLOWED = ',I3//
     ;    ' INCREASE TNOTLR DIMENSION IN ALL COMMONS.'/)
C
C
9       CONTINUE
C
   10 IF(N.NE.1) GO TO 11
      XMU(1) = XMU2
      XMU(2) = - XMU2
      C(1) = 1.
      C(2) = 1.
   11 IF(N.NE.3) GO TO 12
      XMU(1) = XMU3(1)
      XMU(2) = XMU3(2)
      XMU(3) = -XMU3(1)
      C(1) = C3(1)
      C(3) = C3(1)
      C(2) = C3(2)
   12 IF(N.NE.4) GO TO 13
      DO 128 I = 1,2
      XMU(I) = XMU4(I)
      C(I) = C4(I)
  128 C(5-I) = C4(I)
      DO 129 I = 3,4
  129 XMU(I) = - XMU4(5-I)
   13 IF(N.NE.5) GO TO 14
      DO 138 I = 1,2
      XMU(I) = XMU5(I)
      C(I) = C5(I)
  136 C(6-I) = C5(I)
      XMU(5) = 0
      C(5) = C5(3)
      DO 139 I = 4,5
  139 XMU(I) = -XMU5(6-I)
   14 IF(N.NE.6) GO TO 15
      DO 148 I = 1,3
      XMU(I) = XMU6(I)
      C(I) = C6(I)
  148 C(7-I) = C6(I)
      DO 149 I = 4,6
  149 XMU(I) = -XMU6(7-I)
   15 IF(N.NE.7) GO TO 16
      DO 158 I = 1,3
      XMU(I) = XMU7(I)
      C(I) = C7(I)
  158 C(8-I) = C7(I)
      XMU(4) = 0.
```

```
      C(4) = C7(4)
      DO 159 I = 5,7
  159 XMU(I) = -XMU7(8-I)
   16 IF(N.NE.8) GO TO 17
      DO 168 I = 1,4
      XMU(I) = XMU8(I)
      C(I) = C8(I)
  168 C(9-I) = C8(I)
      DO 169 I = 5,8
  169 XMU(I) = -XMU8(9-I)
   17 IF(N.NE.9) GO TO 18
      DO 178 I = 1,4
      XMU(I) = XMU9(I)
      C(I) = C9(I)
  178 C(10-I) = C9(I)
      XMU(5) = 0.
      C(5) = C9(5)
      DO 179 I = 6,9
  179 XMU(I) = -XMU(10-I)
   18 IF(N.NE.10) GO TO 19
      DO 188 I = 1,5
      XMU(I) = XMU10(I)
      C(I) = C10(I)
  188 C(11-I) = C10(I)
      DO 189 I = 6,10
  189 XMU(I) = -XMU10(11-I)
   19 IF(N.NE.15) GO TO 20
      DO 198 I = 1,7
      XMU(I) = XMU15(I)
      C(I) = C15(I)
  198 C(16-I) = C15(I)
      XMU(8) = 0.
      C(8) = C15(8)
      DO 199 I = 9,15
  199 XMU(I) = - XMU(16-I)
   20 CONTINUE
C
C
      DO 200 I = 1,N
  200 XMU(I) = .5*XMU(I) + .5
      DO 21 I = 1,N
      XMUINV(I) = 1./XMU(I)
      DWT(I) = C(I)*0.5
      DWTINV(I) = 1./DWT(I)
   21 XMUDWT(I) = XMU(I)*DWT(I)
C
      RETURN
      END
```

PLANE-PARALLEL SINGLE SCATTERING PROGRAM PPSS1:

SAMPLE IBM JOB CONTROL CARDS AND DATA FILES

```
/*JOBPARM T=1,L=9
//PHASEFFT EXEC PGM=MAIN
//STEPLIB DD DSN=MOT4101.ADNGFFT.LOAD,DISP=SHR
//FT05F001 DD *
   51    32     7     1     1     0     1     1
    0.8
//FT06F001 DD SYSOUT=A
//FT07F001 DD DSN=&TEMP1,UNIT=SCRATCH,DISP=(NEW,DELETE,DELETE),
//            SPACE=(CYL,(1,1))
//FT08F001 DD DSN=&TEMP2,UNIT=SCRATCH,DISP=(NEW,PASS),
//            SPACE=(CYL,(1,1))
//PPSS    EXEC PGM=MAIN
//STEPLIB DD DSN=MOT4101.PPSS1.LOAD,DISP=SHR
//FT05F001 DD *
 &CASE
 NLAYER=32,
 TNOTLR=  0.2520882E-06, 0.4097418E-05, 0.4014033E-05, 0.7848409E-05,
          0.1596691E-04, 0.7304554E-04, 0.3850379E-03, 0.1793371E-03,
          0.2433453E-03, 0.2448388E-03, 0.2478541E-03, 0.2506557E-03,
          0.2361920E-03, 0.2297376E-03, 0.2439593E-03, 0.2650097E-03,
          0.2909857E-03, 0.3124068E-03, 0.3249425E-03, 0.3344070E-03,
          0.3095272E-03, 0.2279736E-03, 0.1256998E-03, 0.8913260E-04,
          0.1802612E-03, 0.4156892E-03, 0.9852635E-03, 0.2502452E-02,
          0.6078091E-02, 0.1590397E-01, 0.4777662E-01, 0.1046715E+00,
 &END
  0.2059553E+00  0.2059541E+00  0.2059497E+00  0.2059422E+00
  0.2050720E+00  0.3171340E-01  0.2313057E-03  0.2261108E-03
  0.2521912E-03  0.3641597E-03  0.4637628E-03  0.5429178E-03
  0.6191996E-03  0.5990531E-03  0.4841997E-03  0.3806465E-03
  0.3337481E-03  0.3345475E-03  0.3681581E-03  0.4311963E-03
  0.5791909E-03  0.1052119E-02  0.5051012E-02  0.1527380E-01
  0.1397186E-01  0.9038797E-02  0.4659929E-02  0.2893881E-02
  0.2289355E-02  0.9466766E-01  0.2802829E+00  0.3485013E+00  /
//FT06F001 DD SYSOUT=A
//FT12F001 DD DSN=&TEMP2,DISP=(OLD,DELETE),UNIT=SCRATCH
//FT10F001 DD DSN=MOT4101.SSFLUX.DATA,
//       DISP=(MOD,KEEP,KEEP),
//       DCB=(DSORG=PS,LRECL=133,RECFM=FB,BLKSIZE=2660)
//FT10F002 DD DSN=MOT4101.SSFLUX.DATA,
//       DISP=(MOD,KEEP,KEEP),
//       DCB=(DSORG=PS,LRECL=133,RECFM=FB,BLKSIZE=2660)
```